Chapter 1
Introduction

A heartbeat system, i.e. a van der Pol system, which is a typical nonlinear chaotic system have many interesting features, and numerous applications. It has been used for the design of various systems including biological ones, such as the heartbeats [1] or the generation of action potentials by neurons, acoustic models, the radiation of mobile phones, and as a model of electrical systems. Chaos, chaos control and chaos synchronization of nonlinear systems, including the van der Pol system have been subject to extensive studies [2-10].

Fractional calculus is an old mathematical topic from 17th century. Although it has a long history, applications are only recently focus of interest. Many systems are known to display fractional order dynamics, such as viscoelastic systems [11], dielectric polarization, electrode–electrolyte polarization, and electromagnetic waves. Furthermore, some systems had been found with chaotic motions in the fractional orders. There is a new topic to investigate the control and dynamics of fractional order dynamical systems recently. The behavior of nonlinear chaotic systems when their models become fractional was also investigated widely and reported [12-22].

Chaos has been extensively studied within the scientific, engineering and mathematical communities as an interesting complex dynamic phenomenon [23-26]. Sensitive dependence on initial conditions is an important exhibit characteristic of chaotic systems. For this reason, chaotic systems are difficult to be synchronized or controlled. Research in the area of the synchronization of dynamical systems has been widely explored in a variety of fields including physical, chemical and ecological systems, secure communications and so on. There are many control methods to synchronize chaotic systems such as adaptive control, sliding mode control, observer-based design methods, impulsive control and other control methods. There are more advantages in synchronization of uncoupled chaotic systems than that of coupled chaotic systems. And a new uncoupled method of synchronization is presented in this thesis. Chaos excited chaos synchronizations of generalized van der Pol systems with integral and fractional order are studied. Synchronizations of two identified autonomous generalized van der Pol chaotic systems are obtained by replacing their corresponding exciting terms by the same function of chaotic states of a third nonautonomous or autonomous. Numerical simulations, such as phase portraits, Poincaré maps and state error plots are given. It is found that chaos excited chaos synchronizations exist for the fractional order systems with the total

fractional order both less than and more than the number of the states of the integer order generalized van der Pol system.

Recently, the traditional trend of understanding and analyzing chaos has evolved to a new phase of investigation: controlling and utilizing chaos. Sometimes, chaos is not only useful but actually important, such as the generation of random numbers in chaotic secure communications system. For this purpose, making a non-chaotic dynamical system chaotic is called ‘‘anticontrol of chaos ’’. Anticontrol of chaos has received great attention in recent years[27-39]. Anticontrol of chaos for integral and fractional order generalized nonautonomous van der Pol system is obtained effectively by adding a constant term. By numerical analyses, such as phase portraits, Poincaré maps and bifurcation diagrams, periodic, and chaotic motions are observed. It is found that the periodic motions of the system are transformed to chaotic motions effectively by the proposed anticontrol scheme.

This thesis is organized as follows. In Chapter 2, a review and the approximation of the fractional order operator is presented. Chaos of the generalized van der Pol system and the nonautonomous and autonomous fractional order generalized van der Pol systems are given. Numerical simulations, such as phase portraits, Poincaré maps and bifurcation diagrams, of various nonautonomous and autonomous fractional order generalized van der Pol systems are presented.

In Chapter 3, the schemes of chaos excited chaos synchronization of two generalized van der Pol systems by replacing the amplitude or the sine time function of their corresponding exciting terms by the same function of chaotic states of a third nonautonomous or autonomous generalized van der Pol system are given. Numerical simulations, such as phase portraits, Poincaré maps error states plots, of synchronizations of various fractional order generalized van der Pol systems are presented.

In Chapter 4, the scheme of anticontrol of chaos by adding a constant term is presented. Numerical simulations, such as phase portraits, Poincaré maps and bifurcation diagrams of anticontrol of chaos for generalized nonautonomous van der Pol system are presented.

In Chapter 5, conclusions are drawn.

Chapter 2

Chaos in a Generalized Heartbeat System and in Its Fractional Order System

2.1. Preliminaries

In this chapter, chaos of a generalized van der Pol system with fractional orders is studied. Chaos in the nonautonomous generalized van der Pol system excited by a sinusoidal time function with fractional orders is studied. Next, chaos in the autonomous generalized van der Pol system with fractional orders is considered.

2.2. The Review and the Approximation of Fractional-Order Operators

There are many ways to define a fractional differential operator [18-20]. The commonly used definition for general fractional derivative is the Riemann-Liouville definition. The Riemann-Liouville definition of the fractional-order derivative is:

$$\begin{aligned} D^{\alpha} y(t) &= \frac{d^n}{dt^n} D^{\alpha-n} y(t) \\ &= \frac{1}{\Gamma(n-\alpha)} \frac{d^n}{dt^n} \int_0^t \frac{y(\tau)}{(t-\tau)^{\alpha-n+1}} d\tau \end{aligned} \tag{2.1}$$

where $\Gamma(\cdot)$ is a gamma function and n is an integer such that $n-1 \le \alpha < n$. This definition is different from the usual intuitive definition of derivative.

Thus, it is necessary to develop approximations to the fractional operators using the standard integer order operators. Fortunately, the Laplace transform which is basic engineering tool for analyzing linear systems is still applicable and works:

$$L\left\{\frac{d^{\alpha} f(t)}{dt^{\alpha}}\right\} = s^{\alpha} L\{f(t)\} - \sum_{k=0}^{n-1} s^k \left[\frac{d^{\alpha-1-k} f(t)}{dt^{\alpha-1-k}}\right]_{t=0}, \text{ for all } \alpha, \tag{2.2}$$

where n is an integer such that $n-1 \le \alpha < n$. Upon considering the initial conditions to be zero, this formula reduces to the more expected form

$$L\left\{\frac{d^{\alpha} f(t)}{dt^{\alpha}}\right\} = s^{\alpha} L\{f(t)\}. \tag{2.3}$$

Using the algorithm in [13, 21], linear transfer function of approximations of the fractional integrator is adopted. Basically the idea is to approximate the system behavior based on

frequency domain arguments. From [22], we get the table of approximating transfer functions for $1/s^{\alpha}$ with different fractional orders, $\alpha = 0.1-0.9$, in steps of 0.1, which give the maximum error 2 dB in calculations (see appendix). These approximations will be used in the following study.

2.3. The Chaos of the Generalized Heartbeat System and Its Fractional Order Form

The van der Pol system [2] was first given to study the oscillations in vacuum tube circuits. The equivalent state space formulation has the form of an autonomous system:

$$\begin{aligned} \frac{dx_1}{dt} &= x_2 \\ \frac{dx_2}{dt} &= -x_1 - \varepsilon(x_1^{\,2} - 1)x_2 \end{aligned} \tag{2.4}$$

where ε is a parameter. The generalized van der Pol system [7-10] has the form of a nonautonomous system which is written as:

$$\begin{aligned} \frac{dx_1}{dt} &= x_2 \\ \frac{dx_2}{dt} &= -x_1 - \varepsilon(1 - x_1^{\,2})(c - ax_1^{\,2})x_2 + b\sin\omega t \end{aligned} \tag{2.5}$$

where ε, a, b, c are parameters, and ω is the circular frequency of the external excitation $b\sin\omega t$. Fig. 2.1 and Fig. 2.2 shows the bifurcation diagram and Lyapunov exponent diagram for the nonautonomous generalized van der Pol system (2.5), and Fig. 2.3~ Fig. 2.6 are the phase portraits and Poincaré maps, while Poincaré maps are taken by period $\frac{2\pi}{\omega}$. The corresponding nonautonomous fractional order system is

$$\begin{aligned} \frac{d^{\alpha}x_1}{dt^{\alpha}} &= x_2 \\ \frac{d^{\beta}x_2}{dt^{\beta}} &= -x_1 - \varepsilon(1 - x_1^{\,2})(c - ax_1^{\,2})x_2 + b\sin\omega t \end{aligned} \tag{2.6}$$

where α, β are fractional numbers.

A modified version of Eq.(2.6) is now proposed. The nonautonomous generalized fractional order van der Pol system (2.6) with two states is transformed into an autonomous generalized fractional order van der Pol system with three states:

$$\frac{d^{\alpha}x_1}{dt^{\alpha}} = x_2$$
$$\frac{d^{\beta}x_2}{dt^{\beta}} = -x_1 - \varepsilon(1-x_1^{\,2})(c-ax_1^{\,2})x_2 + b\sin\omega x_3 \qquad (2.7)$$
$$\frac{d^{\gamma}x_3}{dt^{\gamma}} = 1$$

where α, β, γ are fractional numbers, in which the original time t in Eq.(2.6) is changed to a new state x_3. When $\gamma = 1$, $x_3 = t$, Eq.(2.7) reduces to Eq.(2.6).

In this thesis, we analyze and present simulation results of the chaotic dynamics produced from a new generalized fractional van der Pol system as the fractional order derivatives in the state equations of Eq.(2.6) is varied from 0.1 to 1.3. It is observed that the different orders have large influences upon the overall system dynamics.

2.4. Numerical Simulations for the Fractional Order Generalized Heartbeat Systems

Our study of system (2.7) consists of three parts:

Part 1: γ equals one, and α, β take the same fractional numbers. The system is equivalent to a nonautonomous fractional order system with two states, Eq. (2.6).

Part 2: α, β, γ take the same fractional numbers.

Part 3: γ equals 1.1 or 0.9, and α, β take the same fractional numbers.

In Part 1, γ=1, Eq.(2.7) reduces to Eq.(2.6) with two states x_1 and x_2. α, β take the same fractional numbers and vary from 1.1 to 0.7 in steps of 0.1. Fig. 2.7 shows the bifurcation diagram and Fig. 2.8~ Fig. 2.11 are the phase portraits and Poincaré maps with $\alpha = \beta = 1.1$, while Poincaré maps are taken by period $\frac{2\pi}{\omega}$. Fig. 2.12 shows the bifurcation diagram and Fig. 2.13~ Fig. 2.16 are the phase portraits and Poincaré maps with $\alpha = \beta = 0.9$. Fig. 2.17 shows the bifurcation diagram and Fig. 2.18~ Fig. 2.21 are the phase portraits and Poincaré maps with $\alpha = \beta = 0.8$. Fig. 2.22 shows the bifurcation diagram and Fig. 2.23~ Fig. 2.26 are the phase

portraits and Poincaré maps with $\alpha = \beta = 0.7$. According to the results of simulation in Part 1, it is found that the chaotic motions exist in the nonautonomous system with fractional orders. The lowest total fractional order for chaos existence in this system is 1.4 (2×0.7). When the total fractional order is 1.2 (2×0.6), no chaos exists.

In Part 2, α, β, γ take the same fractional numbers, vary from 1.1 to 0.6 in steps of 0.1. Fig. 2.27 shows the bifurcation diagram and Fig. 2.28~ Fig. 2.31 are the phase portraits and Poincaré maps with $\alpha = \beta = \gamma = 1.1$. When $\alpha = \beta = \gamma$ and vary from 0.9 to 0.6 in steps of 0.1, no chaos exists.

In Part 3, $\gamma = 1.1$, α, β take same fractional numbers and vary from 1.1 to 0.3 in steps of 0.1. Fig. 2.32 shows the bifurcation diagram and Fig. 2.33~ Fig. 2.34 are the phase portraits and Poincaré maps with $\alpha = \beta = 0.9$, γ=1.1. Fig. 2.35 shows the bifurcation diagram and Fig. 2.36~ Fig. 2.37 are the phase portraits and Poincaré maps with $\alpha = \beta = 0.8$, γ=1.1. Fig. 2.38 shows the bifurcation diagram and Fig. 2.39~ Fig. 2.41 are the phase portraits and Poincaré maps with $\alpha = \beta = 0.7$, γ=1.1. Fig. 2.42 shows the bifurcation diagram and Fig. 2.43~ Fig. 2.45 are the phase portraits and Poincaré maps with $\alpha = \beta = 0.6$, γ=1.1. Fig. 2.46 shows the bifurcation diagram and Fig. 2.47~ Fig. 2.50 are the phase portraits and Poincaré maps with $\alpha = \beta = 0.5$, γ=1.1. Fig. 2.51 shows the bifurcation diagram and Fig. 2.52~ Fig. 2.55 are the phase portraits and Poincaré maps with $\alpha = \beta = 0.4$, γ=1.1. Fig. 2.56 shows the bifurcation diagram and Fig. 2.57~ Fig. 2.60 are the phase portraits and Poincaré maps with $\alpha = \beta = 0.3$, γ=1.1. According to the results of simulation in Part 3, it is found that the chaotic motions exist when γ take 1.1 and α, β vary from 0.9 to 0.3 in steps of 0.1. When α, β take the fractional number less than 0.3, no chaos is found.

$\gamma = 0.9$, α, β take the same fractional numbers 1.1, 1.2, 1.3 and 1.4, only periodic motions are found, no chaos exists.

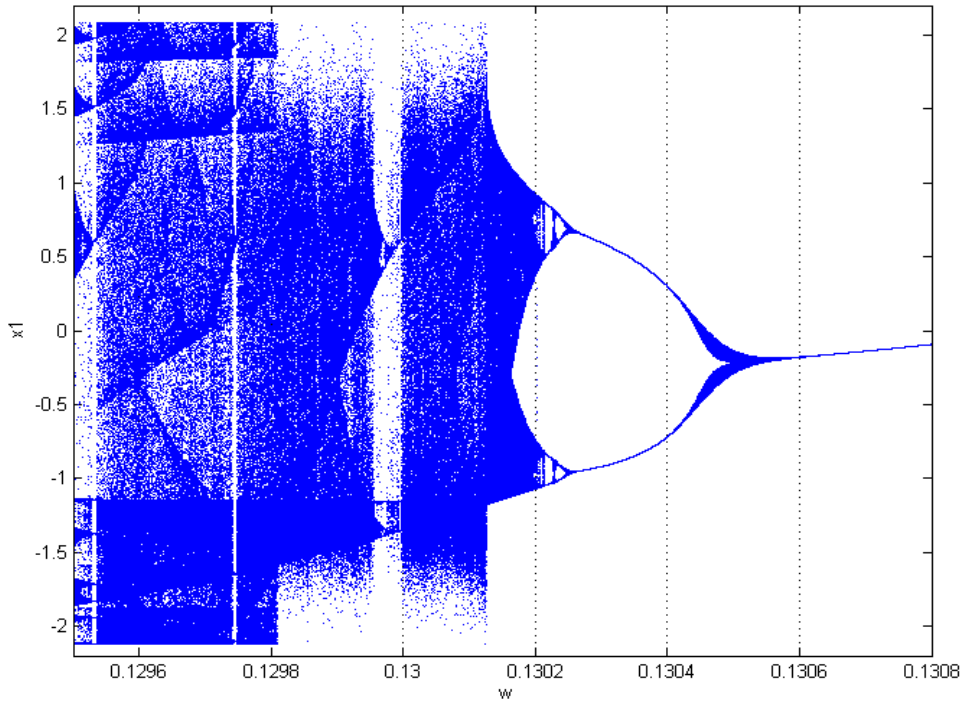

Fig.2.1 The bifurcation diagram of the nonautonomous generalized van der Pol system.

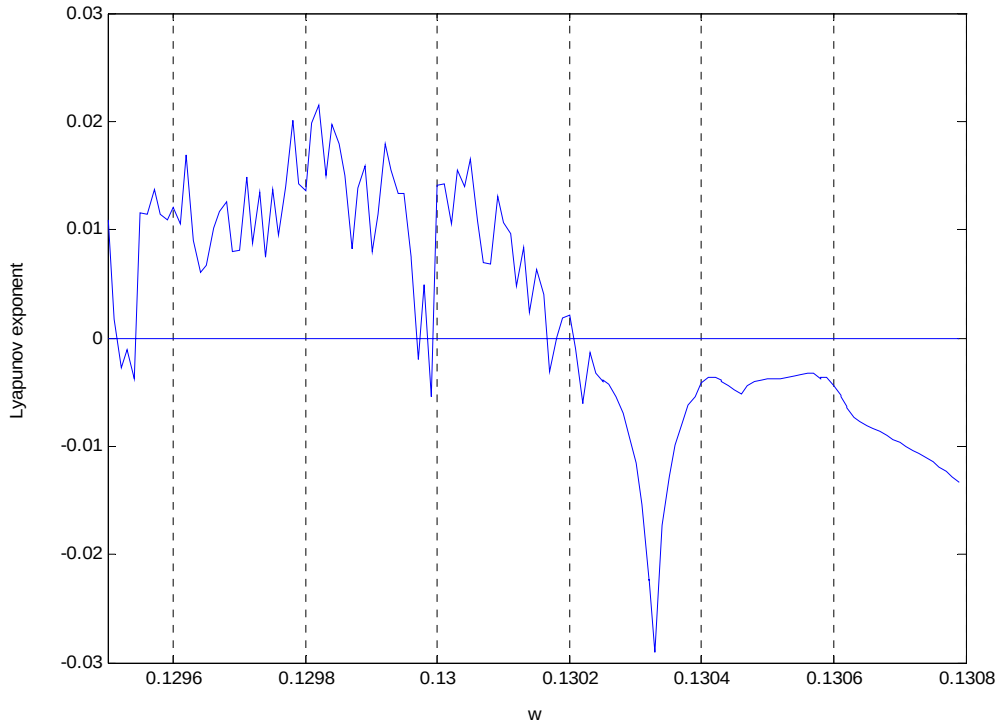

Fig. 2.2 Lyapunov exponent diagram of the nonautonomous generalized van der Pol system for ω between 0.1295 and 0.1308

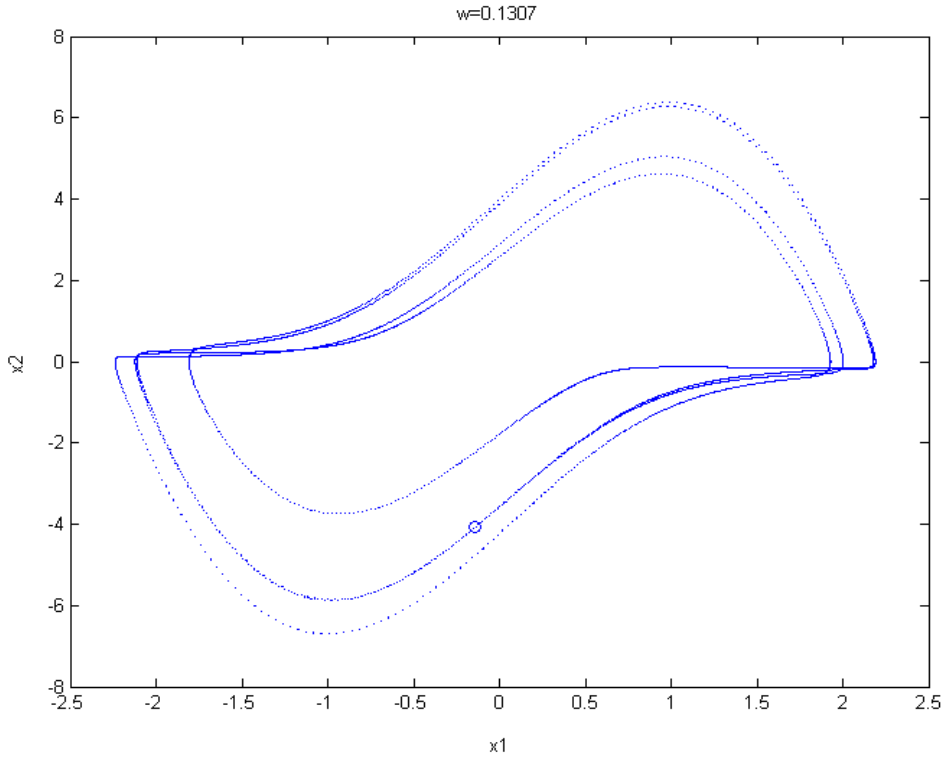

Fig. 2.3 The phase portrait and the Poincaré map of the nonautonomous generalized van der Pol system.

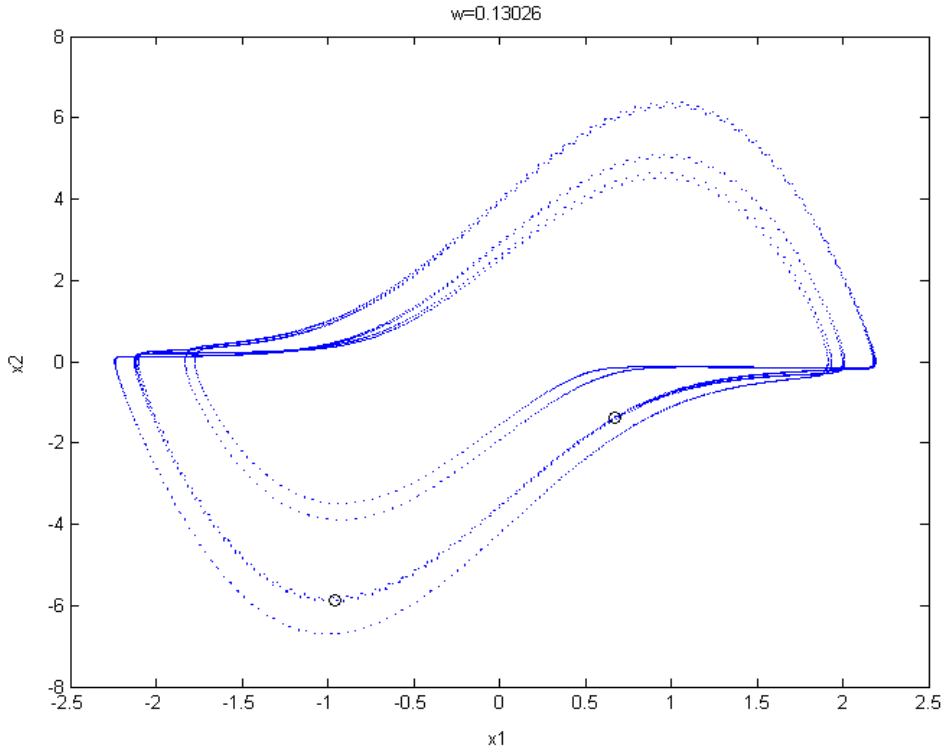

Fig. 2.4 The phase portrait and the Poincaré map of the nonautonomous generalized van der Pol system.

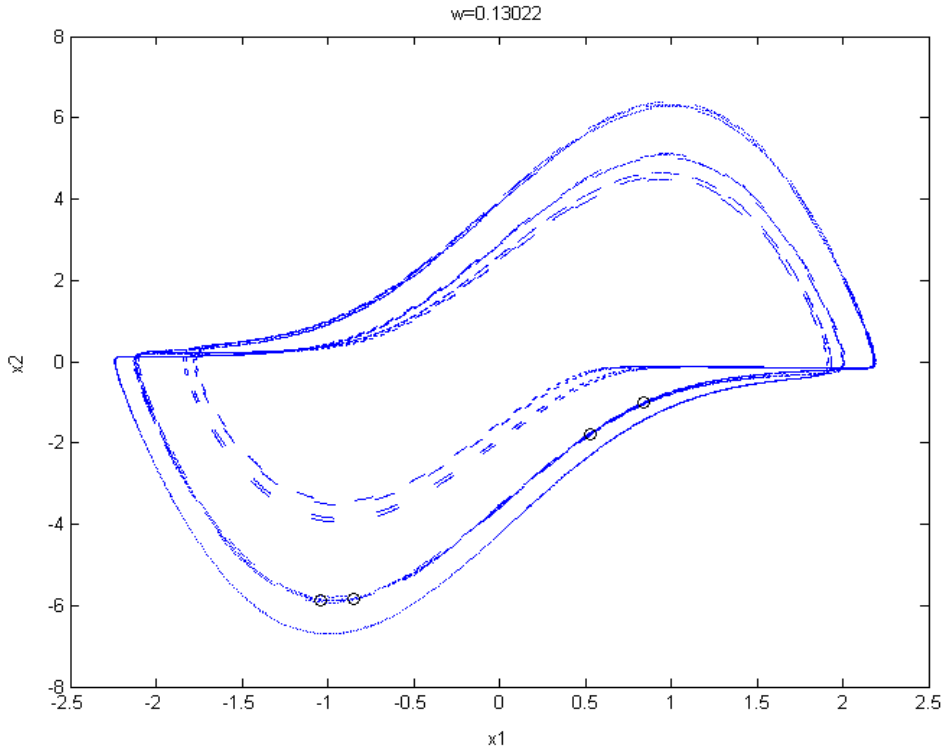

Fig. 2.5 The phase portrait and the Poincaré map of the nonautonomous generalized van der Pol system.

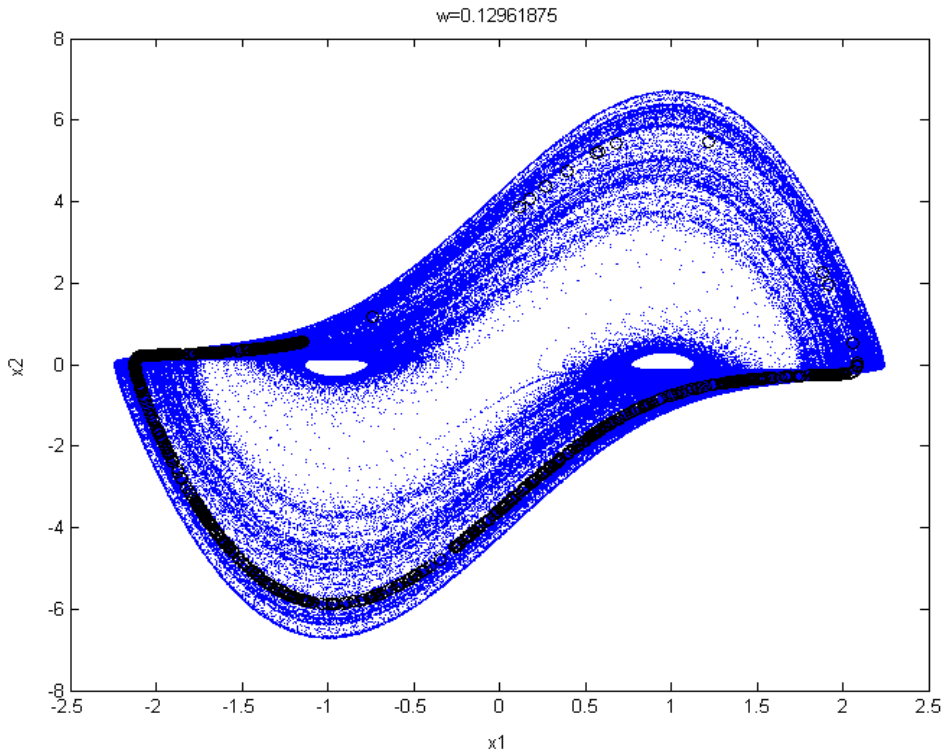

Fig. 2.6 The phase portrait and the Poincaré map of the nonautonomous generalized van der Pol system.

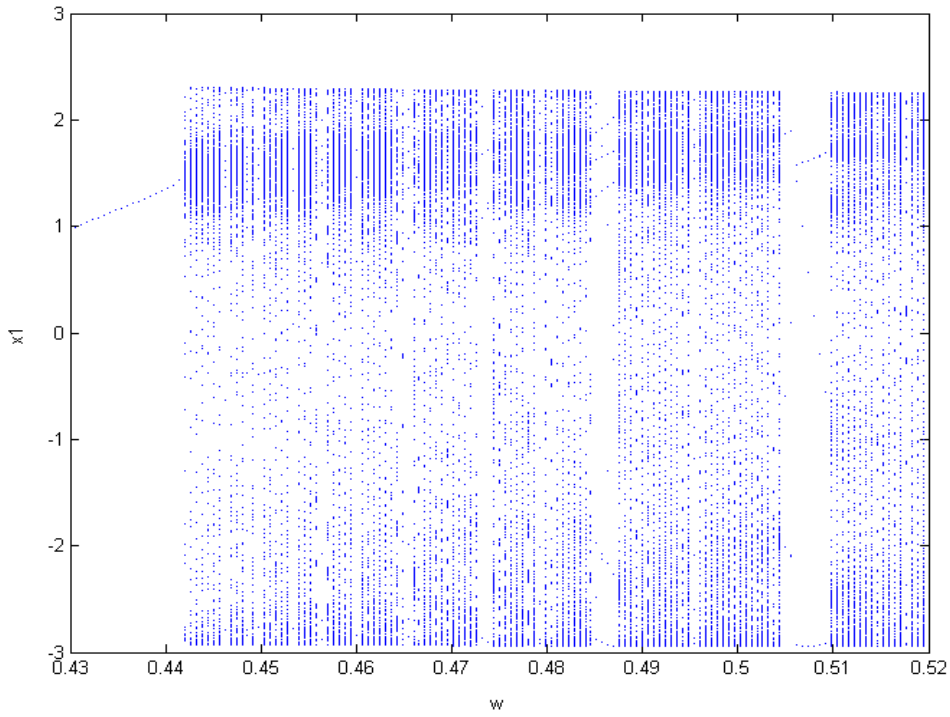

Fig. 2.7 The bifurcation diagram of the nonautonomous fractional order system with order $\alpha = \beta = 1.1$, $\gamma = 1$

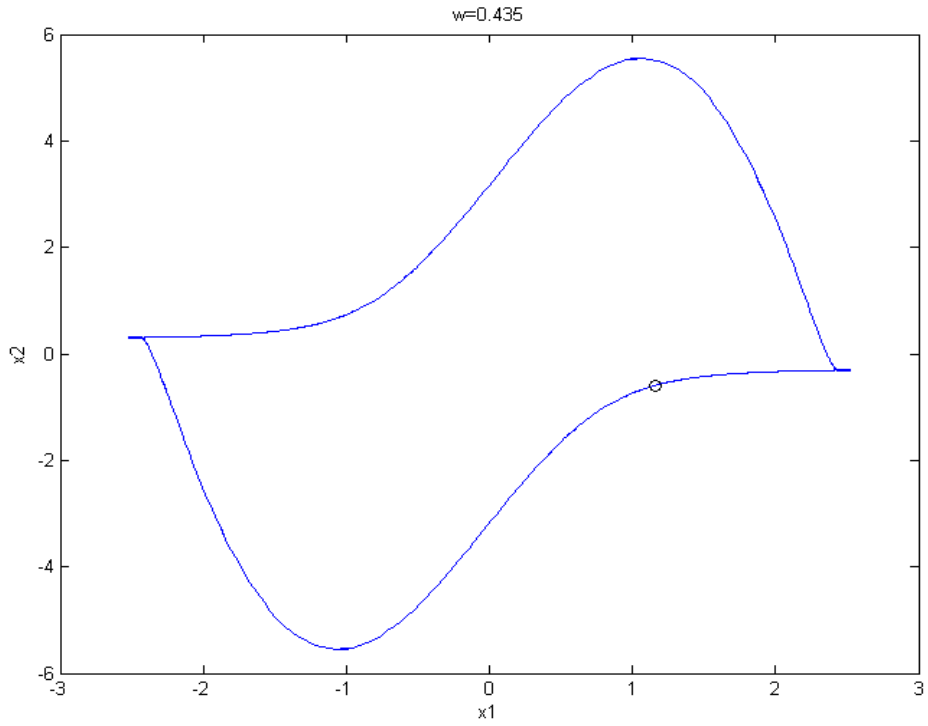

Fig. 2.8 The phase portrait and Poincaré map of the nonautonomous fractional order system with order $\alpha = \beta = 1.1$, $\gamma = 1, \omega = 0.435$.

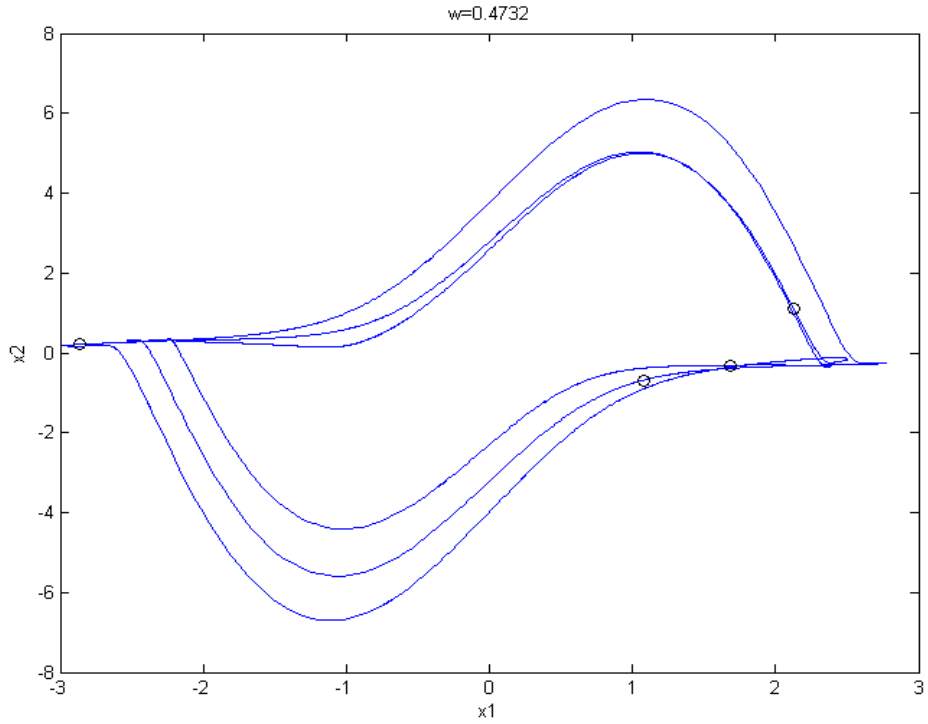

Fig. 2.9 The phase portrait and Poincaré maps of the nonautonomous fractional order system with order $\alpha = \beta = 1.1$, $\gamma = 1, \omega = 0.4732$.

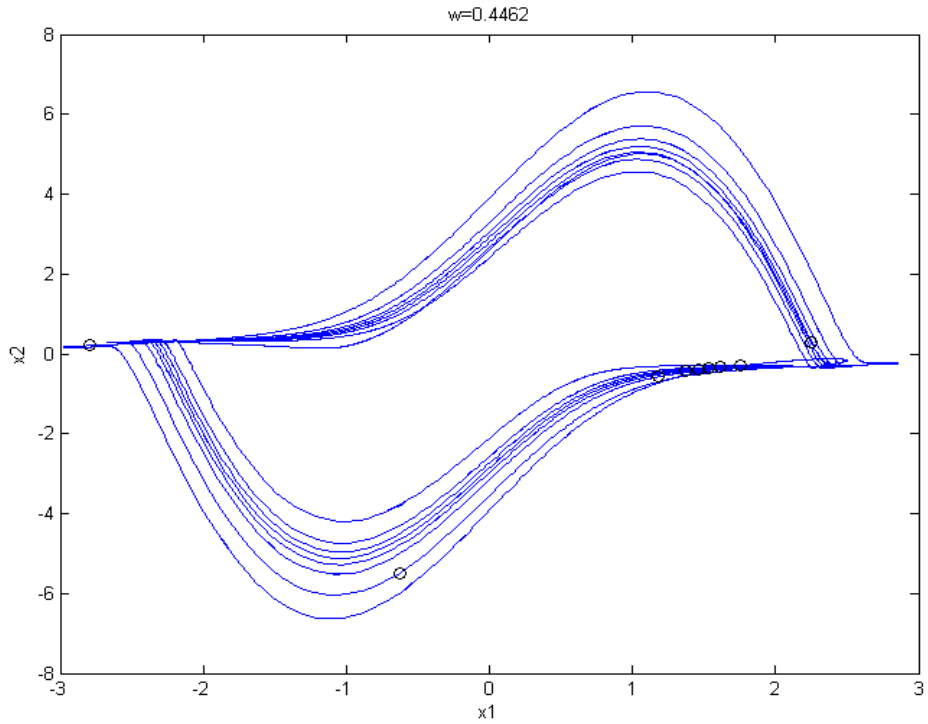

Fig. 2.10 The phase portrait and Poincaré maps of the nonautonomous fractional order system with order $\alpha = \beta = 1.1$, $\gamma = 1, \omega = 0.4462$.

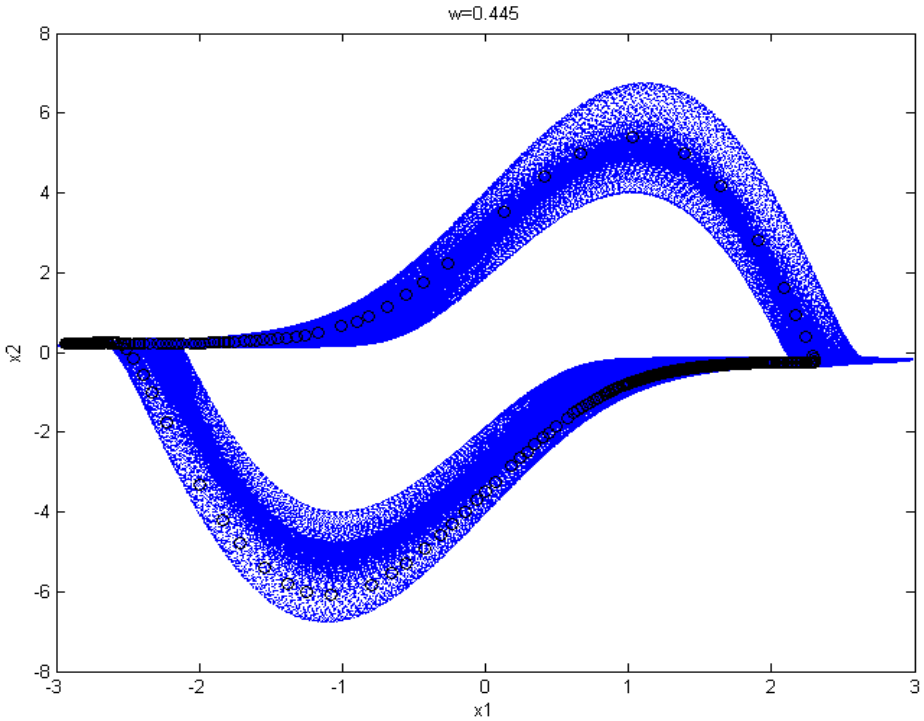

Fig. 2.11 The phase portrait and Poincaré maps of the nonautonomous fractional order system with order $\alpha = \beta = 1.1$, $\gamma = 1, \omega = 0.445$.

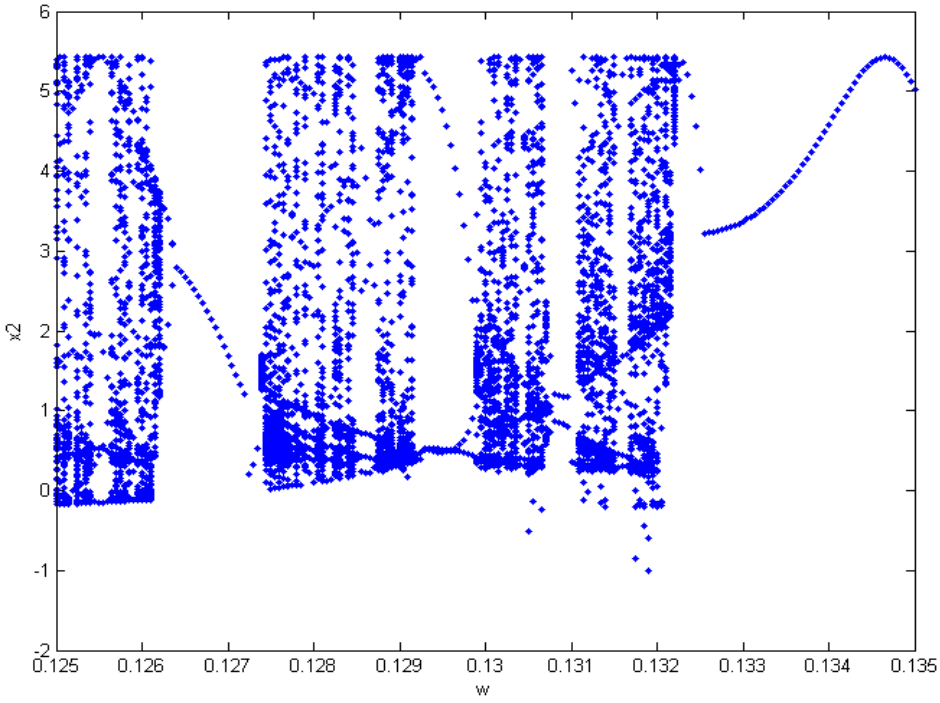

Fig. 2.12 The bifurcation diagram of the nonautonomous fractional order system with order $\alpha = \beta = 0.9$, $\gamma = 1$.

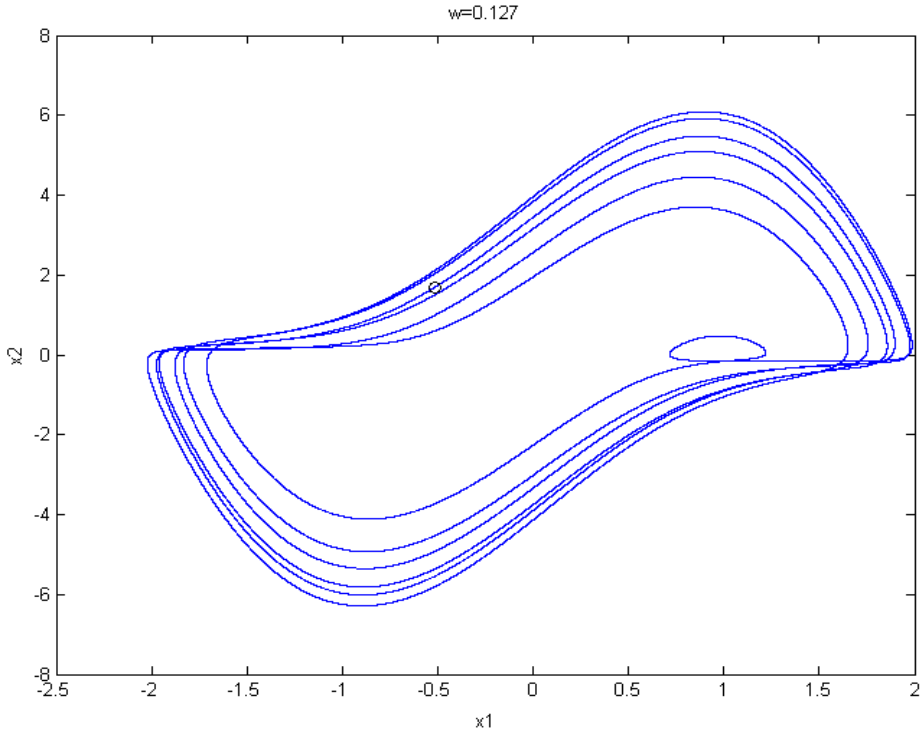

Fig. 2.13 The phase portrait and Poincaré map of the nonautonomous fractional order system with order $\alpha = \beta = 0.9$, $\gamma = 1, \omega = 0.127$.

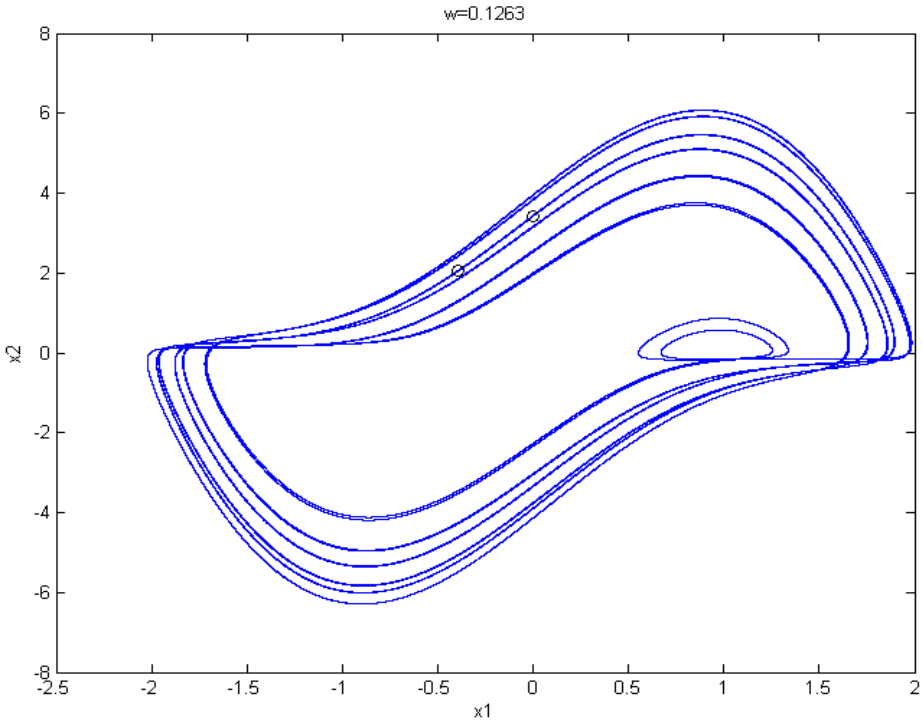

Fig. 2.14 The phase portrait and Poincaré maps of the nonautonomous fractional order system with order $\alpha = \beta = 0.9$, $\gamma = 1, \omega = 0.1263$.

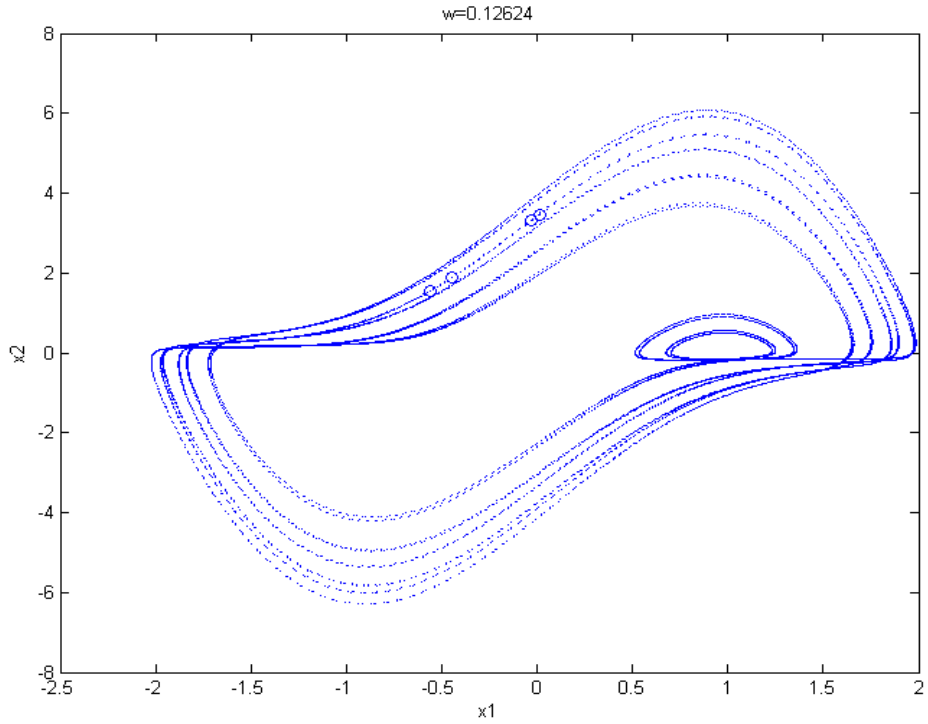

Fig. 2.15 The phase portrait and Poincaré maps of the nonautonomous fractional order system with order $\alpha = \beta = 0.9$, $\gamma = 1, \omega = 0.12624$.

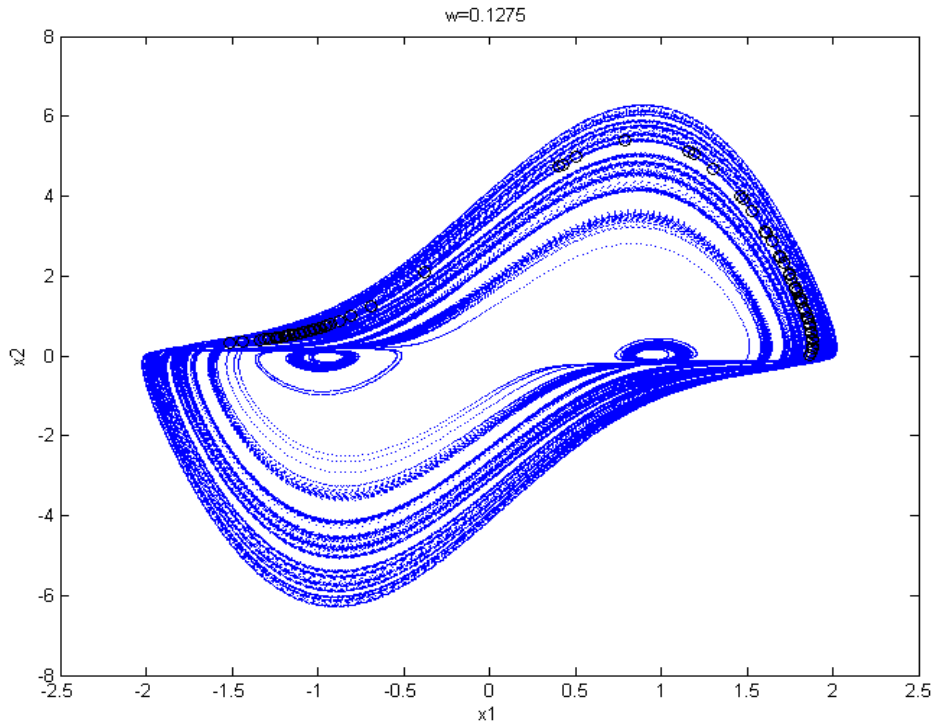

Fig. 2.16 The phase portrait and Poincaré maps of the nonautonomous fractional order system with order $\alpha = \beta = 0.9$, $\gamma = 1, \omega = 0.1275$.

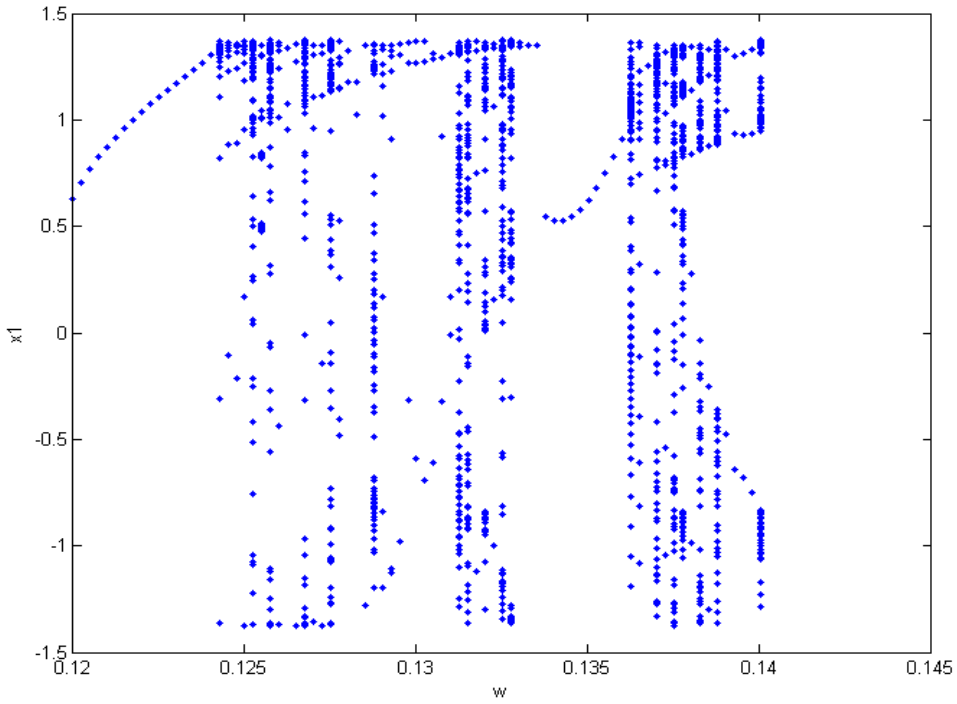

Fig. 2.17 The bifurcation diagram of the nonautonomous fractional order system with order $\alpha = \beta = 0.8$, $\gamma = 1$.

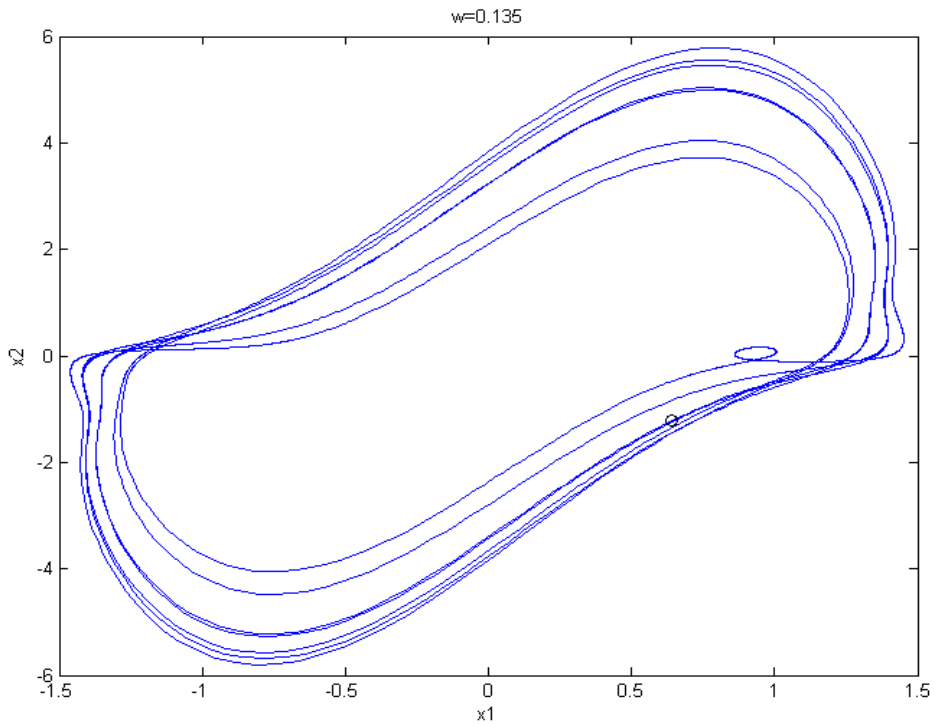

Fig. 2.18 The phase portrait and Poincaré map of the nonautonomous fractional order system with order $\alpha = \beta = 0.8$, $\gamma = 1, \omega = 0.135$.

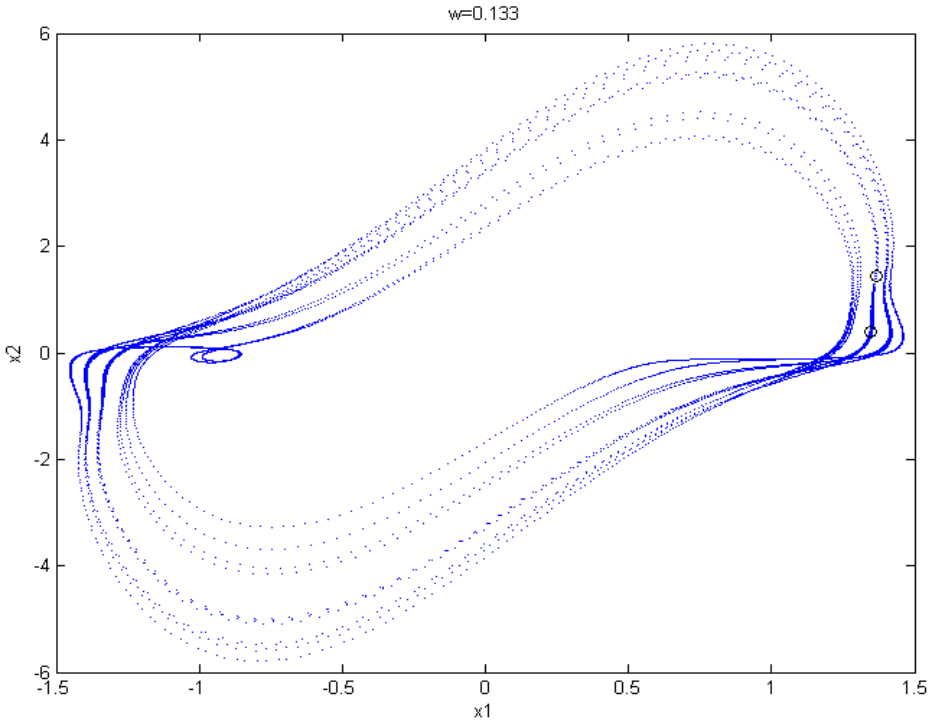

Fig. 2.19 The phase portrait and Poincaré maps of the nonautonomous fractional order systemwith order $\alpha = \beta = 0.8$, $\gamma = 1, \omega = 0.133$.

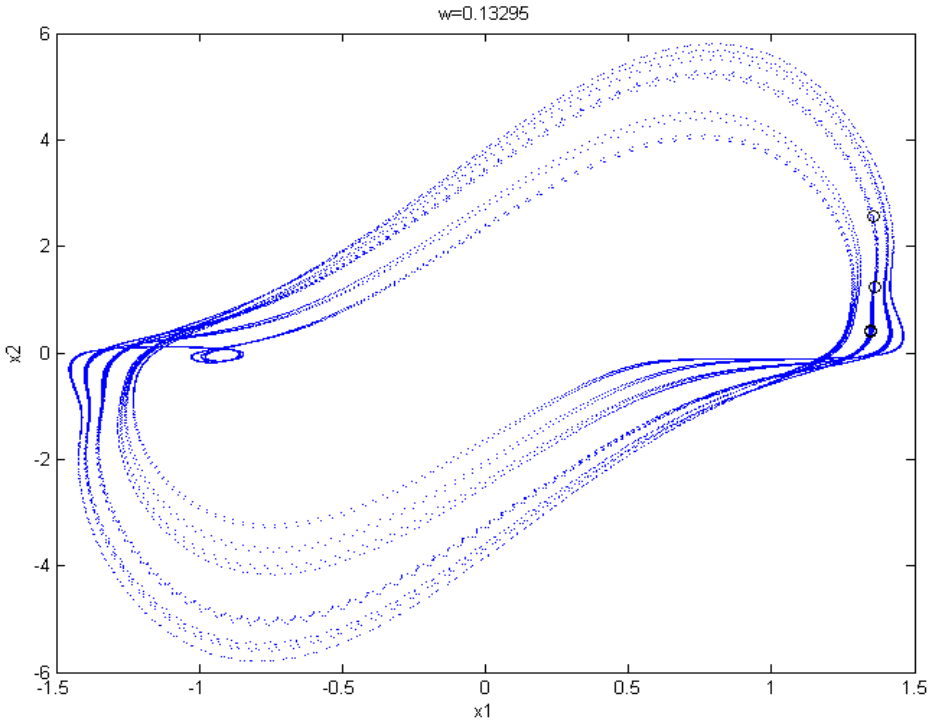

Fig. 2.20 The phase portrait and Poincaré maps of the nonautonomous fractional order systemwith order $\alpha = \beta = 0.8$, $\gamma = 1, \omega = 0.13295$.

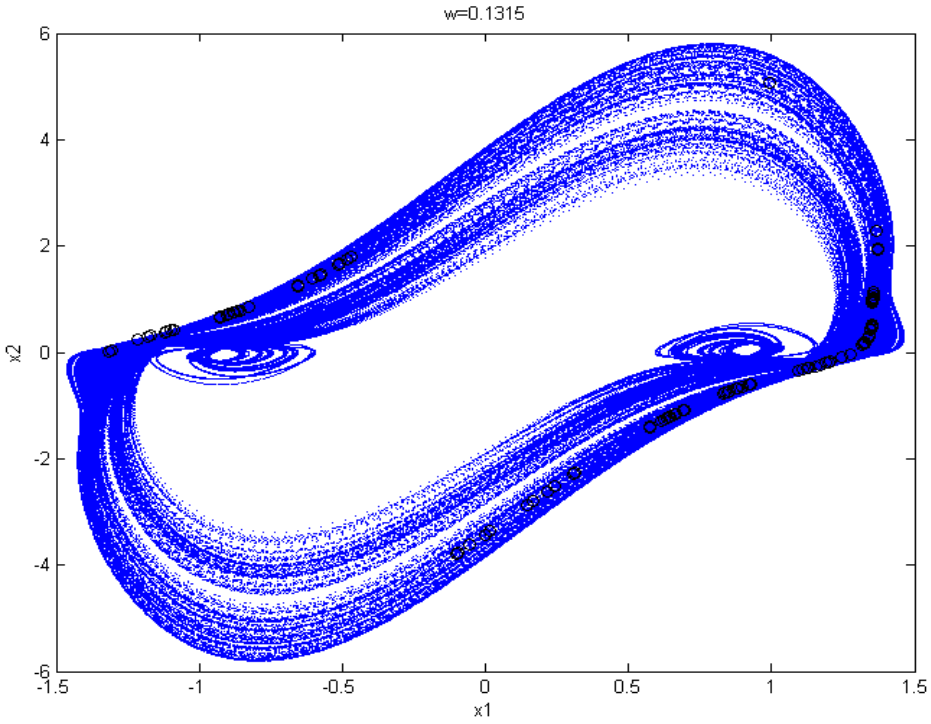

Fig. 2.21 The phase portrait and Poincaré maps of the nonautonomous fractional order system with order $\alpha = \beta = 0.8$, $\gamma = 1, \omega = 0.1315$.

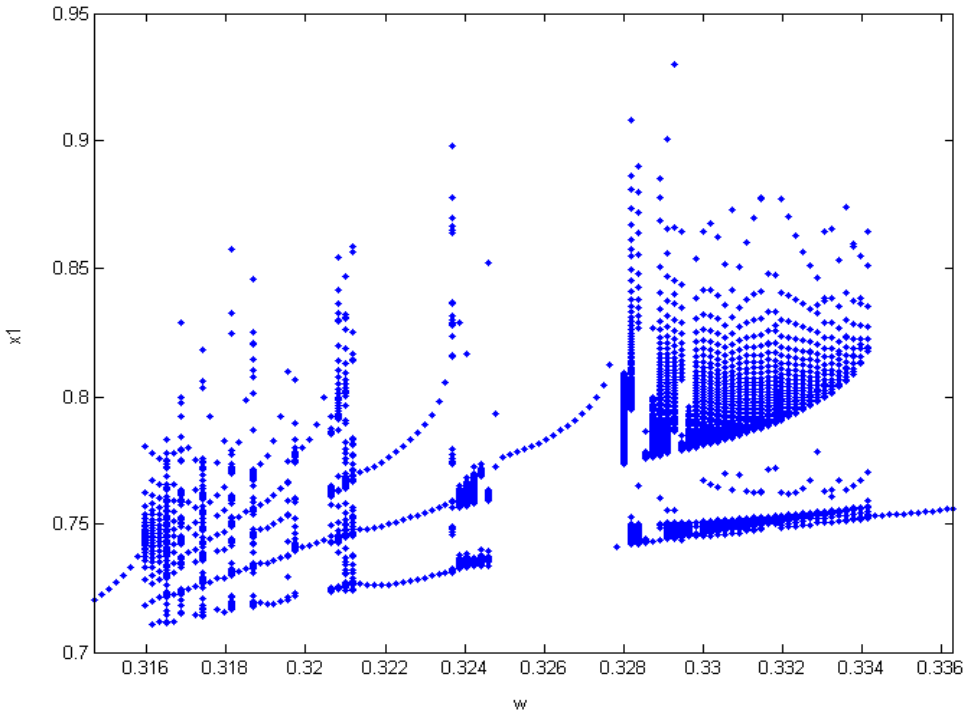

Fig. 2.22 The bifurcation diagram of the nonautonomous fractional order system with order $\alpha = \beta = 0.7$, $\gamma = 1$

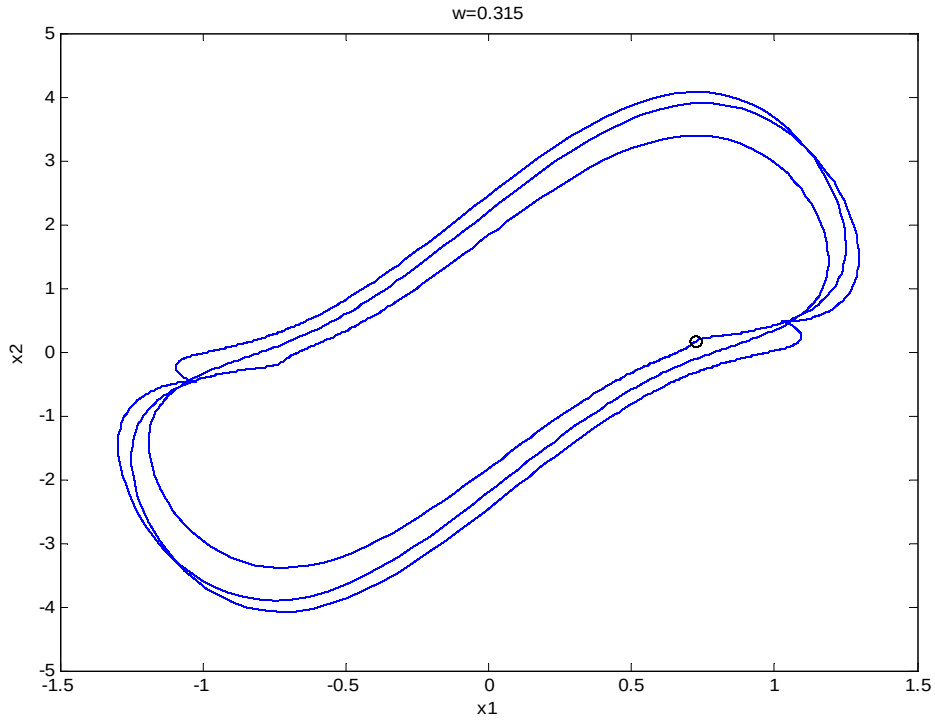

Fig. 2.23 The phase portrait and Poincaré map of the nonautonomous fractional order system with order $\alpha = \beta = 0.7$, $\gamma = 1, \omega = 0.315$.

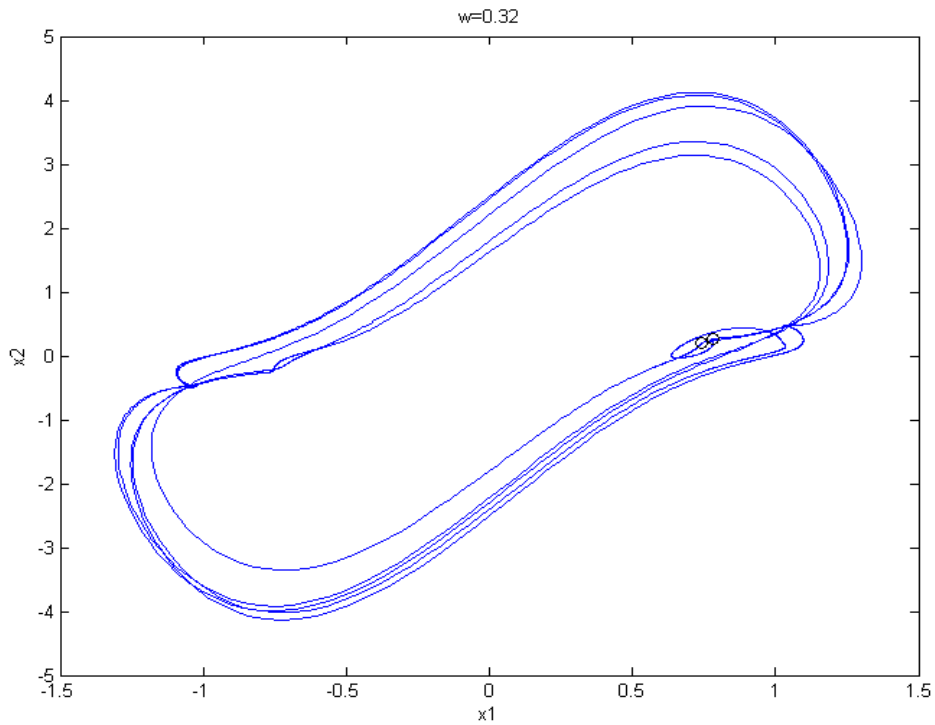

Fig. 2.24 The phase portrait and Poincaré maps of the nonautonomous fractional order system with order $\alpha = \beta = 0.7$, $\gamma = 1, \omega = 0.32$.

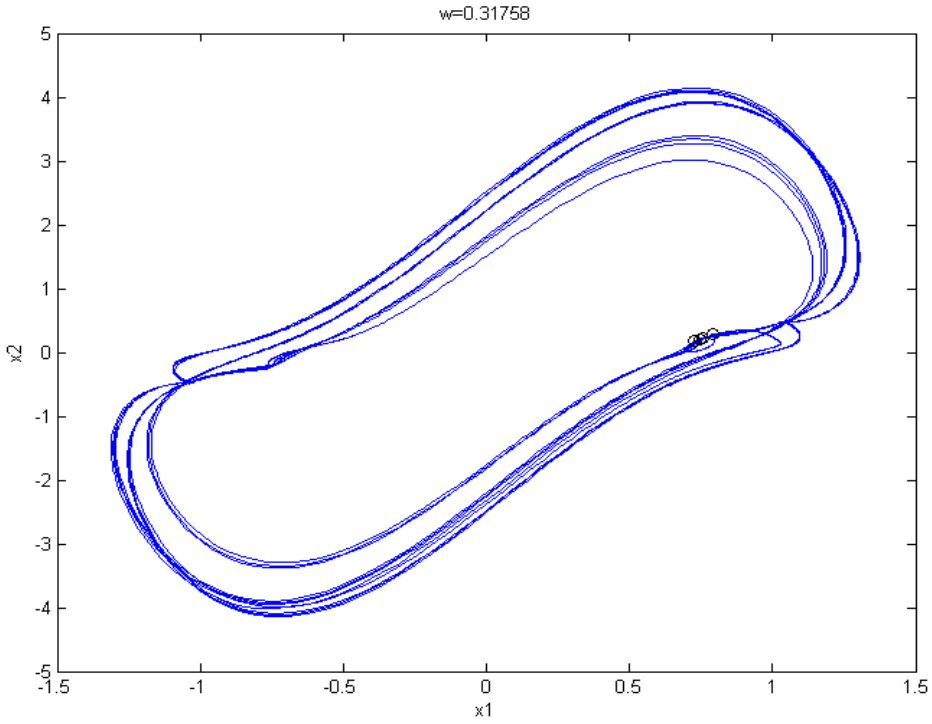

Fig. 2.25 The phase portrait and Poincaré maps of the nonautonomous fractional order system with order $\alpha = \beta = 0.7$, $\gamma = 1, \omega = 0.31758$.

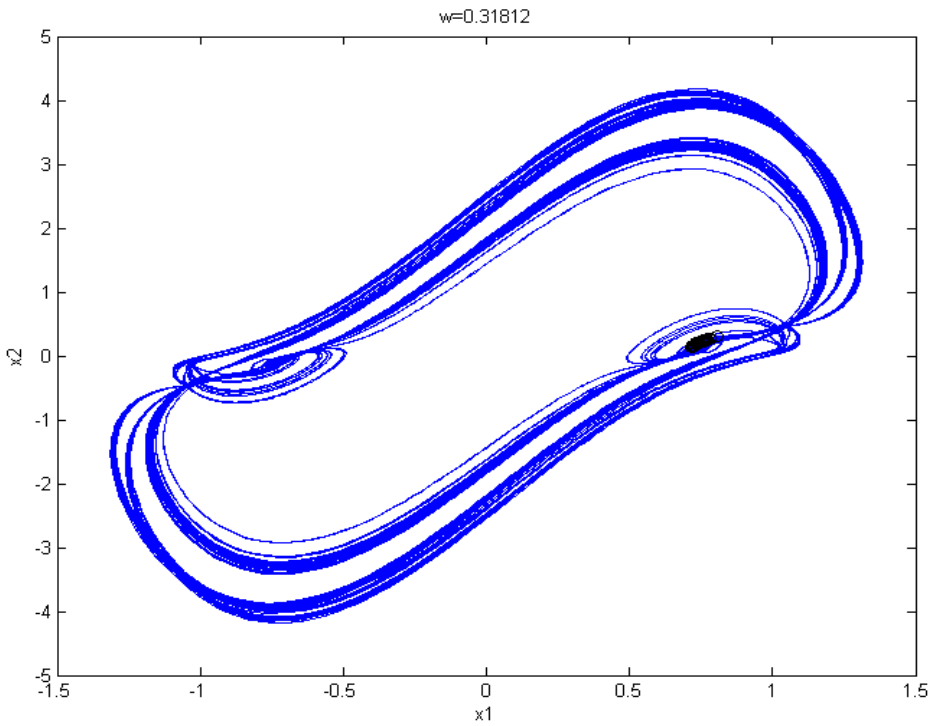

Fig. 2.26 The phase portrait and Poincaré maps of the nonautonomous fractional order system with order $\alpha = \beta = 0.7$, $\gamma = 1, \omega = 0.31812$.

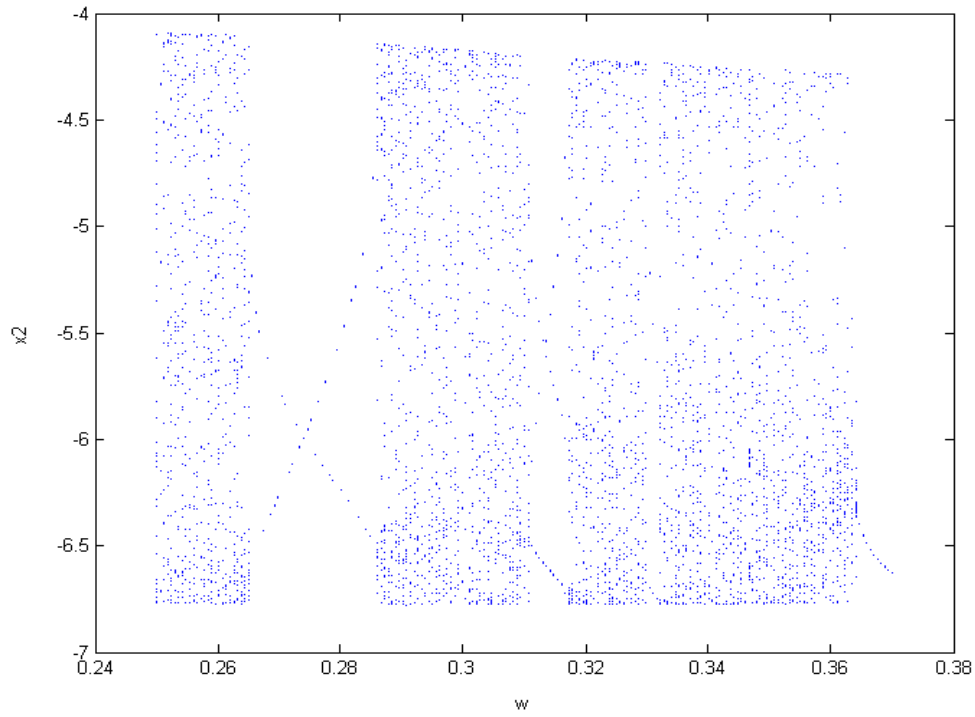

Fig. 2.27 The bifurcation diagram of the autonomous fractional order system with order $\alpha = \beta = \gamma = 1.1$

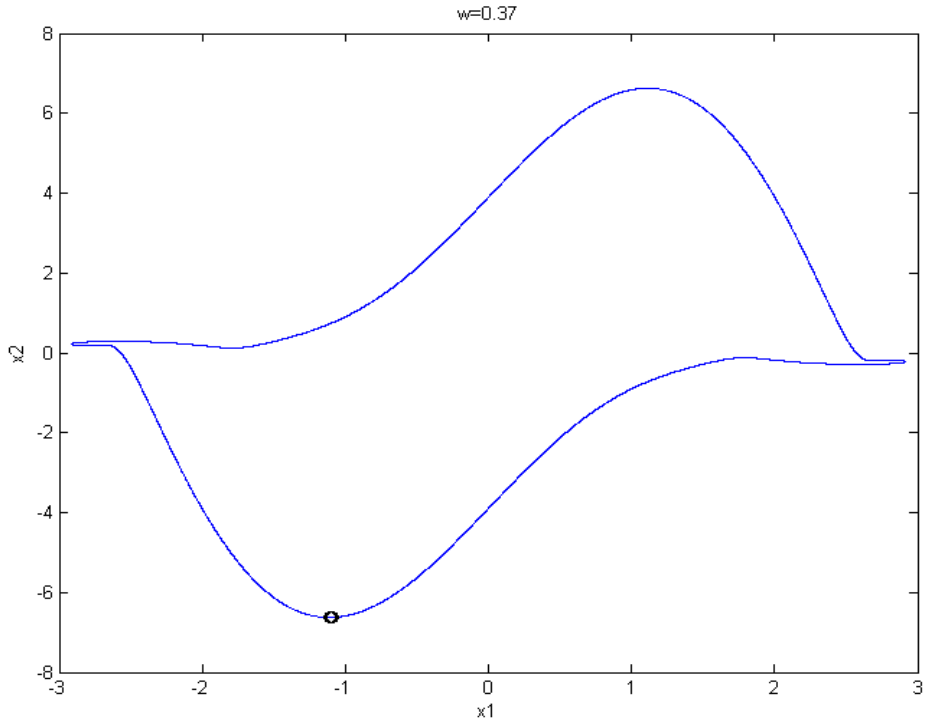

Fig. 2.28 The phase portrait and Poincaré map of the autonomous fractional order system with order $\alpha = \beta = \gamma = 1.1, \omega = 0.37$.

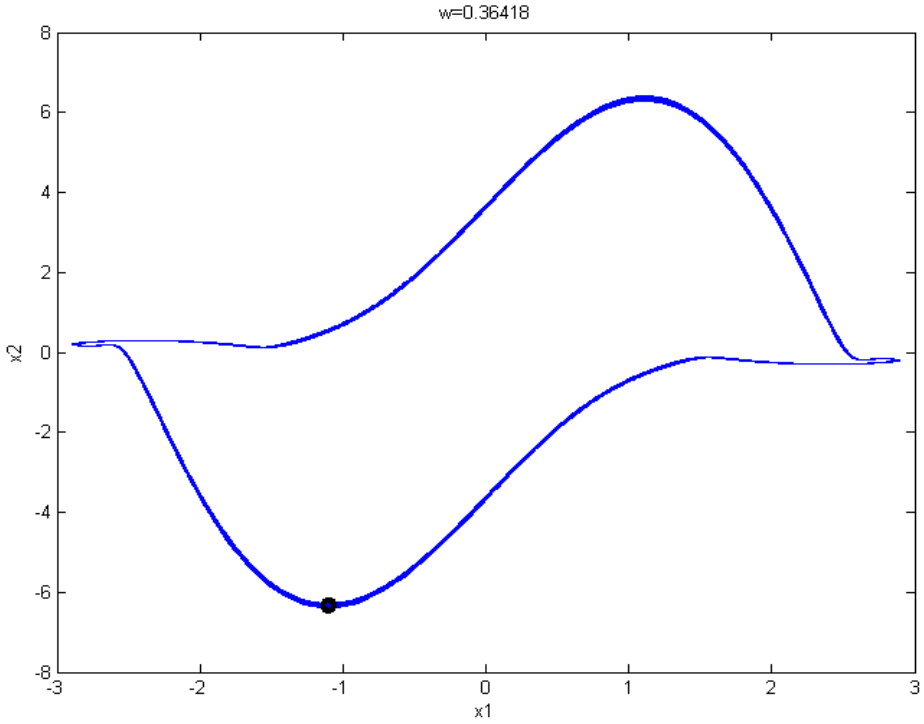

Fig. 2.29 The phase portrait and Poincaré maps of the autonomous fractional order system with order $\alpha = \beta = \gamma = 1.1, \omega = 0.36418$.

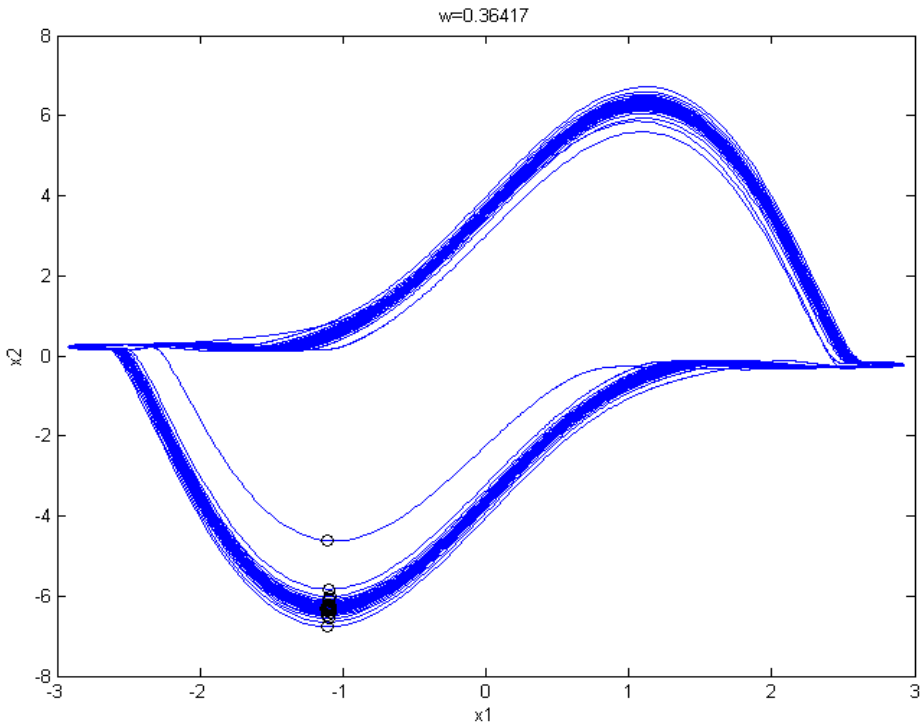

Fig. 2.30 The phase portrait and Poincaré maps of the autonomous fractional order system with order $\alpha = \beta = \gamma = 1.1, \omega = 0.36417$.

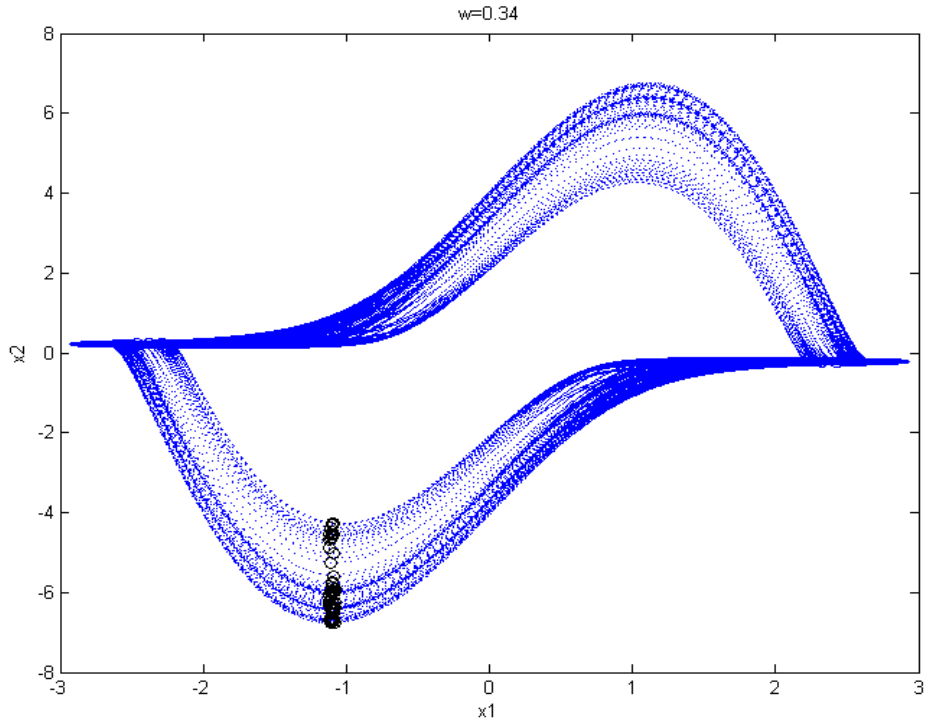

Fig. 2.31 The phase portrait and Poincaré maps of the autonomous fractional order system with order $\alpha = \beta = \gamma = 1.1, \omega = 0.34$.

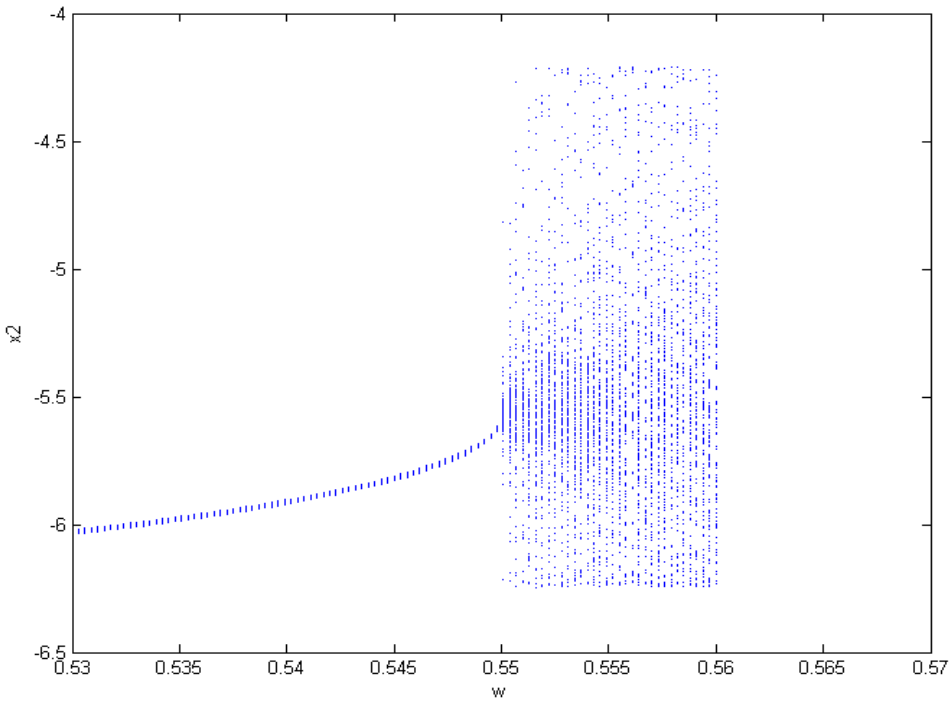

Fig. 2.32 The bifurcation diagram of the autonomous fractional order system with order $\alpha = \beta = 0.9$, $\gamma = 1.1$

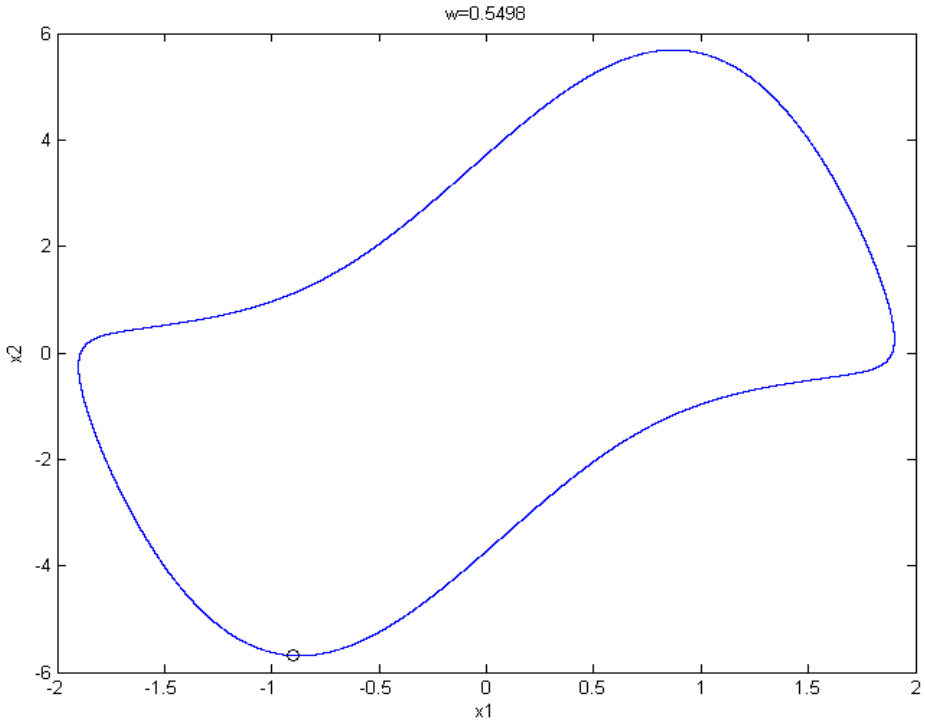

Fig. 2.33 The phase portrait and Poincaré map of the autonomous fractional order system with order $\alpha = \beta = 0.9$, $\gamma = 1.1, \omega = 0.5498$.

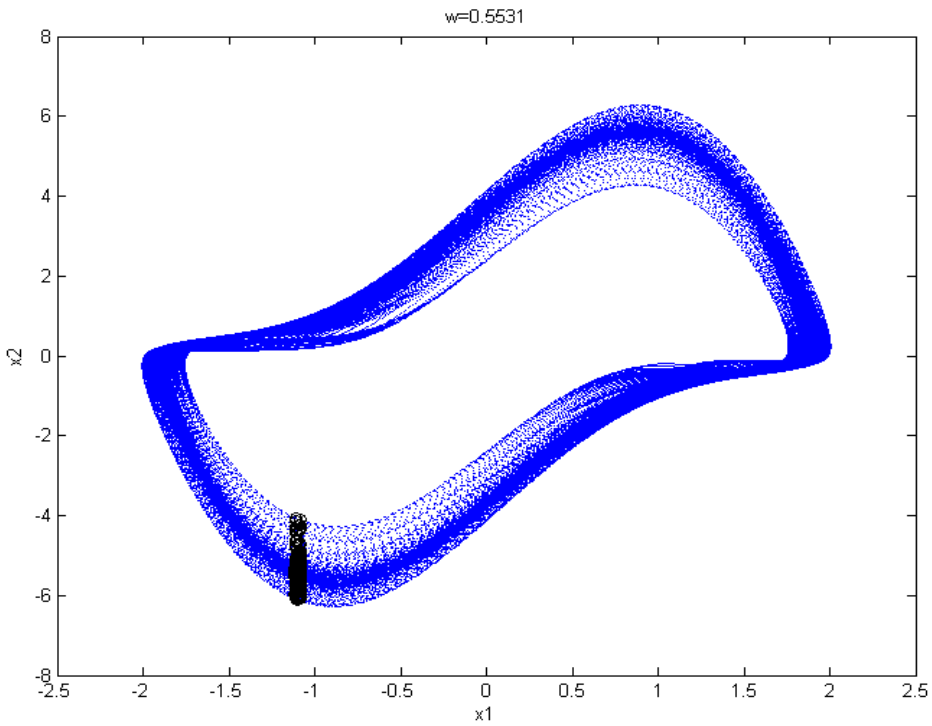

Fig. 2.34 The phase portrait and Poincaré maps of the autonomous fractional order system with order $\alpha = \beta = 0.9$, $\gamma = 1.1, \omega = 0.5531$.

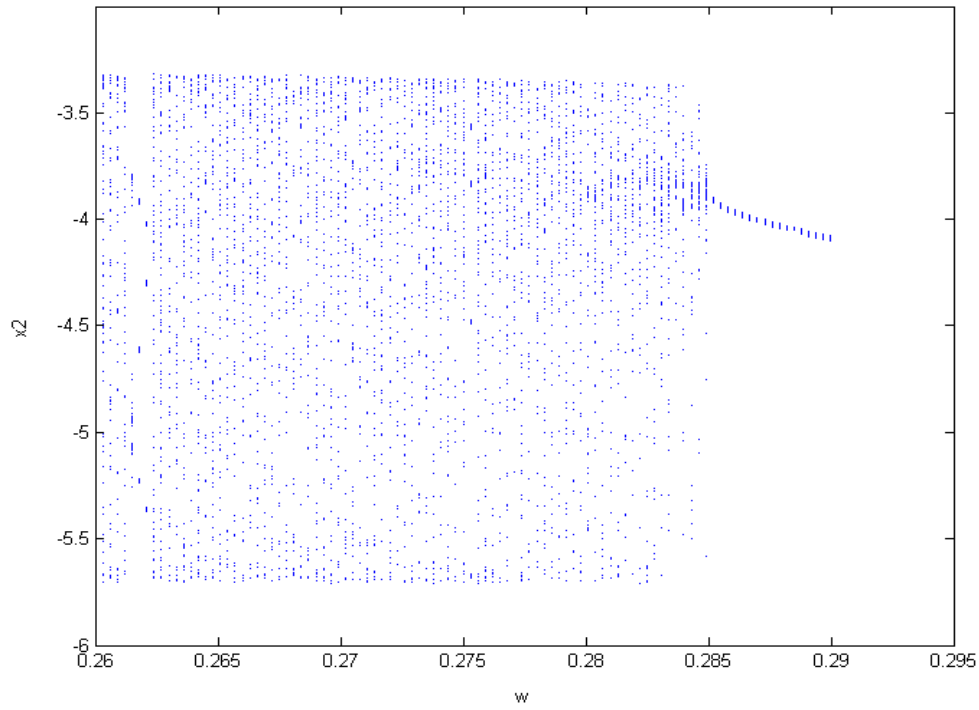

Fig. 2.35 The bifurcation diagram of the autonomous fractional order system with order $\alpha = \beta = 0.8$, $\gamma = 1.1$

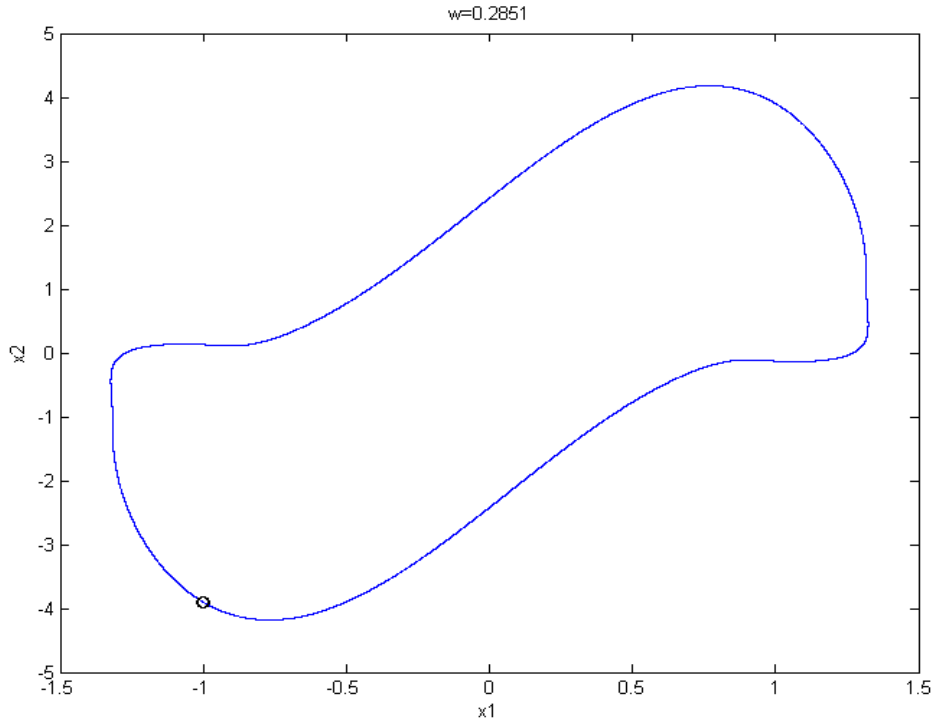

Fig. 2.36 The phase portrait and Poincaré map of the autonomous fractional order system with order $\alpha = \beta = 0.8$, $\gamma = 1.1, \omega = 0.2851$.

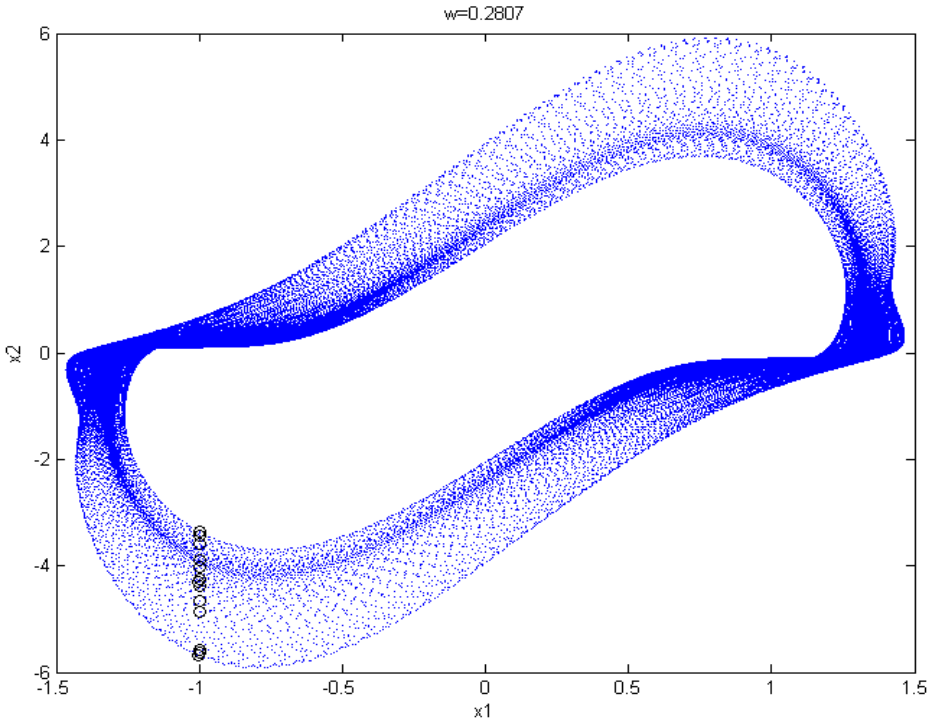

Fig. 2.37 The phase portrait and Poincaré maps of the autonomous fractional order system with order $\alpha = \beta = 0.8$, $\gamma = 1.1, \omega = 0.2807$.

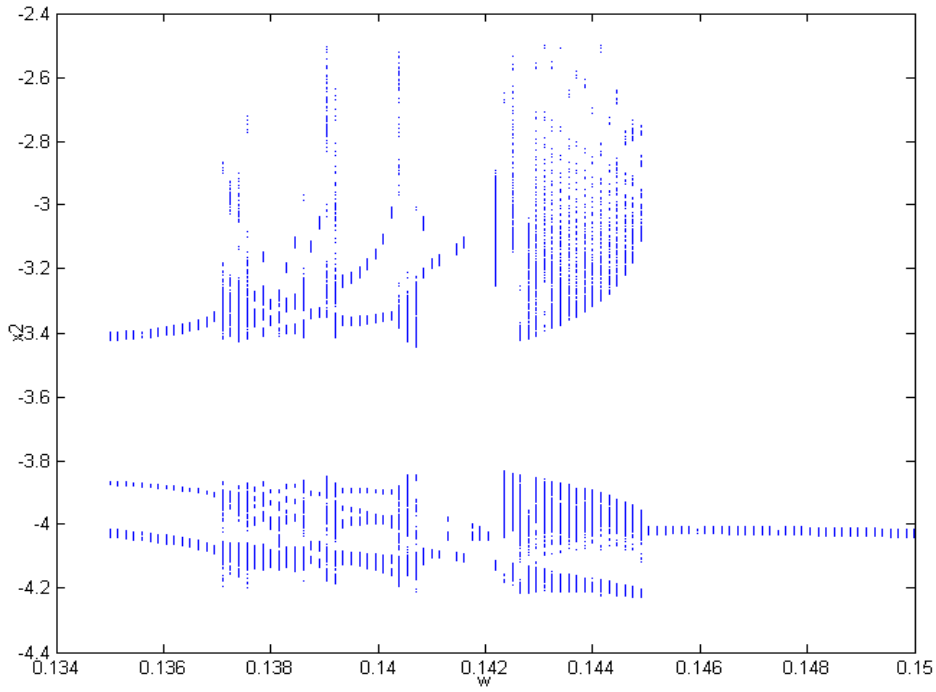

Fig. 2.38 The bifurcation diagram of the autonomous fractional order system with order $\alpha = \beta = 0.7$, $\gamma = 1.1$

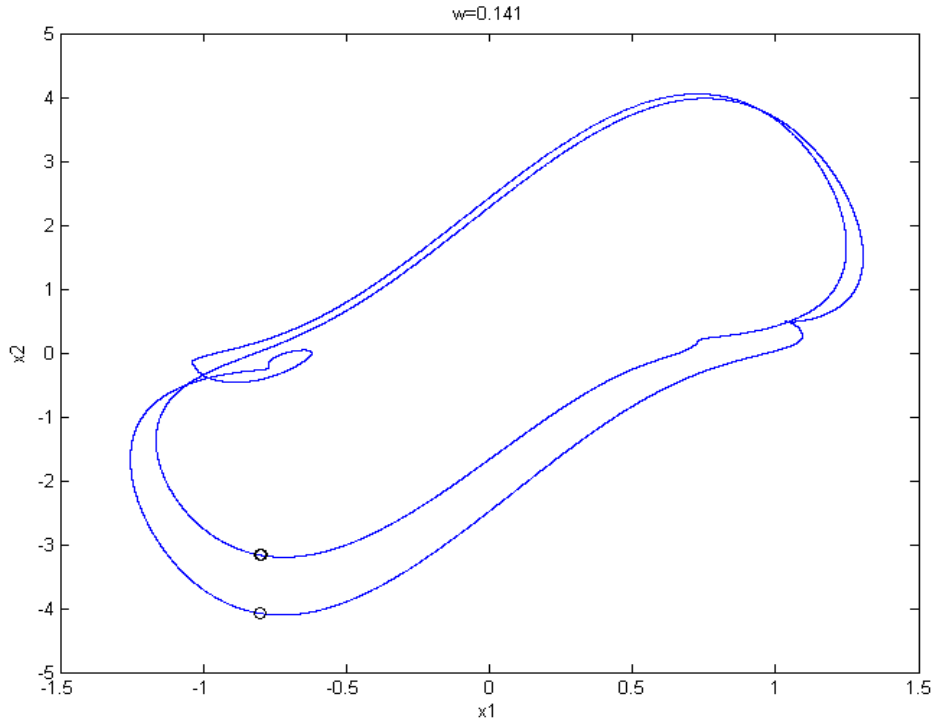

Fig. 2.39 The phase portrait and Poincaré maps of the autonomous fractional order system with order $\alpha = \beta = 0.7$, $\gamma = 1.1, \omega = 0.141$.

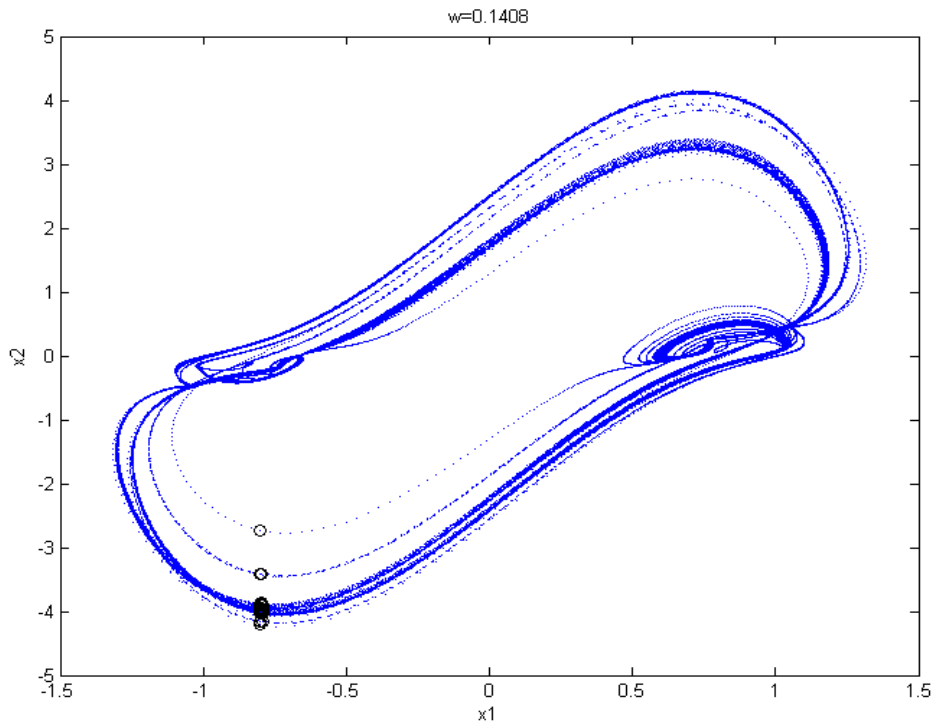

Fig. 2.40 The phase portrait and Poincaré maps of the autonomous fractional order system with order $\alpha = \beta = 0.7$, $\gamma = 1.1, \omega = 0.1408$.

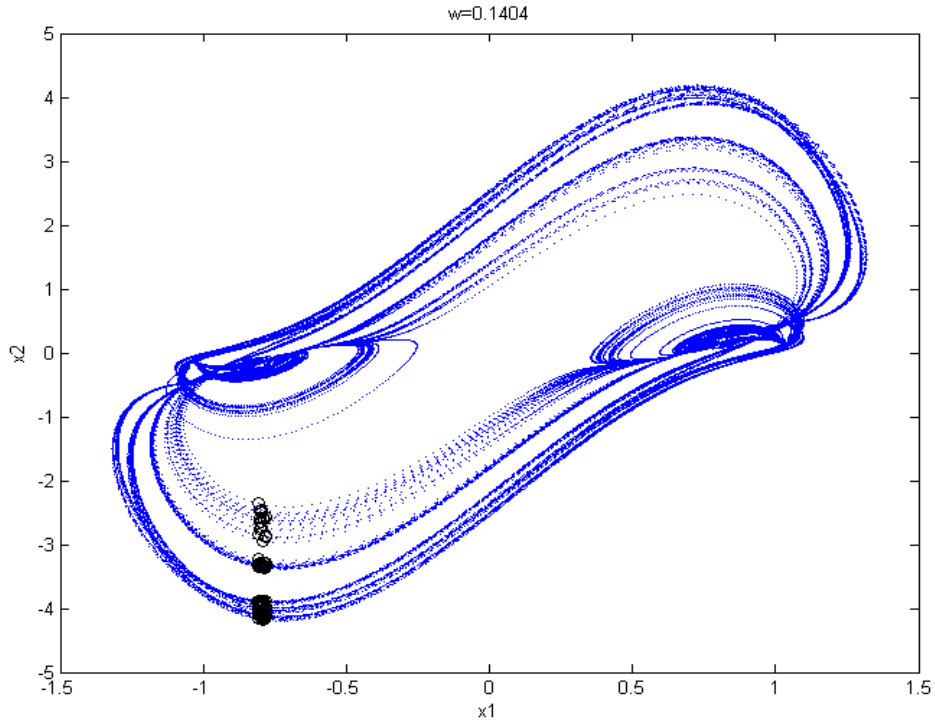

Fig. 2.41 The phase portrait and Poincaré maps of the autonomous fractional order system with order $\alpha = \beta = 0.7$, $\gamma = 1.1, \omega = 0.1404$.

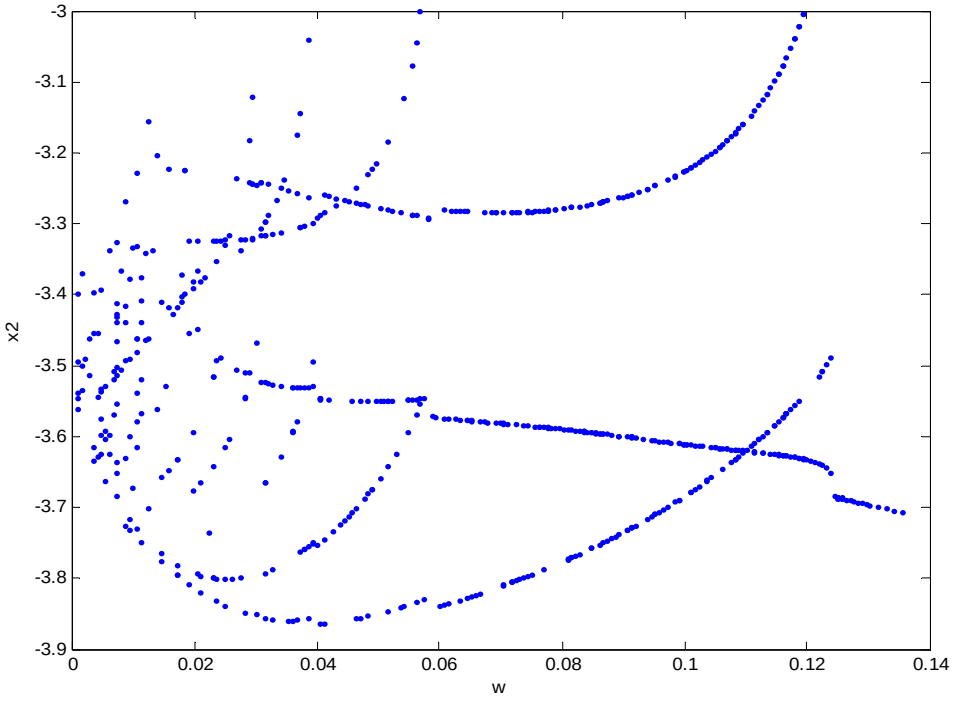

Fig. 2.42 The bifurcation diagram of the autonomous fractional order system with order $\alpha = \beta = 0.6$, $\gamma = 1.1$

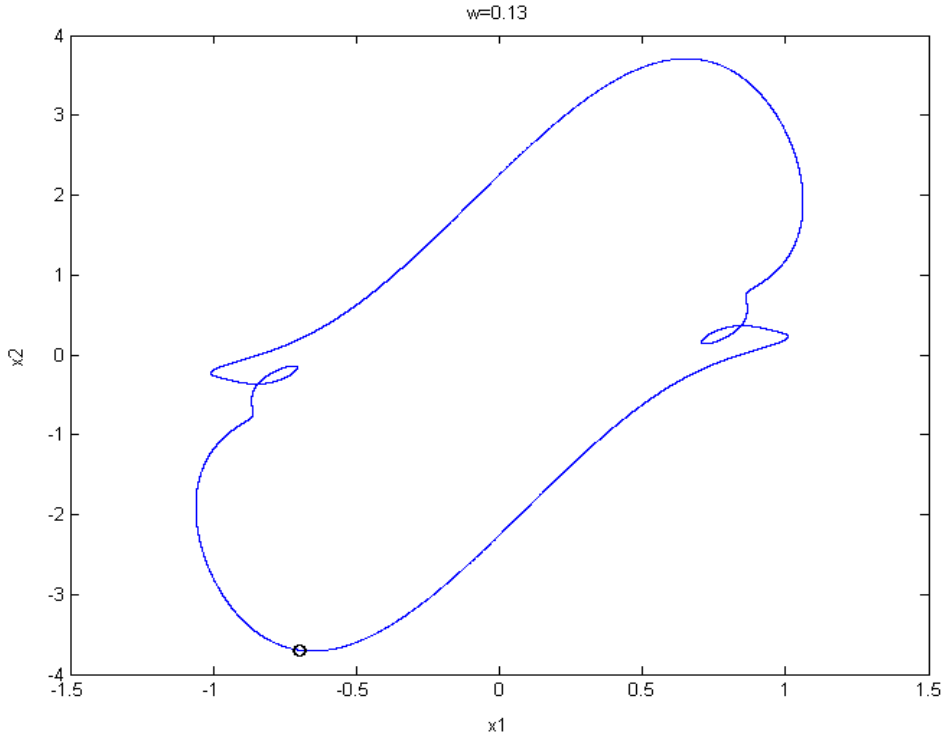

Fig. 2.43 The phase portrait and Poincaré map of the autonomous fractional order system with order $\alpha = \beta = 0.6$, $\gamma = 1.1, \omega = 0.13$.

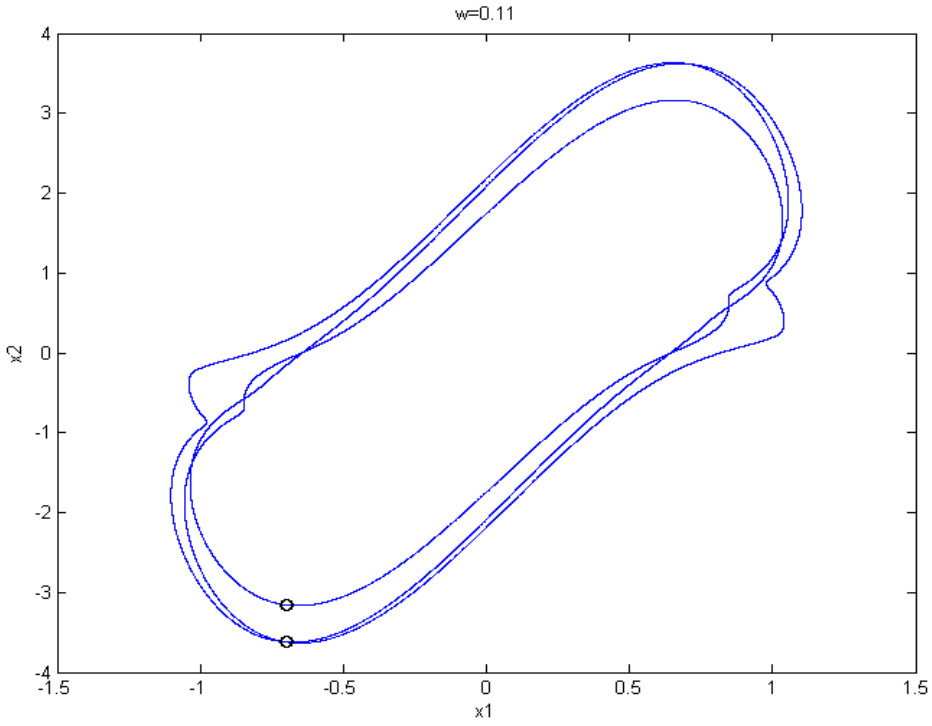

Fig. 2.44 The phase portrait and Poincaré maps of the autonomous fractional order system with order $\alpha = \beta = 0.6$, $\gamma = 1.1, \omega = 0.11$.

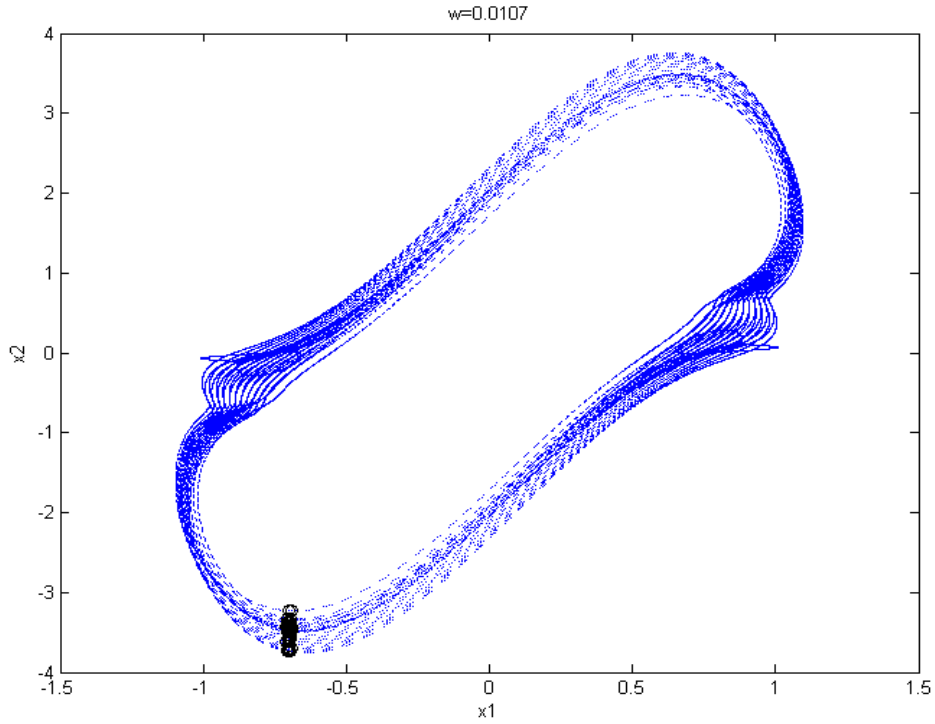

Fig. 2.45 The phase portrait and Poincaré maps of the autonomous fractional order system with order $\alpha = \beta = 0.6$, $\gamma = 1.1, \omega = 0.0107$.

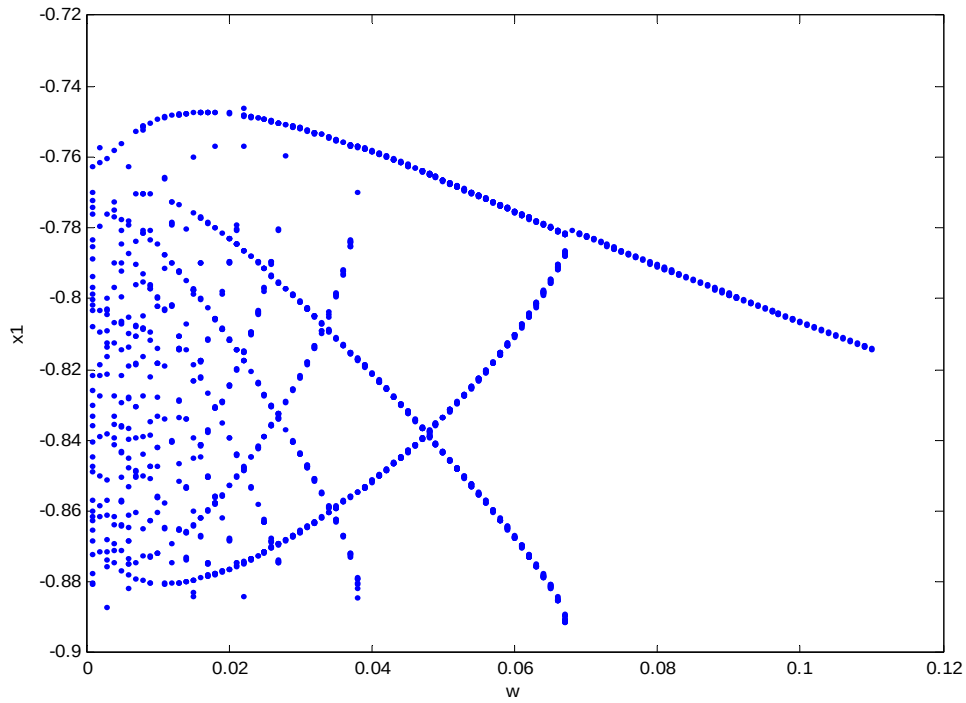

Fig. 2.46 The bifurcation diagram of the autonomous fractional order system with order $\alpha = \beta = 0.5$, $\gamma = 1.1$

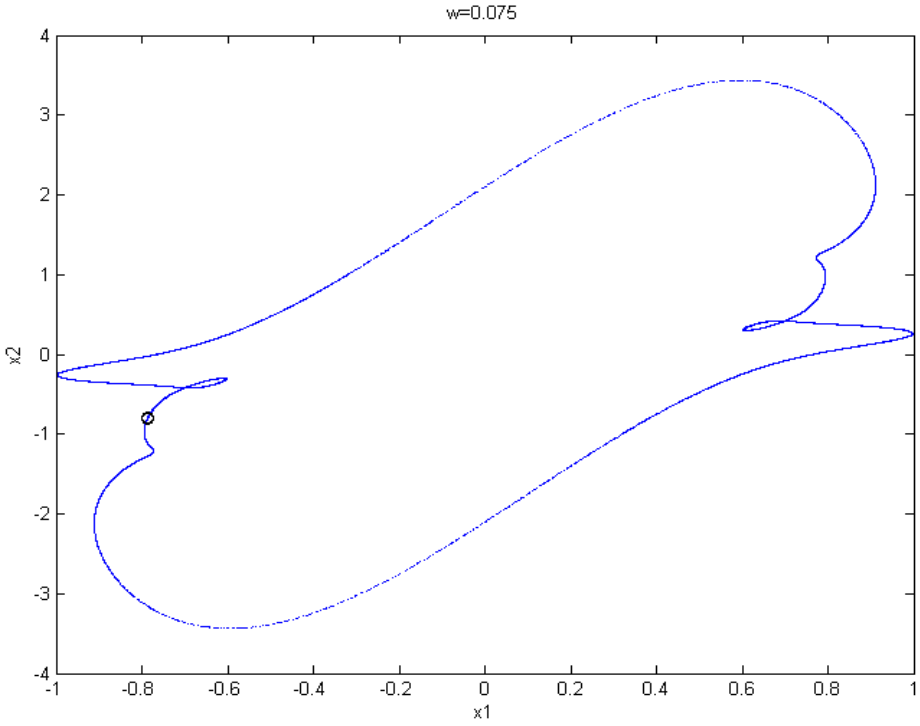

Fig. 2.47 The phase portrait and Poincaré map of the autonomous fractional order system with order $\alpha = \beta = 0.5$, $\gamma = 1.1, \omega = 0.075$.

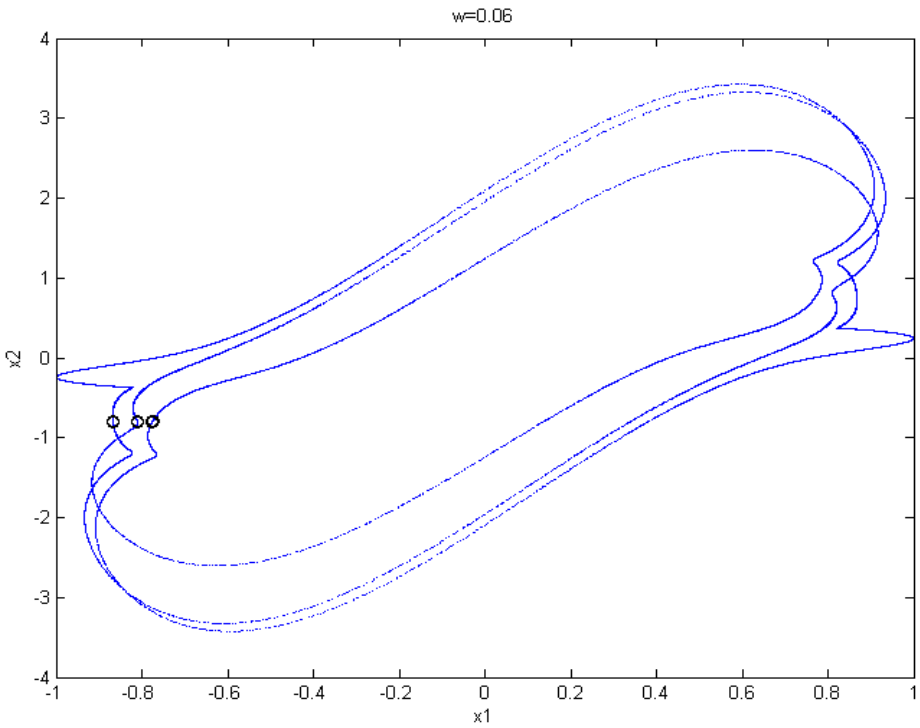

Fig. 2.48 The phase portrait and Poincaré maps of the autonomous fractional order system with order $\alpha = \beta = 0.5$, $\gamma = 1.1, \omega = 0.06$.

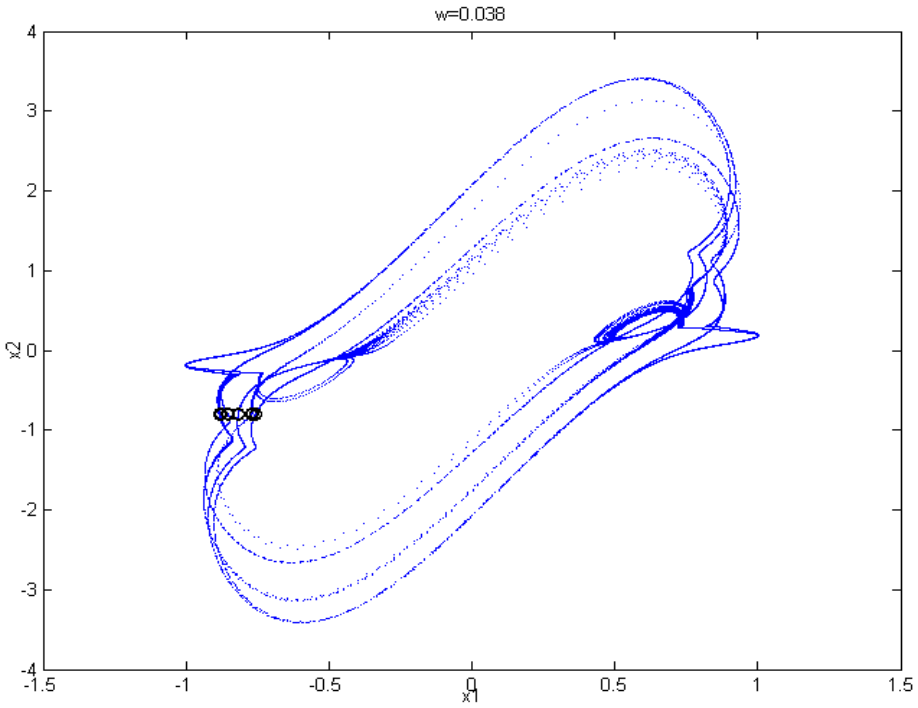

Fig. 2.49 The phase portrait and Poincaré maps of the autonomous fractional order system with order $\alpha = \beta = 0.5$, $\gamma = 1.1, \omega = 0.038$.

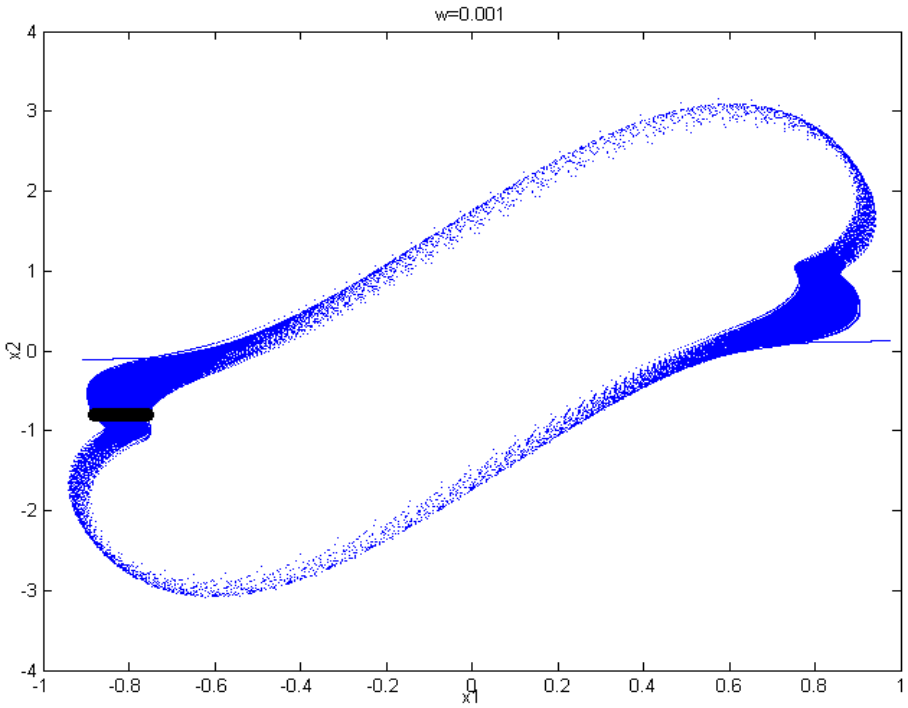

Fig. 2.50 The phase portrait and Poincaré maps of the autonomous fractional order system with order $\alpha = \beta = 0.5$, $\gamma = 1.1, \omega = 0.001$.

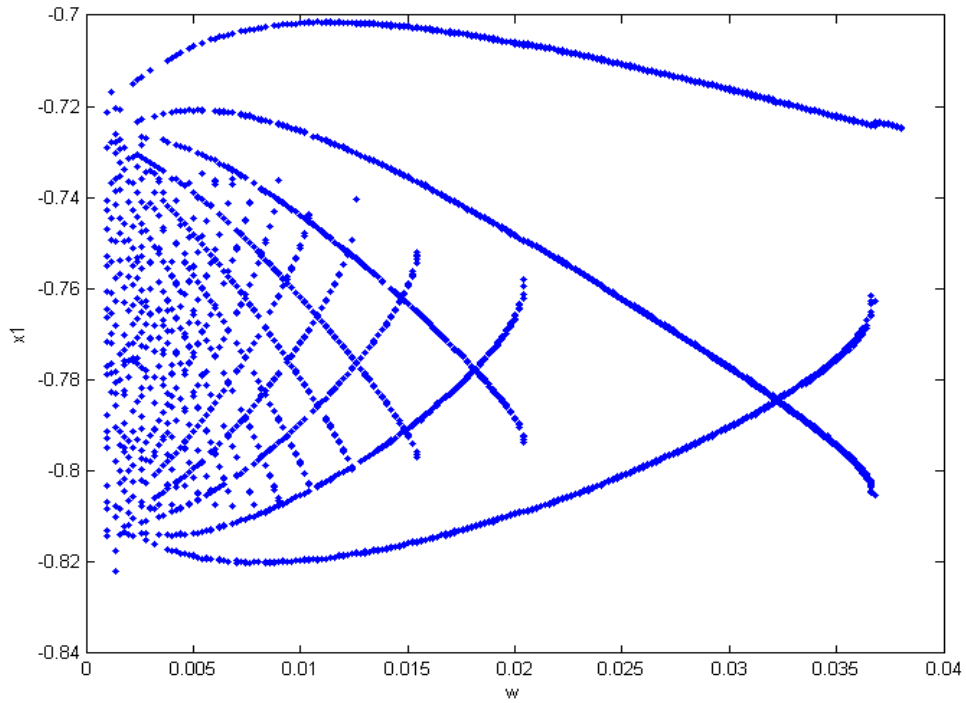

Fig. 2.51 The bifurcation diagram of the autonomous fractional order system with order $\alpha = \beta = 0.4$, $\gamma = 1.1$

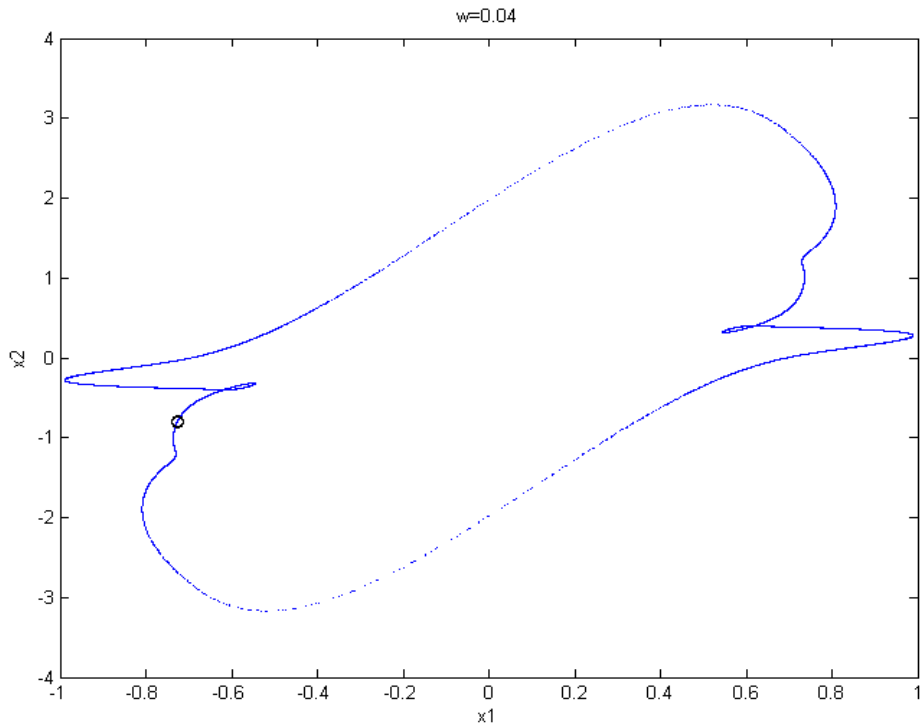

Fig. 2.52 The phase portrait and Poincaré map of the autonomous fractional order system with order $\alpha = \beta = 0.4$, $\gamma = 1.1, \omega = 0.04$.

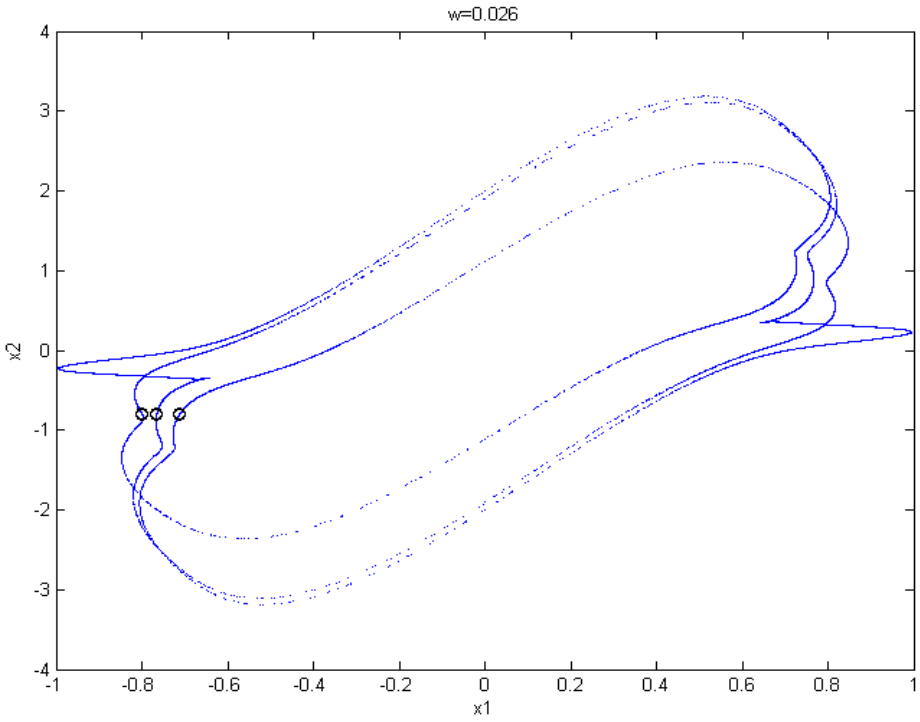

Fig. 2.53 The phase portrait and Poincaré maps of the autonomous fractional order system with order $\alpha = \beta = 0.4$, $\gamma = 1.1, \omega = 0.026$.

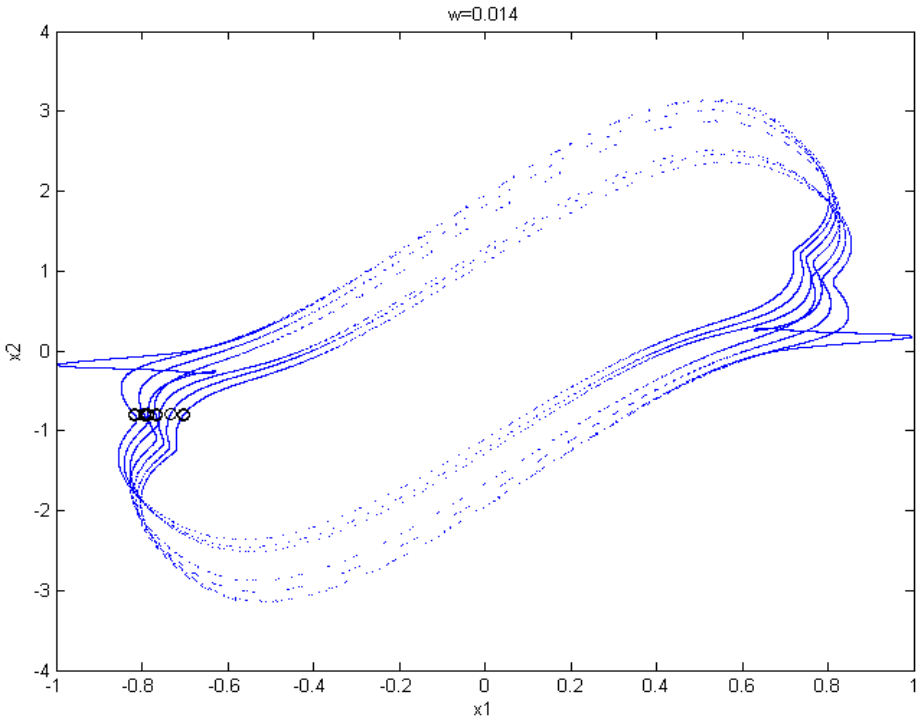

Fig. 2.54 The phase portrait and Poincaré maps of the autonomous fractional order system with order $\alpha = \beta = 0.4$, $\gamma = 1.1, \omega = 0.014$.

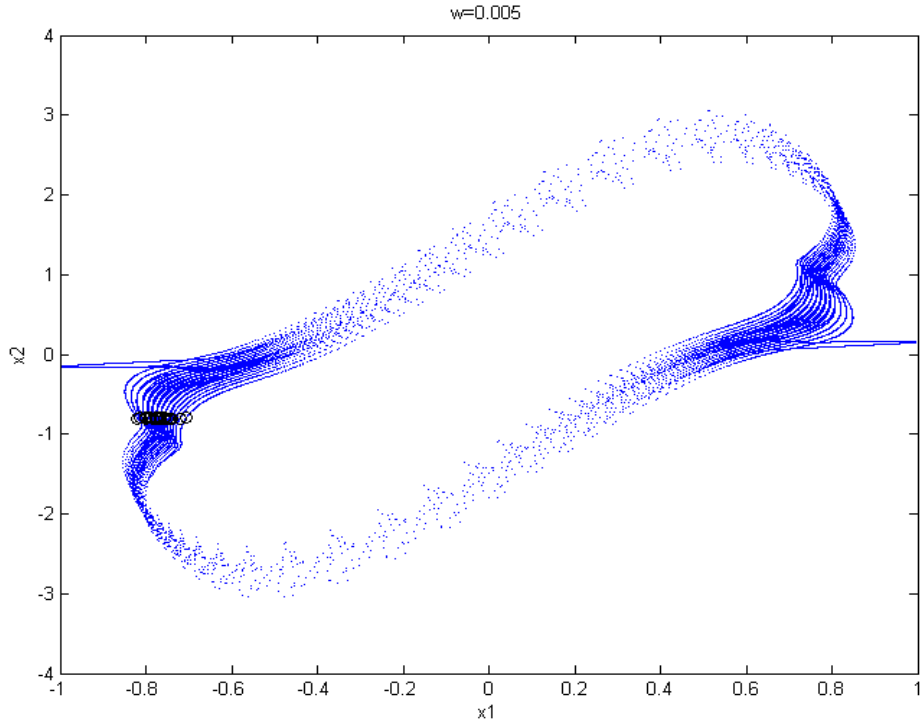

Fig. 2.55 The phase portrait and Poincaré maps of the autonomous fractional order system with order $\alpha = \beta = 0.4$, $\gamma = 1.1, \omega = 0.005$.

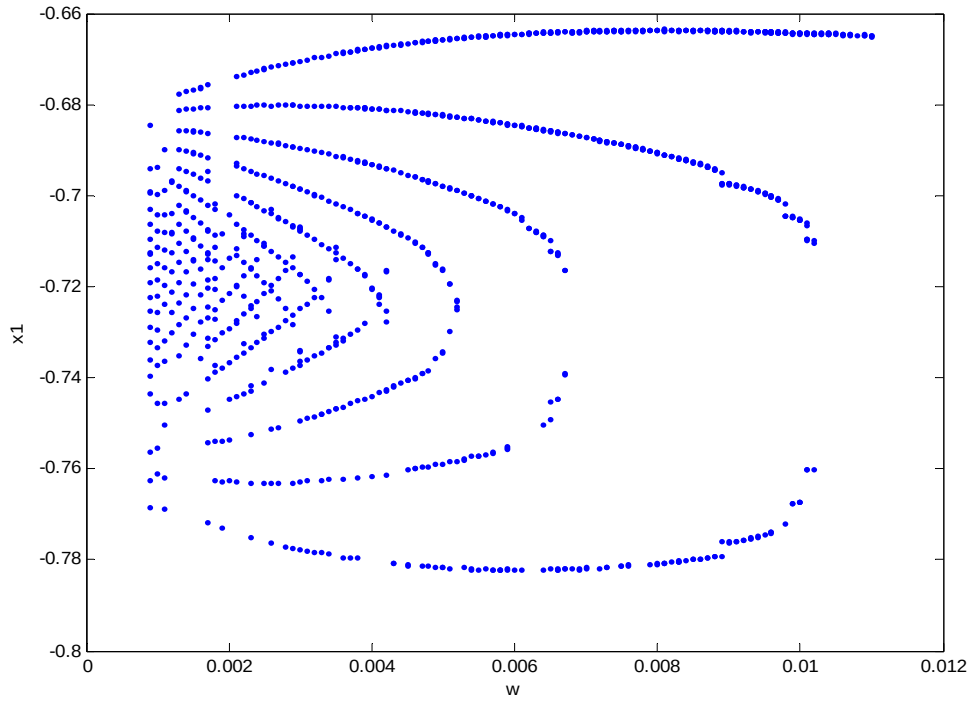

Fig. 2.56 The bifurcation diagram of the autonomous fractional order system with order $\alpha = \beta = 0.3$, $\gamma = 1.1$

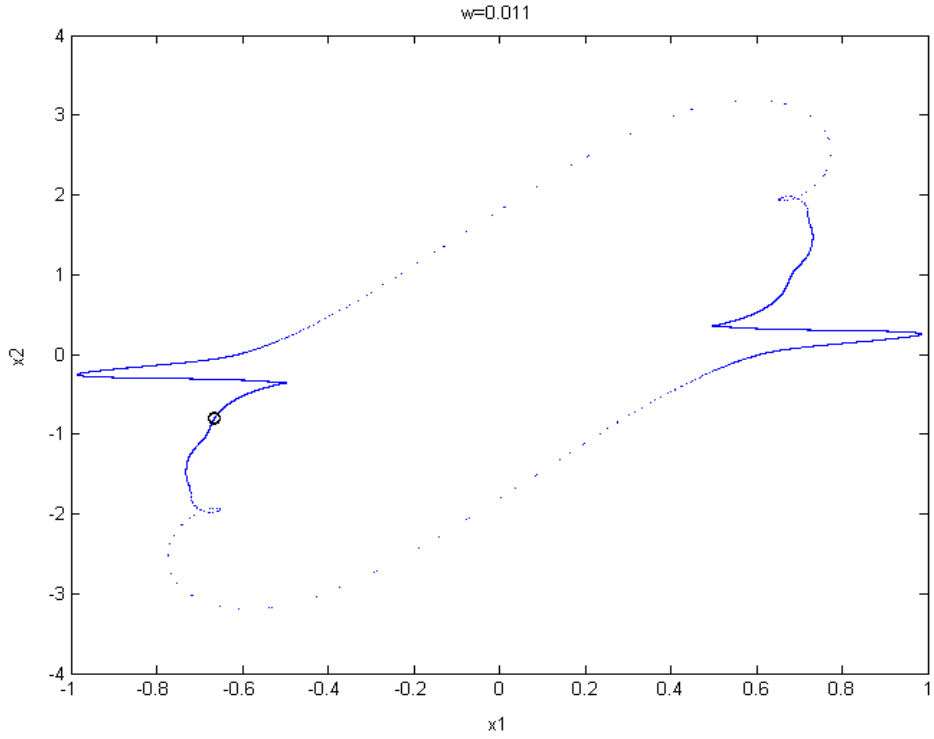

Fig. 2.57 The phase portrait and Poincaré map of the autonomous fractional order system with order $\alpha = \beta = 0.3$, $\gamma = 1.1, \omega = 0.011$.

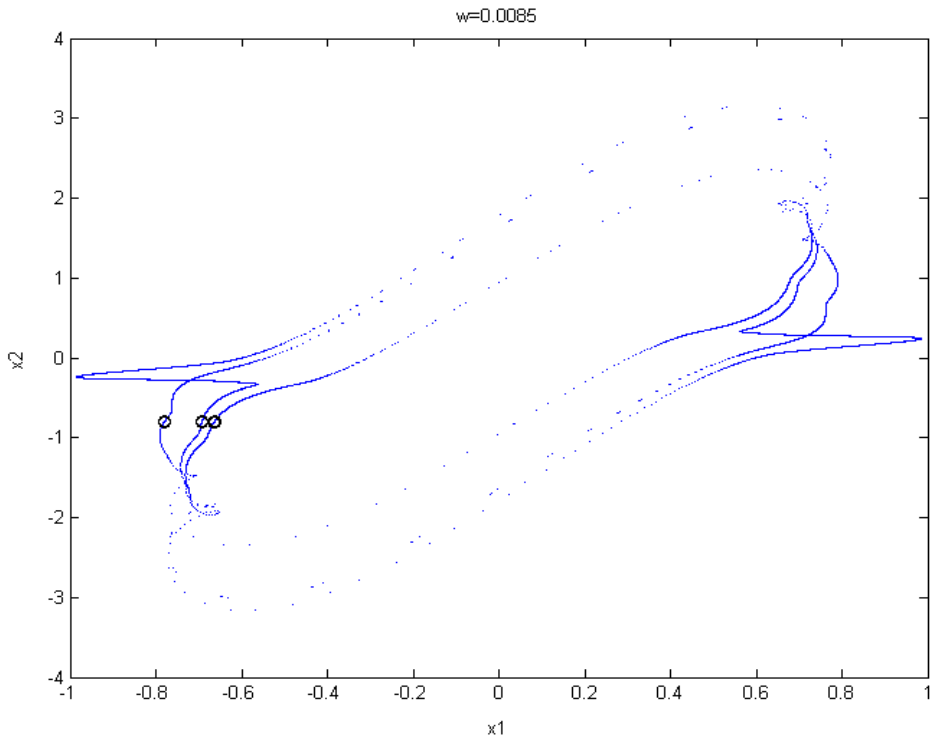

Fig. 2.58 The phase portrait and Poincaré maps of the autonomous fractional order system with order $\alpha = \beta = 0.3$, $\gamma = 1.1, \omega = 0.0085$.

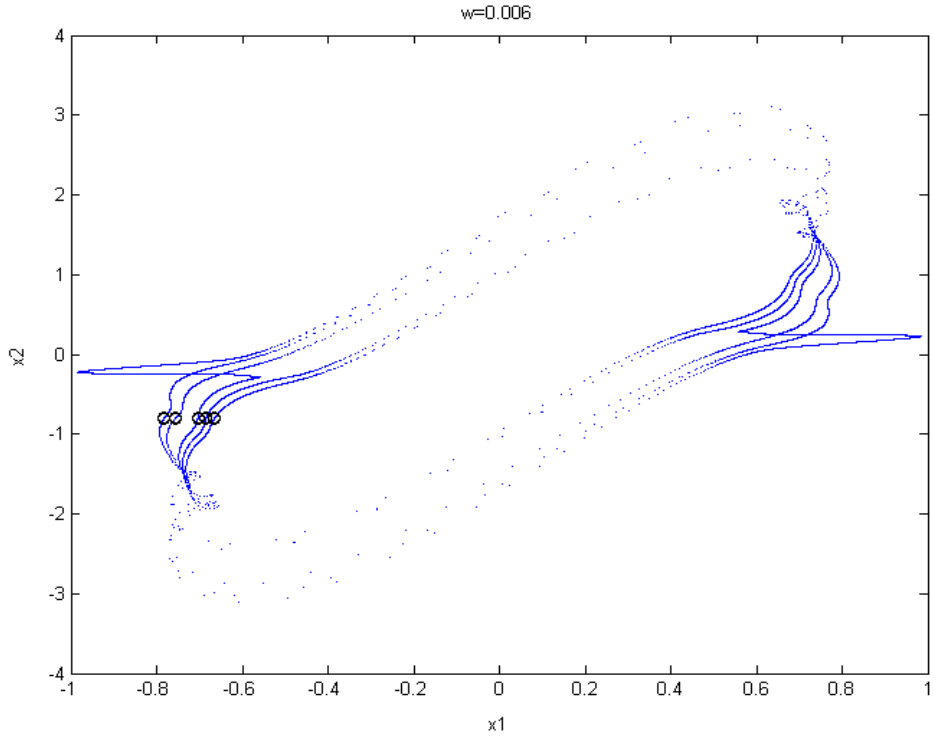

Fig. 2.59 The phase portrait and Poincaré maps of the autonomous fractional order system with order $\alpha = \beta = 0.3$, $\gamma = 1.1, \omega = 0.006$.

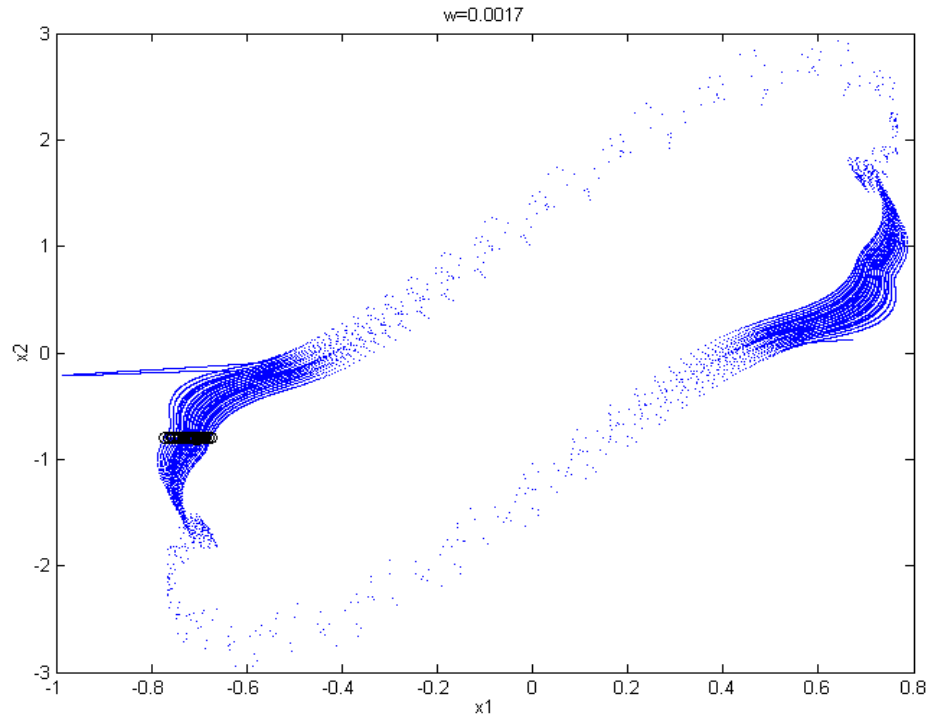

Fig. 2.60 The phase portrait and Poincaré maps of the autonomous fractional order system with order $\alpha = \beta = 0.3$, $\gamma = 1.1, \omega = 0.0017$.

Chapter 3

Chaos Excited Chaos Synchronizations of Integral and Fractional Order Generalized Heartbeat Systems

3.1. Preliminaries

In this chapter, chaos excited chaos synchronizations of generalized van der Pol systems with integral and fractional order are studied. Synchronizations of two identified autonomous generalized van der Pol chaotic systems are obtained by replacing their corresponding exciting terms by the same function of chaotic states of a third nonautonomous or autonomous generalized van der Pol system.

3.2. Schemes of Chaos Excited Chaos Synchronizations of Integral and Fractional Order Generalized Heartbeat Systems

The generalized van der Pol system [7-10] is a nonautonomous system:

$$\begin{aligned} \frac{dx_1}{dt} &= x_2 \\ \frac{dx_2}{dt} &= -x_1 - \varepsilon(1-x_1^{\,2})(c-ax_1^{\,2})x_2 + b\sin\omega t \end{aligned} \tag{3.1}$$

where ε, a, b, c are parameters, and ω is the circular frequency of the external excitation $b\sin\omega t$. The corresponding nonautonomous fractional order system is

$$\begin{aligned} \frac{d^{\alpha}x_1}{dt^{\alpha}} &= x_2 \\ \frac{d^{\beta}x_2}{dt^{\beta}} &= -x_1 - \varepsilon(1-x_1^{\,2})(c-ax_1^{\,2})x_2 + b\sin\omega t \end{aligned} \tag{3.2}$$

where α, β are fractional numbers.

A modified version of Eq.(3.2) is now proposed. The nonautonomous generalized fractional order van der Pol system (3.2) with two states is transformed into an autonomous generalized fractional order van der Pol system with three states:

$$\frac{d^{\alpha}x_1}{dt^{\alpha}} = x_2$$
$$\frac{d^{\beta}x_2}{dt^{\beta}} = -x_1 - \varepsilon(1-x_1^{\,2})(c-ax_1^{\,2})x_2 + b\sin\omega x_3 \qquad (3.3)$$
$$\frac{d^{\gamma}x_3}{dt^{\gamma}} = 1$$

where α, β, γ are fractional numbers, in which the original time t in Eq.(3.2) is changed to a new state x_3. When $\gamma = 1$, $x_3 = t$, Eq.(3.3) reduces to Eq.(3.2).

Two methods of chaos excited chaos synchronization[40-67] are proposed. In Case 1, two identical generalized fractional order van der Pol systems to be synchronized are

$$\frac{d^{\alpha}x_1}{dt^{\alpha}} = x_2$$
$$\frac{d^{\beta}x_2}{dt^{\beta}} = -x_1 - \varepsilon(1-x_1^{\,2})(c-ax_1^{\,2})x_2 + Z \qquad (3.4)$$

and

$$\frac{d^{\alpha}y_1}{dt^{\alpha}} = y_2$$
$$\frac{d^{\beta}y_2}{dt^{\beta}} = -y_1 - \varepsilon(1-y_1^{\,2})(c-ay_1^{\,2})y_2 + Z \qquad (3.5)$$

where the exciting term $b\sin\omega t$ in Eq.(3.2) is replaced in Eqs.(3.4) and (3.5) by Z which is a function of the chaotic states of a third nonautonomous chaotic system

$$\frac{d^{\alpha}z_1}{dt^{\alpha}} = z_2$$
$$\frac{d^{\beta}z_2}{dt^{\beta}} = -z_1 - \varepsilon(1-z_1^{\,2})(c-az_1^{\,2})z_2 + b\sin(\omega t) \qquad (3.6)$$

Z is chosen as $Z = bgz_1$, $Z = bgz_2$, $Z = gz_1\sin(\omega t)$, $Z = gz_2\sin(\omega t)$, respectively, where g is a constant with different values. Error states are defined: $e_1 = x_1 - y_1$, $e_2 = x_2 - y_2$.

In Case 2, two identical generalized fractional order van der Pol systems to be synchronized remain unchanged, as Eqs.(3.4) and (3.5). But Z is a function of the chaotic states of a third autonomous system

$$\frac{d^{\alpha}z_1}{dt^{\alpha}} = y_2$$
$$\frac{d^{\beta}z_2}{dt^{\beta}} = -z_1 - \varepsilon(1-z_1^{\,2})(c-az_1^{\,2})z_2 + b\sin(\omega_z z_3) \qquad (3.7)$$
$$\frac{d^{\gamma}z_3}{dt^{\gamma}} = 1$$

Z is chosen as $Z = bgz_1$, $Z = bgz_2$, $Z = bg\exp(z_1)$, $Z = bg\exp(z_2)$, $Z = g\exp(z_1)\sin(\omega t)$, $Z = g\exp(z_2)\sin(\omega t)$ respectively. g is a constant with different values.

3.3. Numerical Simulations for the Synchronization of Fractional Order Generalized Heartbeat Systems

The systems to be synchronized are systems (3.4) and (3.5) in following two cases. The parameters a=3, b=1.0091, c=1.2 and d=0.07 of system Eq.(3.4)、Eq.(3.5)、Eq.(3.6) and Eq.(3.7) are fixed. Our study of two cases consists of ten parts:

Case 1: The third system is a nonautonomous system with two states, Eq.(3.6).

Part (1): $Z = bgz_1$ where z_1 is the chaotic state of system (3.6), g is an ajustable constant. Fig. 3.1~ Fig. 3.5 show the phase portraits and Poincaré maps of the fractional order synchronized systems and time history of error states plot where α, β take the same fractional numbers and vary from 1.1 to 0.7 in steps of 0.1. When α, β take the fractional number less than 0.7, no chaotic synchronization is found.

Part (2): $Z = bgz_2$ where z_2 is the chaotic state of system (3.6). Fig. 3.6~ Fig. 3.10 show the phase portraits and Poincaré maps of the fractional order synchronized systems and time history of error states plot where α, β take the same fractional numbers and vary from 1.1 to 0.7 in steps of 0.1. When α, β take the fractional number less than 0.7, no chaotic synchronization is found.

Part (3): $Z = gz_1\sin(\omega t)$ where z_1 is the chaotic state of system (3.6). Fig. 3.11~ Fig. 3.15 show the phase portraits and Poincaré maps of the fractional order synchronized systems and time history of error states plot where α, β take the same fractional numbers and vary from 1.1 to 0.7 in steps of 0.1. When α, β take the fractional number less than 0.7, no chaotic synchronization is found.

Part (4): $Z = gz_2\sin(\omega t)$ where z_2 is the chaotic state of system (3.6). Fig. 3.16~ Fig.

3.20 show the phase portraits and Poincaré maps of the fractional order synchronized systems and time history of error states plot where α, β take the same fractional numbers and vary from 1.1 to 0.7 in steps of 0.1. When α, β take the fractional number less than 0.7, no chaotic synchronization is found.

Case 2: The third system is an autonomous system with three states, Eq.(3.7).

Part (1): $Z = bgz_1$ where z_1 is the chaotic state of system (3.7). Fig. 3.21~ Fig. 3.28 show the phase portraits and Poincaré maps of the fractional order synchronized systems and time history of error states plot where γ takes 1.1, and α, β take the same fractional numbers and vary from 1.1 to 0.3 in steps of 0.1. When $\gamma < 1$, no chaos exists in system(3.7). When α, β take the fractional number less than 0.3, no chaotic synchronization is found.

Part (2): $Z = bgz_2$ where z_2 is the chaotic state of system (3.7). Fig. 3.29~ Fig. 3.36 show the phase portraits and Poincaré maps of the fractional order synchronized systems and time history of error states plot where γ takes 1.1, and α, β take the same fractional numbers and vary from 1.1 to 0.3 in steps of 0.1. When $\gamma < 1$, no chaos exists in system(3.7). When α, β take the fractional number less than 0.3, no chaotic synchronization is found.

Part (3): $Z = bg\exp(z_1)$ where z_1 is the chaotic state of system (3.7). Fig. 3.37~ Fig. 3.44 show the phase portraits and Poincaré maps of the fractional order synchronized systems and time history of error states plot where γ takes 1.1, and α, β take the same fractional numbers and vary from 1.1 to 0.3 in steps of 0.1. When $\gamma < 1$, no chaos exists in system(3.7). When α, β take the fractional number less than 0.3, no chaotic synchronization is found.

Part (4): $Z = bg\exp(z_2)$ where z_2 is the chaotic state of system (3.7). Fig. 3.45~ Fig. 3.52 show the phase portraits and Poincaré maps of the fractional order synchronized

systems and time history of error states plot where γ takes 1.1, and α, β take the same fractional numbers and vary from 1.1 to 0.3 in steps of 0.1. When $\gamma < 1$, no chaos exists in system(3.7).When α, β take the fractional number less than 0.3, no chaotic synchronization is found.

Part (5): $Z = g\exp(z_1)\sin(\omega t)$ where z_1 is the chaotic state of system (3.7). Fig. 3.53~ Fig. 3.56 show the phase portraits and Poincaré maps of the fractional order synchronized systems and time history of error states plot where γ takes 1.1, and α, β take the same fractional numbers and vary from 1.1 to 0.7 in steps of 0.1. When $\gamma < 1$, no chaos exists in system(3.7). When α, β take the fractional number less than 0.7, no chaotic synchronization is found.

Part (6): $Z = g\exp(z_2)\sin(\omega t)$ where z_2 is the chaotic state of system (3.7). Fig. 3.57~ Fig. 3.60 show the phase portraits and Poincaré maps of the fractional order synchronized systems and time history of error states plot where γ takes 1.1, and α, β take the same fractional numbers and vary from 1.1 to 0.7 in steps of 0.1. When $\gamma < 1$, no chaos exists in system(3.7). When α, β take the fractional number less than 0.7, no chaotic synchronization is found.

The ranges of g for various chaos synchronization cases are listed in Table 1.

Table 1. The ranges of g for various chaos synchronization cases.

Case 1: The third system is a nonautonomous system with two states, Eq.(3.6).				
	Part (1) $Z = bgz_1$	Part (2) $Z = bgz_2$	Part (3) $Z = gz_1\sin(\omega t)$	Part (4) $Z = gz_2\sin(\omega t)$
$\alpha = \beta = 1.1$	0.23~1.64	0.18~4.20	0.51~2.27	0.32~6.51
$\alpha = \beta = 1$	0.09~3.43	0.14~7.6	0.15~3.7	0.7~9.8
$\alpha = \beta = 0.9$	0.11~6.13	0.05~9.59	0.6~14.9	0.5~6.1

$\alpha=\beta=0.8$	0.18~8.23	0.1~13.53	0.3~8.5	0.5~14.4
$\alpha=\beta=0.7$	0.07~12.27	0.3~14.65	0.09~14.9	0.12~26.6
Case 2: The third system is an autonomous system with three states, Eq.(3.7).				
	Part (1) $Z=bgz_1$	Part (2) $Z=bgz_2$	Part (3) $Z=bg\exp(z_1)$	Part (4) $Z=bg\exp(z_2)$
$\alpha=\beta=\gamma=1.1$	0.8~1.64	0.1~4.16	0.29~0.015	0.12~0.015
$\alpha=\beta=0.9,\ \gamma=1.1$	0.16~0.52	0.2~0.132	0.0001~1.36	0.001~0.18
$\alpha=\beta=0.8,\ \gamma=1.1$	0.1~11.6	0.07~13.5	0.0001~1.9	0.001~0.5
$\alpha=\beta=0.7,\ \gamma=1.1$	0.04~10.4	0.02~19.1	0.0001~3.6	0.001~1.9
$\alpha=\beta=0.6,\ \gamma=1.1$	0.06~6.6	0.05~21.3	0.0001~2.3	0.001~2.0
$\alpha=\beta=0.5,\ \gamma=1.1$	0.05~8.7	0.04~34.2	0.0001~3.2	0.001~3.6
$\alpha=\beta=0.4,\ \gamma=1.1$	0.06~10.1	0.1~38.2	0.02~3.7	0.001~4
$\alpha=\beta=0.3,\ \gamma=1.1$	0.06~11.9	0.04~50	0.01~4.7	0.01~5.5
	Part (5) $Z=g\exp(z_1)\sin(\omega t)$		Part (6) $Z=g\exp(z_2)\sin(\omega t)$	
$\alpha=\beta=\gamma=1.1$	0.44~0.08		0.13~0.01	
$\alpha=\beta=0.9,\ \gamma=1.1$	0.03~2.14		0.003~0.33	
$\alpha=\beta=0.8,\ \gamma=1.1$	0.06~3.48		0.02~0.63	
$\alpha=\beta=0.7,\ \gamma=1.1$	0.05~5.22		0.007~1.93	

By the results of simulation, it is found that the chaos excited chaos synchronizations are obtained in Case(1) for lowest total fractional order $0.7\times 2=1.4$, while synchronizations can be achieved in Case(2) for lowest total fractional order $0.3\times 2=0.6$.

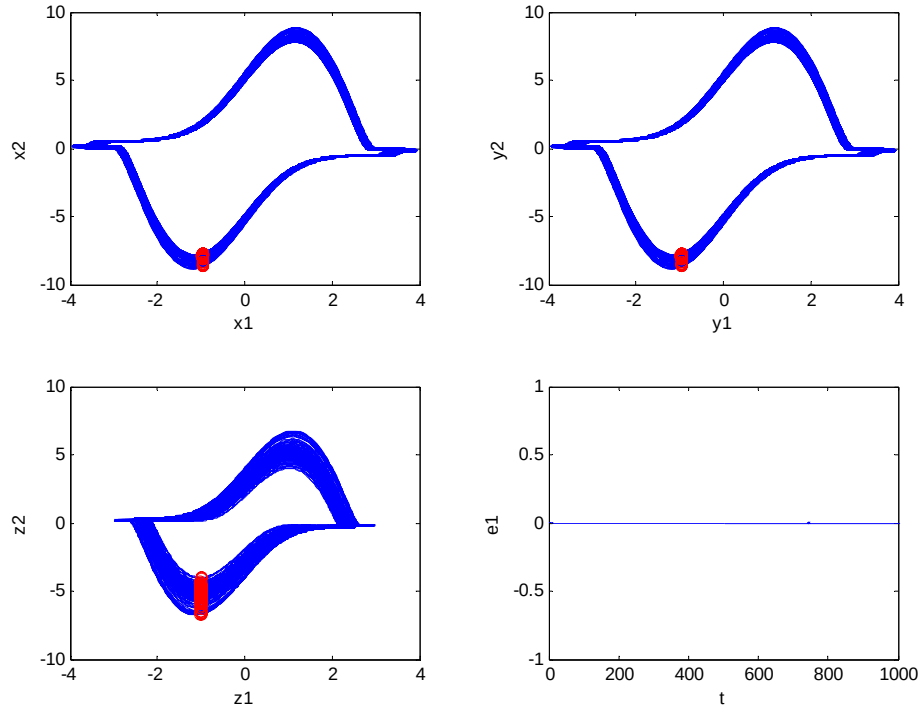

Fig. 3.1 Phase portraits and Poincaré maps of the synchronized fractional order systems and time history of states error for $Z = bgz_1$ with order $\alpha = \beta = 1.1$, ω=0.445, g=1.5 .

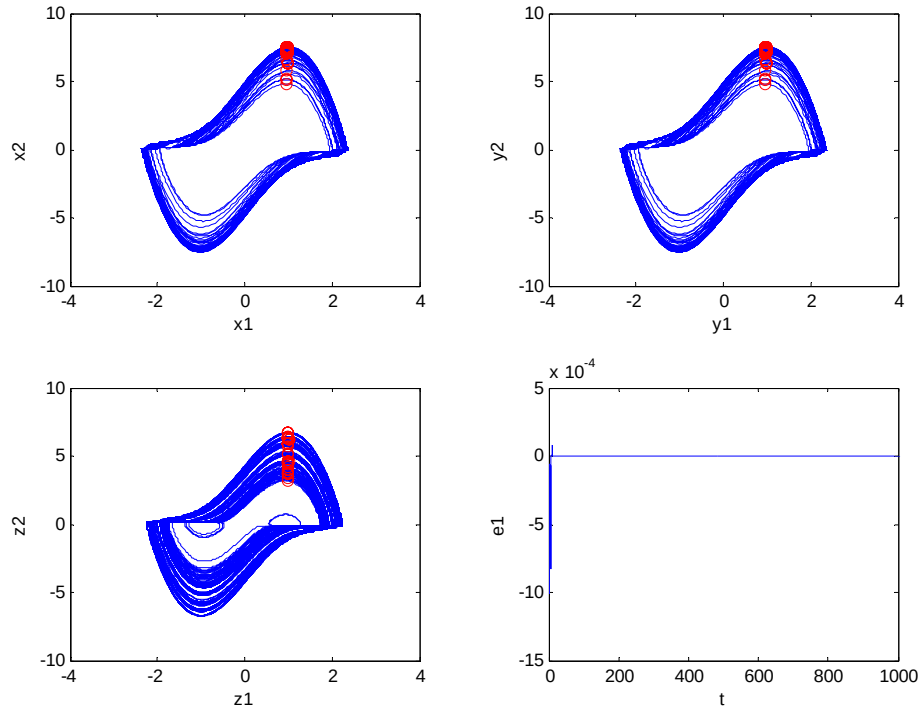

Fig. 3.2 Phase portraits and Poincaré maps of the synchronized fractional order systems and time history of states error for $Z = bgz_1$ with order $\alpha = \beta = 1$, ω=0.1301, g=1 .

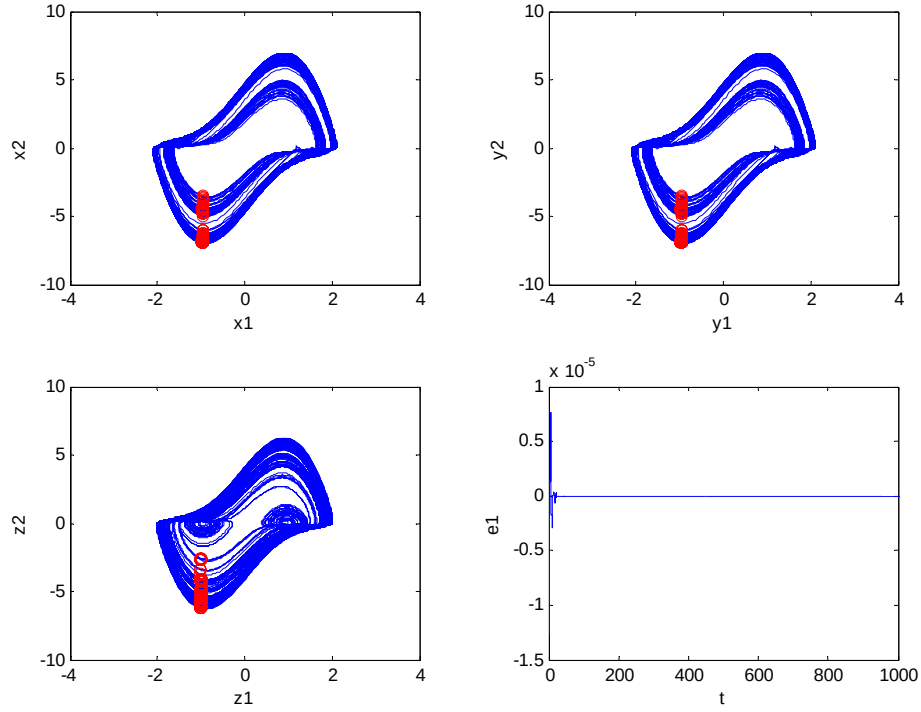

Fig. 3.3 Phase portraits and Poincaré maps of the synchronized fractional order systems and time history of states error for $Z = bgz_1$ with order $\alpha = \beta = 0.9$, ω=0.132, g=1 .

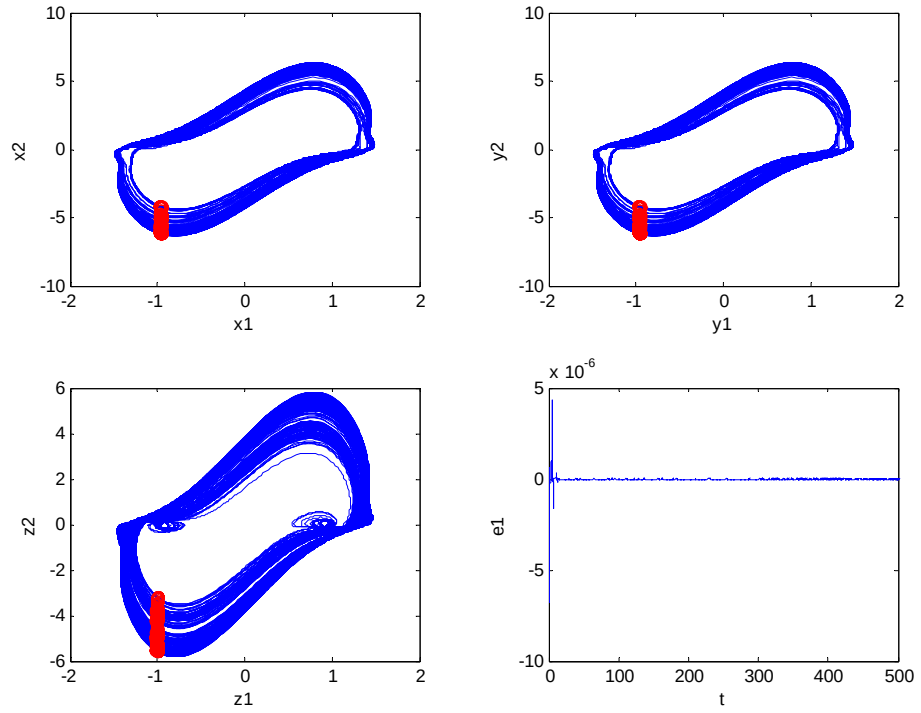

Fig. 3.4 Phase portraits and Poincaré maps of the synchronized fractional order systems and time history of states error for $Z = bgz_1$ with order $\alpha = \beta = 0.8$, ω=0.1315, g=0.8 .

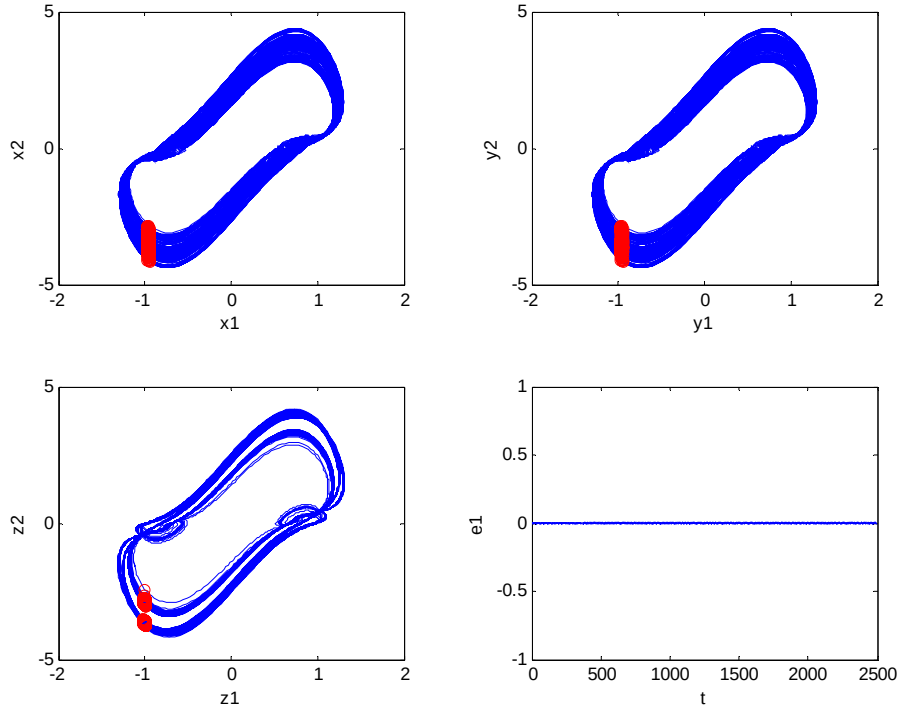

Fig. 3.5 Phase portraits and Poincaré maps of the synchronized fractional order systems and time history of states error for $Z = bgz_1$ with order $\alpha = \beta = 0.7$, ω=0.31812, g=0.3 .

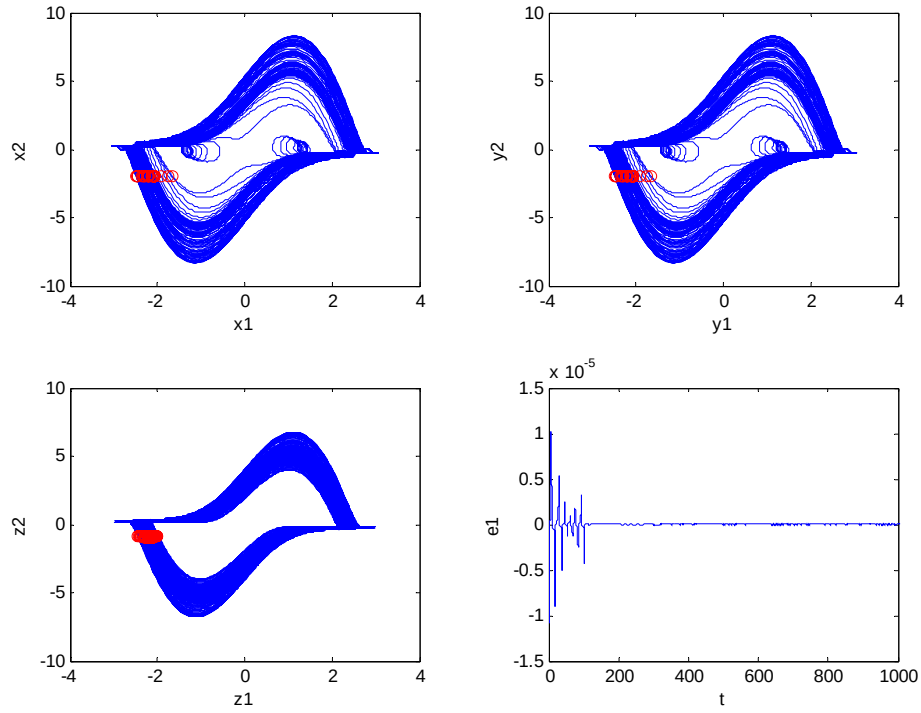

Fig. 3.6 Phase portraits and Poincaré maps of the synchronized fractional order systems and time history of states error for $Z = bgz_2$ with order $\alpha = \beta = 1.1$, ω=0.445, g=0.8 .

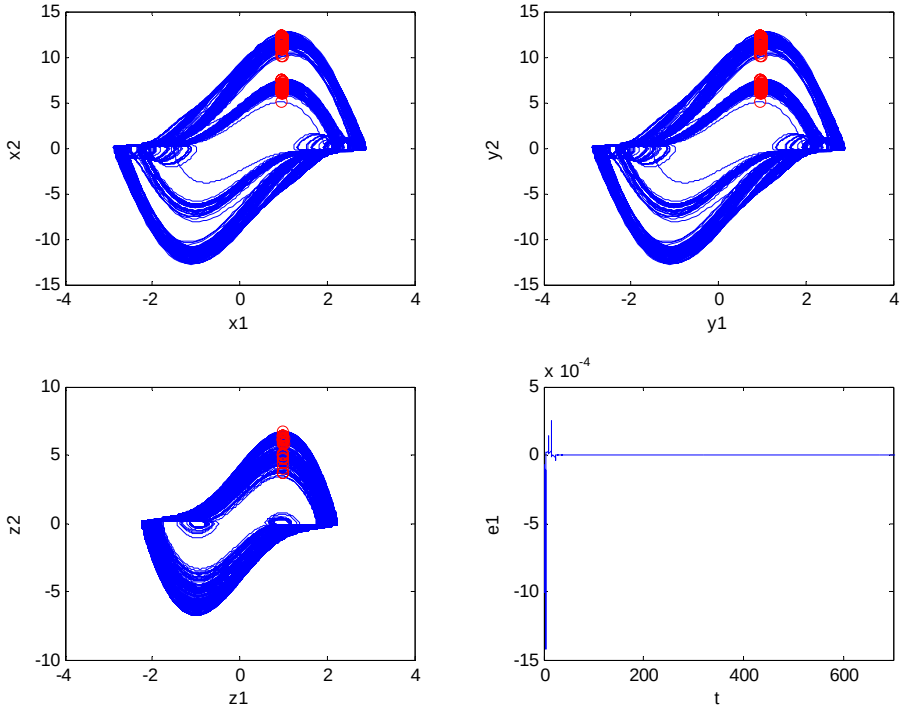

Fig. 3.7 Phase portraits and Poincaré maps of the synchronized fractional order systems and time history of states error for $Z = bgz_2$ with order $\alpha = \beta = 1$, ω=0.12961875, g=3 .

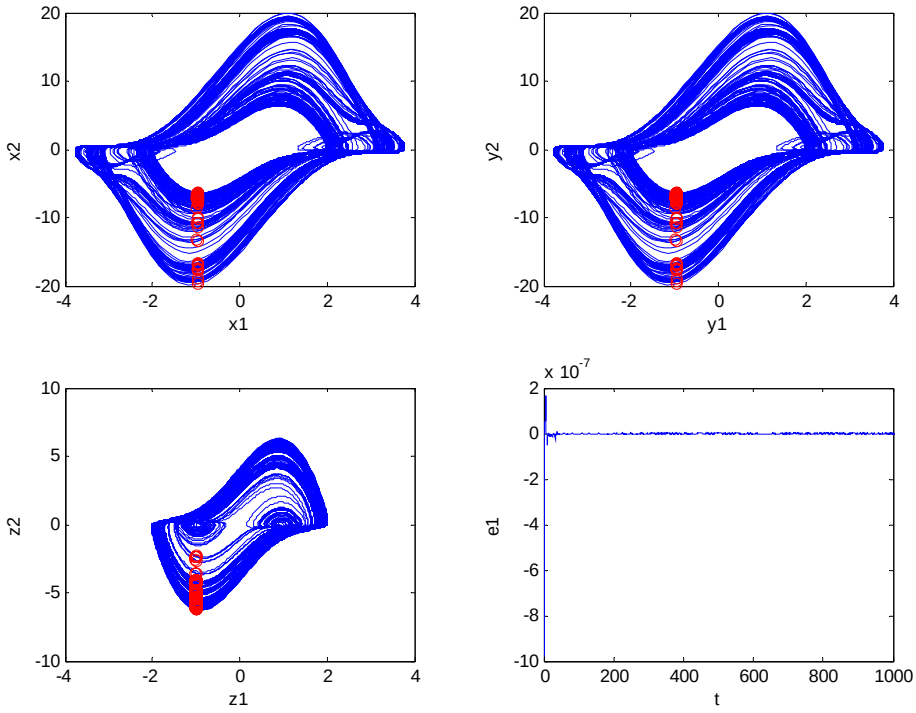

Fig. 3.8 Phase portraits and Poincaré maps of the synchronized fractional order systems and time history of states error for $Z = bgz_2$ with order $\alpha = \beta = 0.9$, ω=0.132, g=9 .

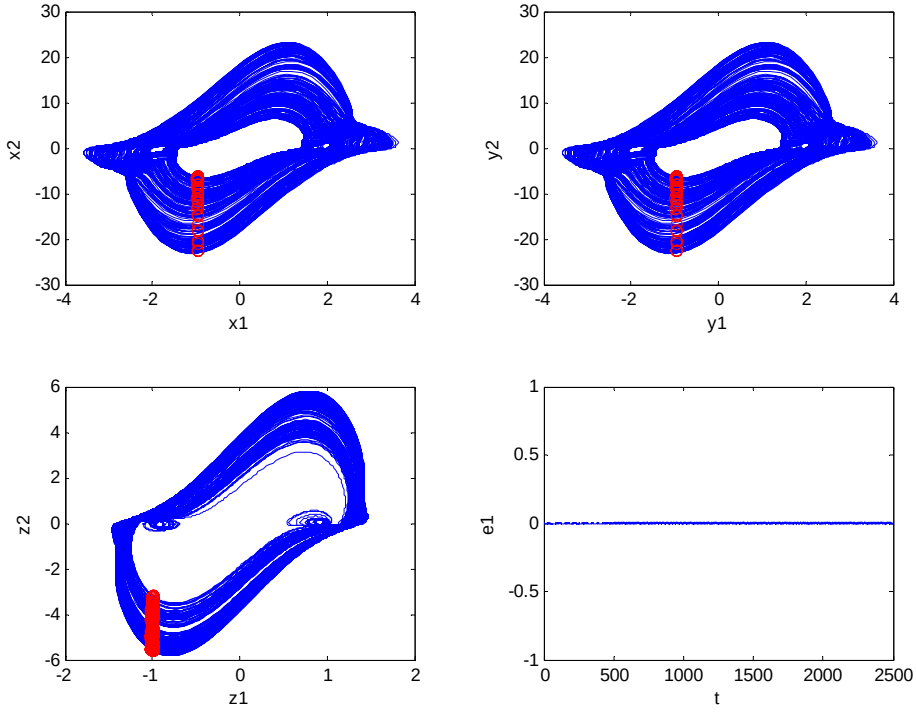

Fig. 3.9 Phase portraits and Poincaré maps of the synchronized fractional order systems and time history of states error for $Z = bgz_2$ with order $\alpha = \beta = 0.8$, ω=0.1315, g=13 .

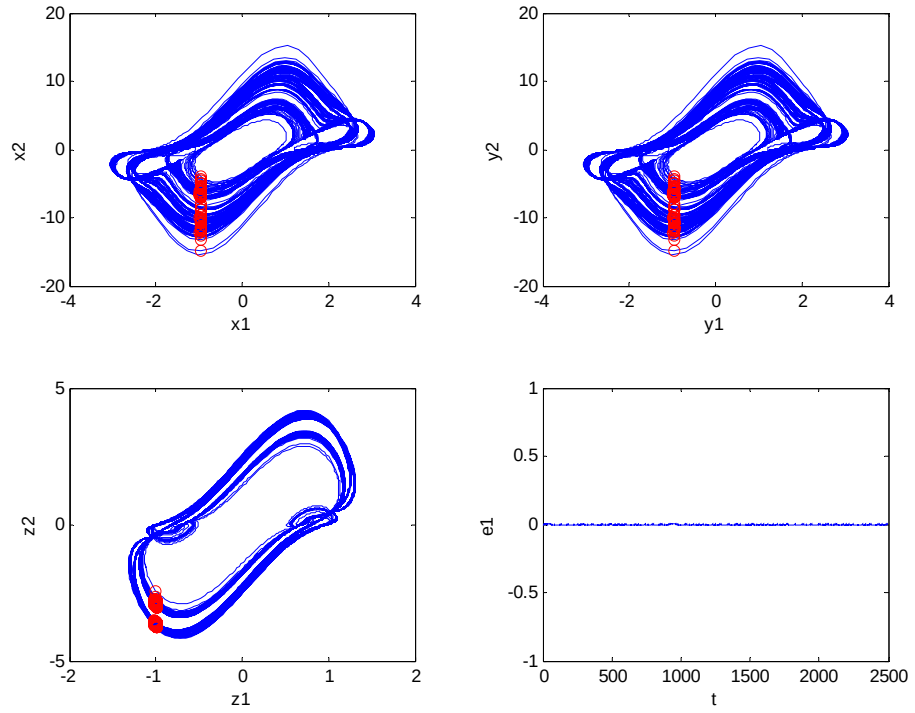

Fig. 3.10 Phase portraits and Poincaré maps of the synchronized fractional order systems and time history of states error for $Z = bgz_2$ with order $\alpha = \beta = 0.7$, ω=0.31812, g=14.65 .

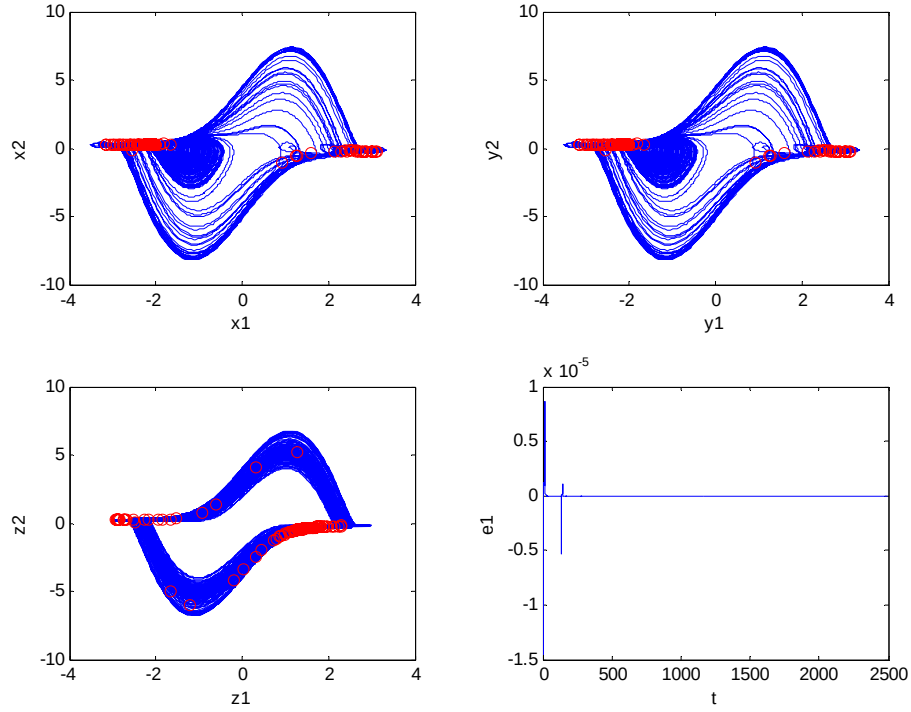

Fig. 3.11 Phase portraits and Poincaré maps of the synchronized fractional order systems and time history of states error for $Z = gz_1 \sin(\omega t)$ with order $\alpha = \beta = 1.1$, ω=0.445, g=1.5 .

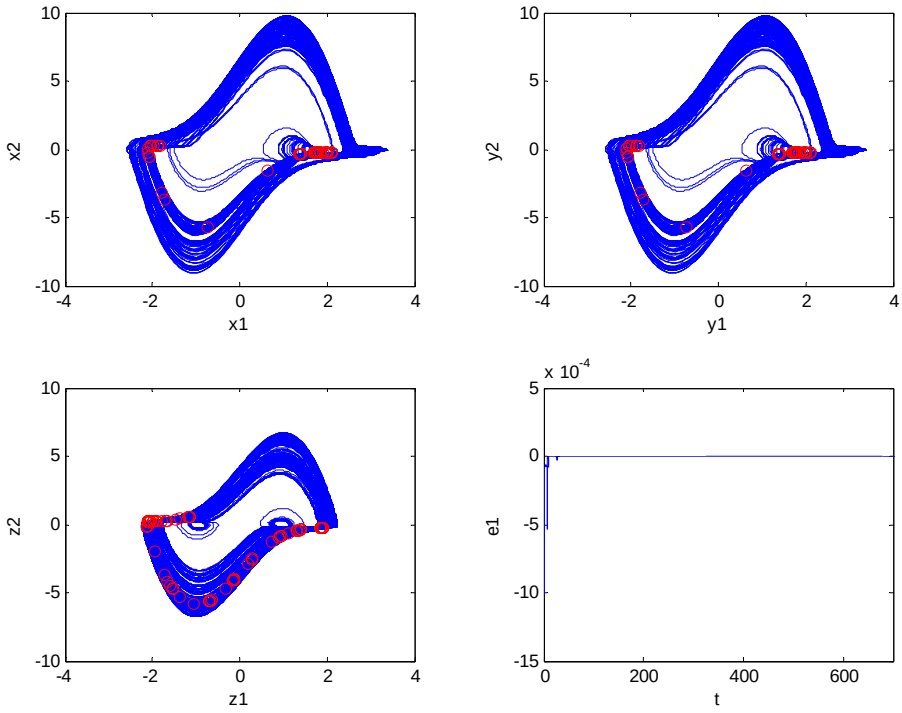

Fig. 3.12 Phase portraits and Poincaré maps of the synchronized fractional order systems and time history of states error for $Z = gz_1 \sin(\omega t)$ with order $\alpha = \beta = 1$, ω=0.12961875, g=3 .

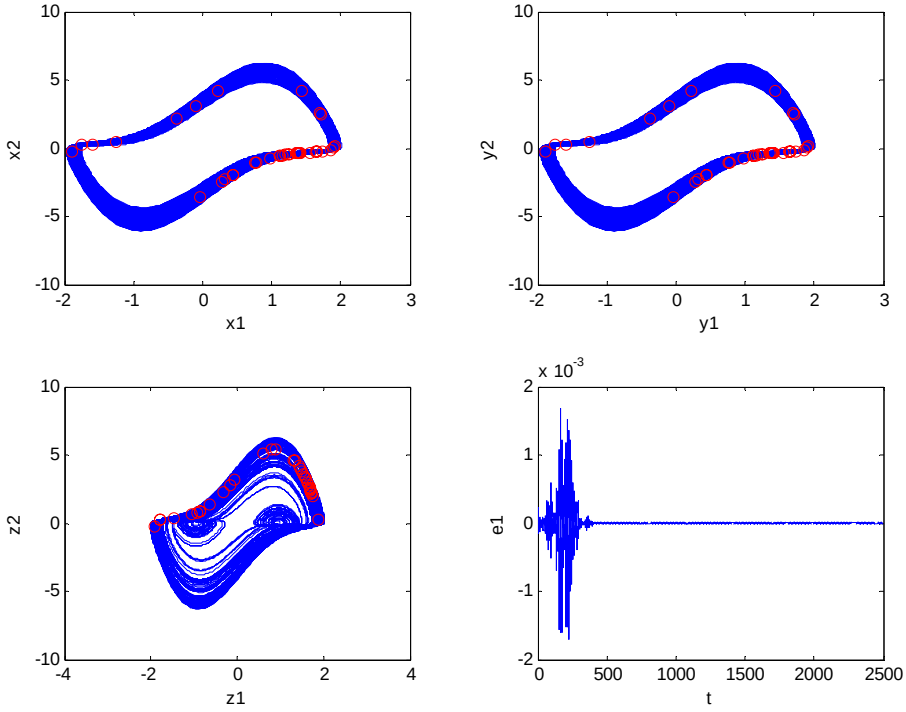

Fig. 3.13 Phase portraits and Poincaré maps of the synchronized fractional order systems and time history of states error for $Z = gz_1 \sin(\omega t)$ with order $\alpha = \beta = 0.9$, ω=0.132, g=0.5 .

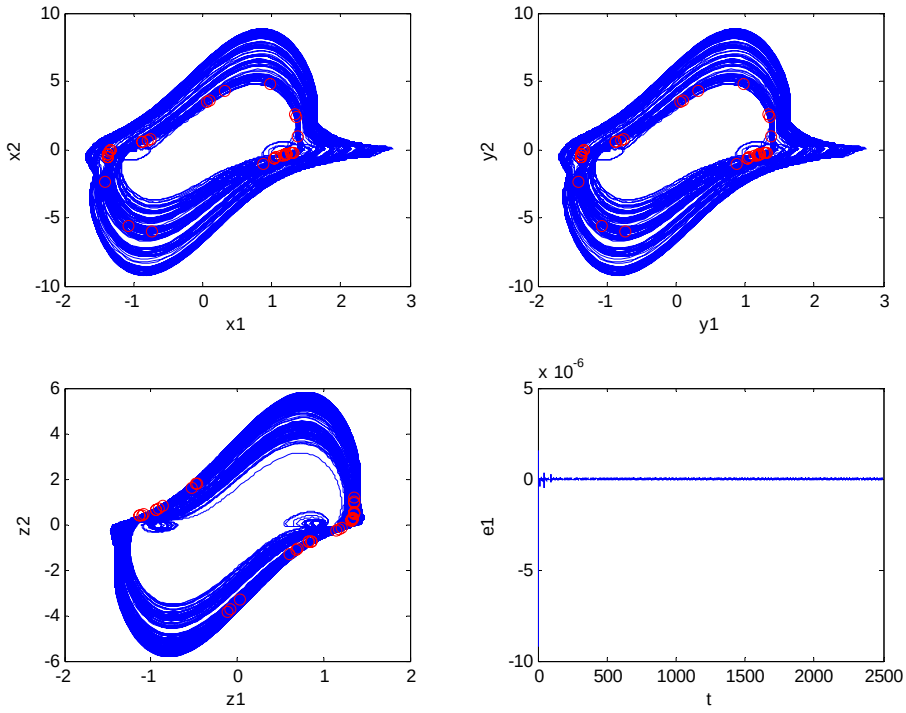

Fig. 3.14 Phase portraits and Poincaré maps of the synchronized fractional order systems and time history of states error for $Z = gz_1 \sin(\omega t)$ with order $\alpha = \beta = 0.8$, ω=0.1315, g=5 .

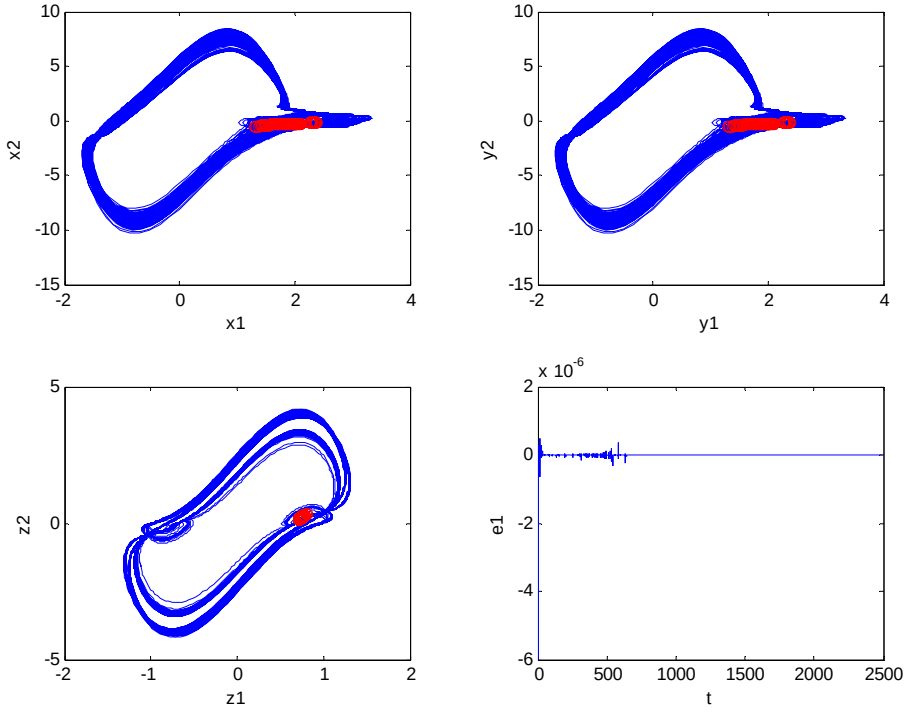

Fig. 3.15 Phase portraits and Poincaré maps of the synchronized fractional order systems and time history of states error for $Z = gz_1 \sin(\omega t)$ with order $\alpha = \beta = 0.7$, ω=0.31812, g=10 .

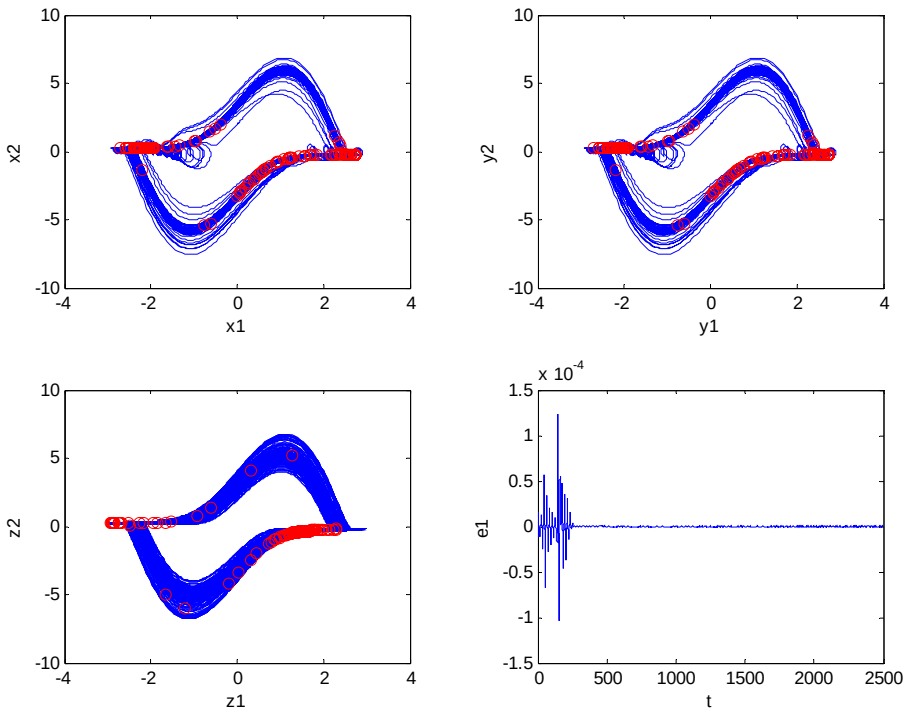

Fig. 3.16 Phase portraits and Poincaré maps of the synchronized fractional order systems and time history of states error for $Z = gz_2 \sin(\omega t)$ with order $\alpha = \beta = 1.1$, ω=0.445, g=1 .

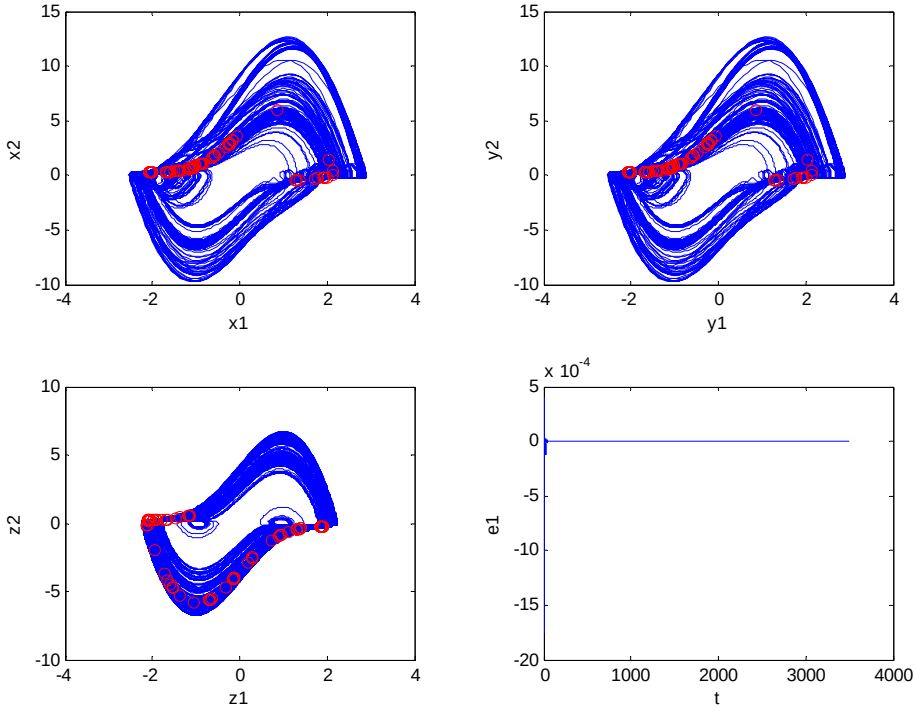

Fig. 3.17 Phase portraits and Poincaré maps of the synchronized fractional order systems and time history of states error for $Z = gz_2 \sin(\omega t)$ with order $\alpha = \beta = 1$, ω=0.12961875, g=3 .

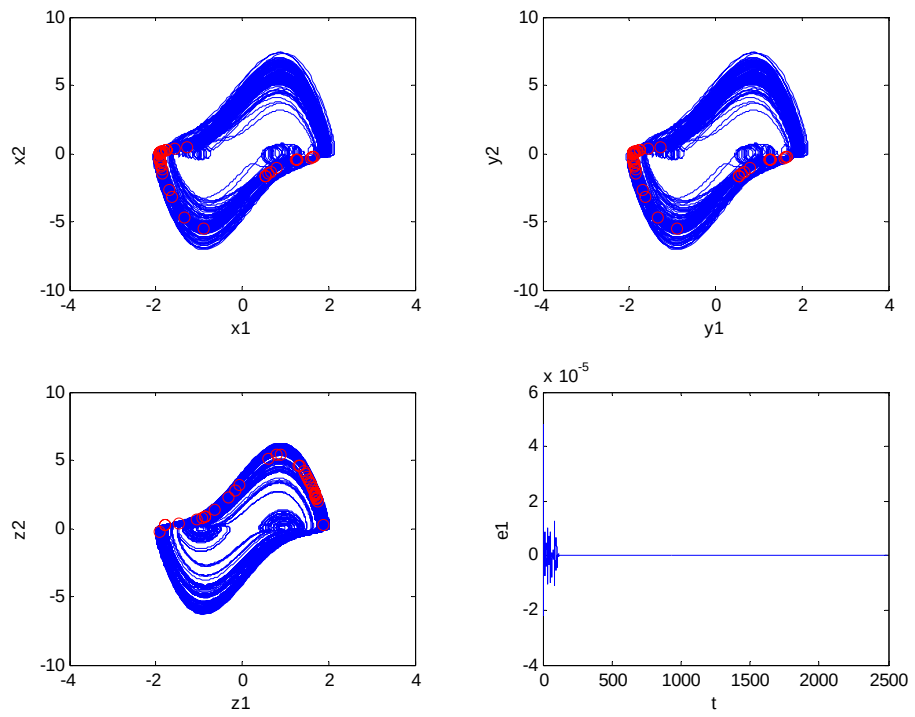

Fig. 3.18 Phase portraits and Poincaré maps of the synchronized fractional order systems and time history of states error for $Z = gz_2 \sin(\omega t)$ with order $\alpha = \beta = 0.9$, ω=0.132, g=1 .

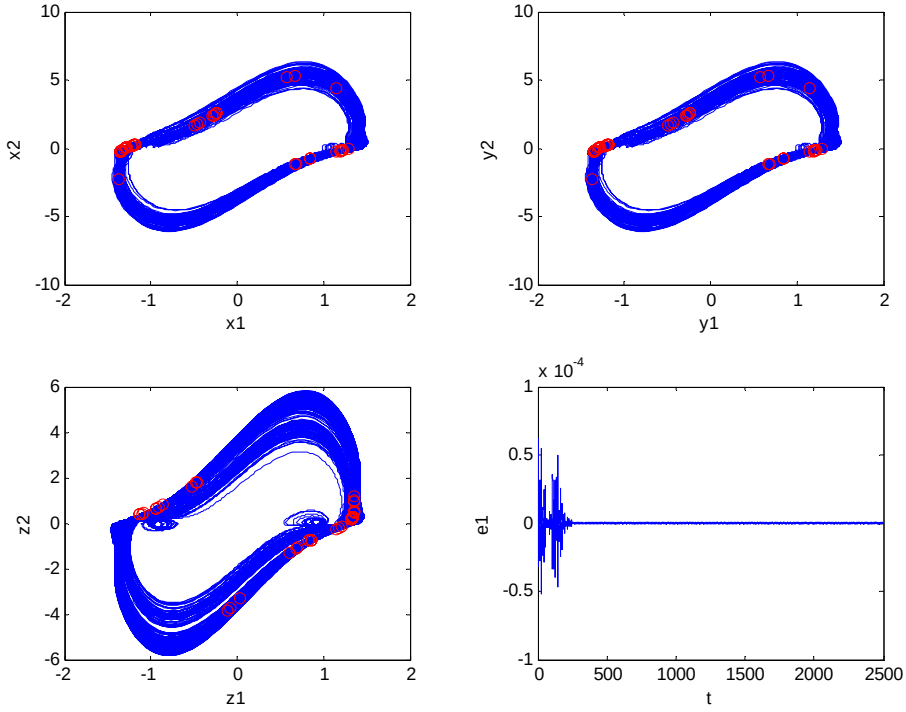

Fig. 3.19 Phase portraits and Poincaré maps of the synchronized fractional order systems and time history of states error for $Z = gz_2 \sin(\omega t)$ with order $\alpha = \beta = 0.8$, ω=0.1315, g=0.5 .

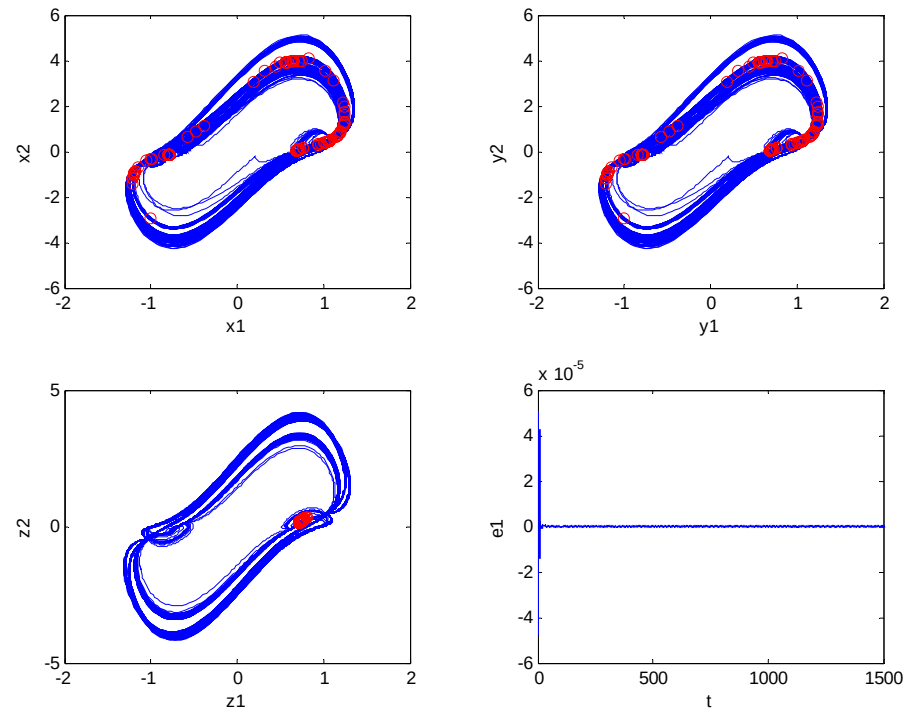

Fig. 3.20 Phase portraits and Poincaré maps of the synchronized fractional order systems and time history of states error for $Z = gz_2 \sin(\omega t)$ with order $\alpha = \beta = 0.7$, ω=0.31812, g=0.5 .

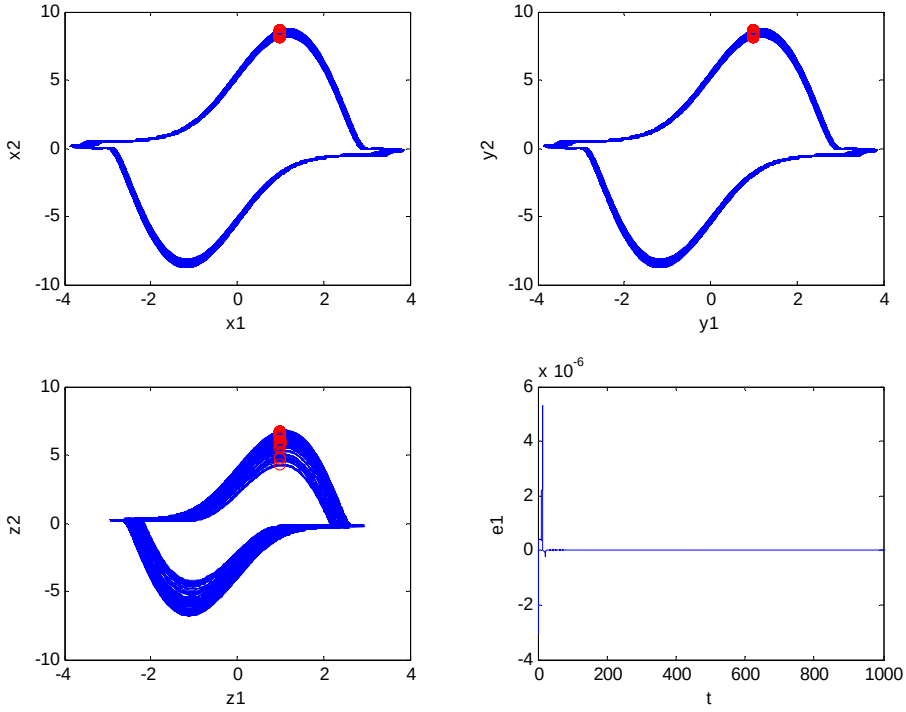

Fig. 3.21 Phase portraits and Poincaré maps of the synchronized fractional order systems and time history of states error for $Z = bgz_1$ with order $\alpha = \beta = \gamma = 1.1$, ω=0.34, g=1.5 .

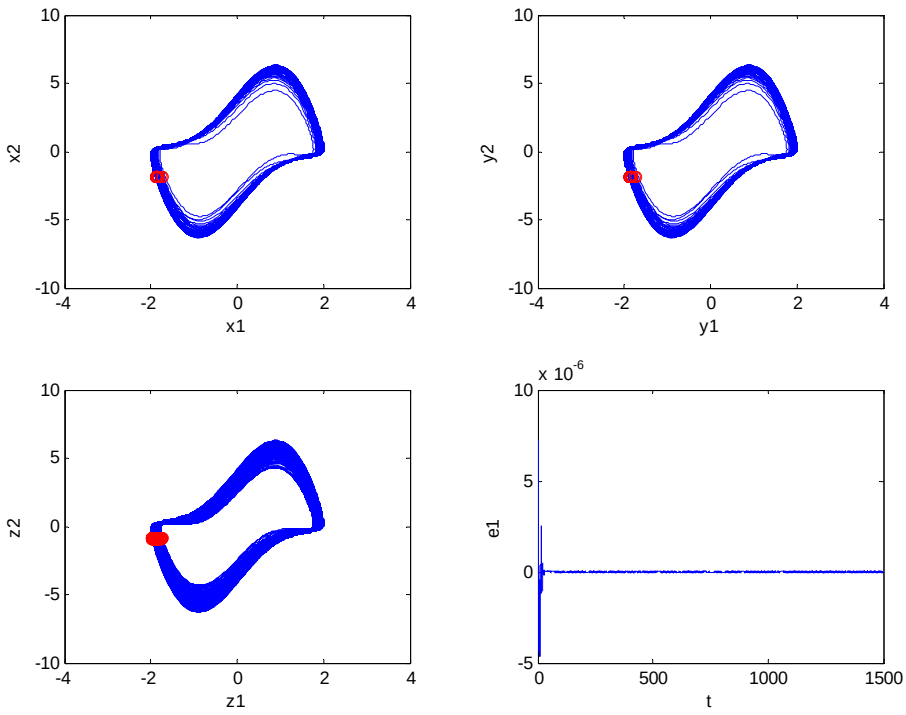

Fig. 3.22 Phase portraits and Poincaré maps of the synchronized fractional order systems and time history of states error for $Z = bgz_1$ with order $\alpha = \beta = 0.9,\ \gamma = 1.1,\ \omega$=0.62, g=0.5 .

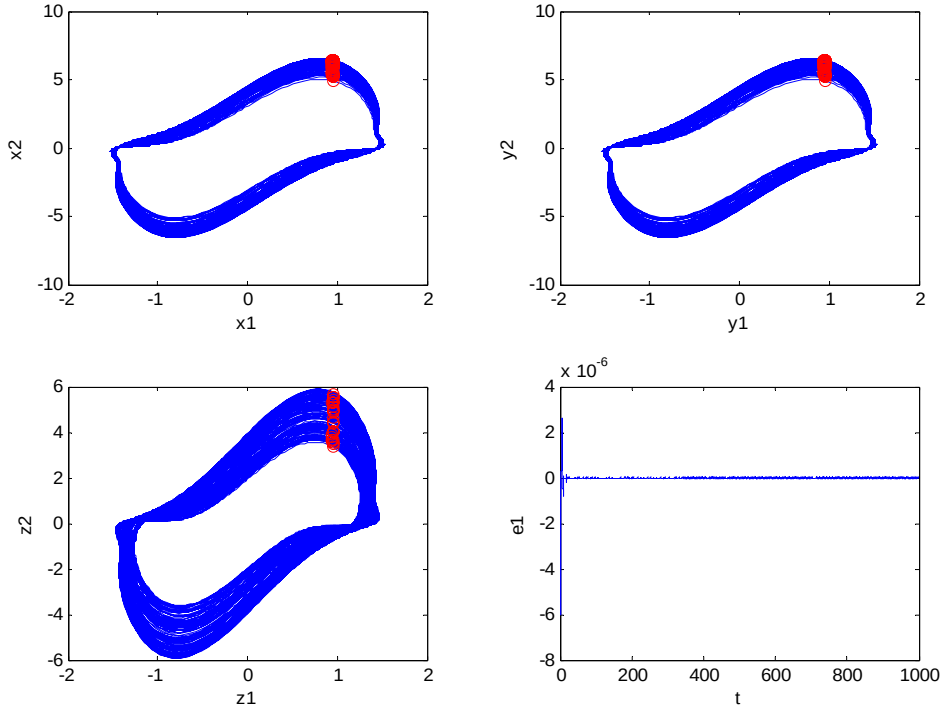

Fig. 3.23 Phase portraits and Poincaré maps of the synchronized fractional order systems and time history of states error for $Z = bgz_1$ with order $\alpha = \beta = 0.8,\ \gamma = 1.1,\ \omega$=0.2807, g=1 .

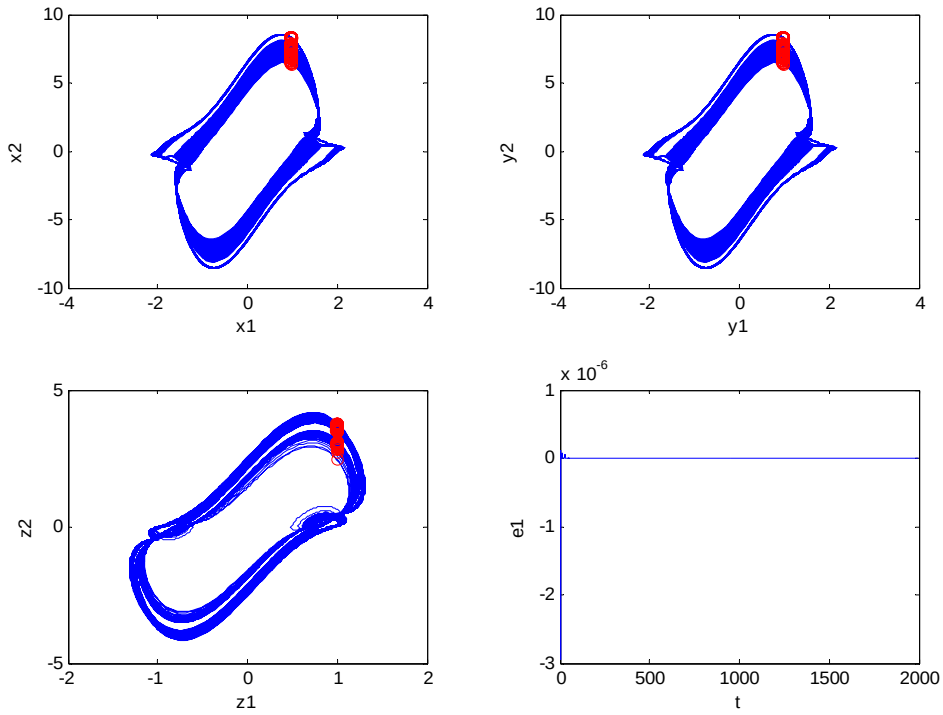

Fig. 3.24 Phase portraits and Poincaré maps of the synchronized fractional order systems and time history of states error for $Z = bgz_1$ with order $\alpha = \beta = 0.7,\ \gamma = 1.1,\ \omega$=0.144, g=5 .

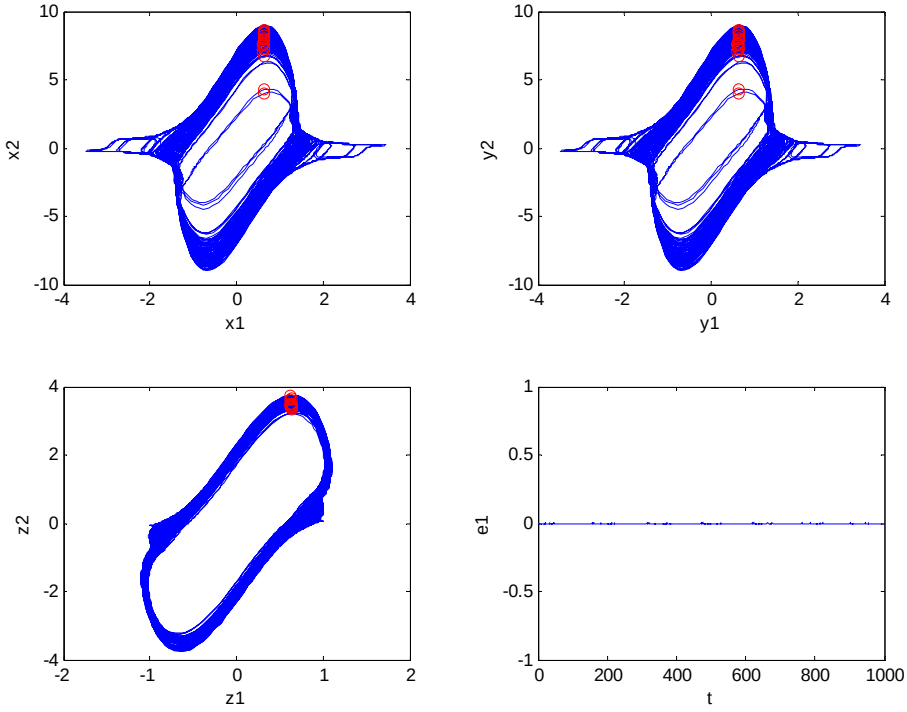

Fig. 3.25 Phase portraits and Poincaré maps of the synchronized fractional order systems and time history of states error for $Z = bgz_1$ with order $\alpha = \beta = 0.6,\ \gamma = 1.1,\ \omega$=0.0107, g=6.6 .

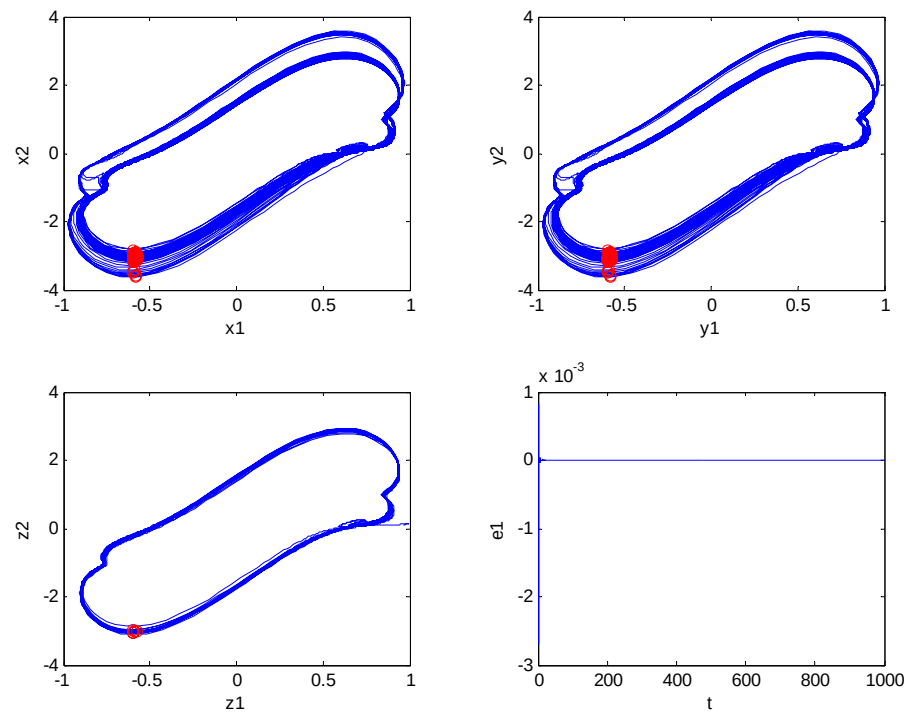

Fig. 3.26 Phase portraits and Poincaré maps of the synchronized fractional order systems and time history of states error for $Z = bgz_1$ with order $\alpha = \beta = 0.5,\ \gamma = 1.1,\ \omega$=0.001, g=0.5 .

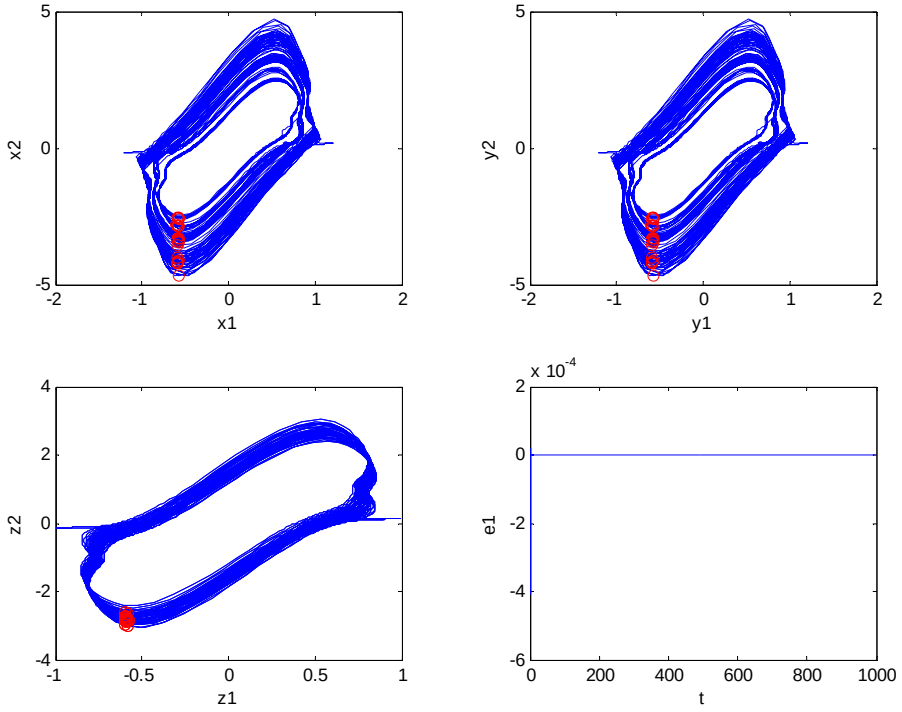

Fig. 3.27 Phase portraits and Poincaré maps of the synchronized fractional order systems and time history of states error for $Z = bgz_1$ with order $\alpha = \beta = 0.4,\ \gamma = 1.1,\ \omega$=0.005, g=0.5 .

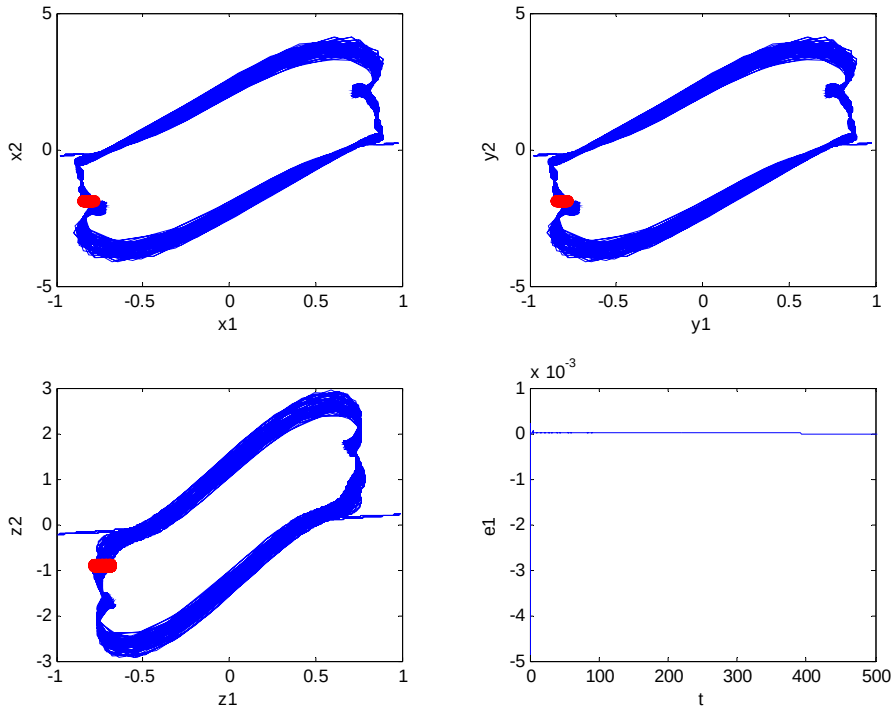

Fig. 3.28 Phase portraits and Poincaré maps of the synchronized fractional order systems and time history of states error for $Z = bgz_1$ with order $\alpha = \beta = 0.3,\ \gamma = 1.1,\ \omega$=0.0017, g=1 .

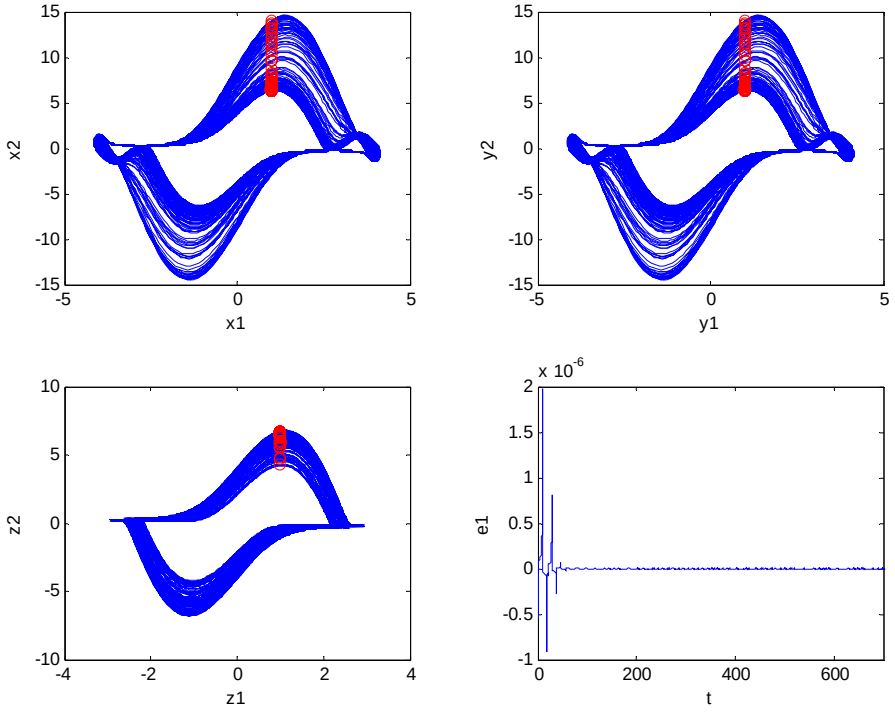

Fig. 3.29 Phase portraits and Poincaré maps of the synchronized fractional order systems and time history of states error for $Z = bgz_2$ with order $\alpha = \beta = \gamma = 1.1$, ω=0.34, g=4 .

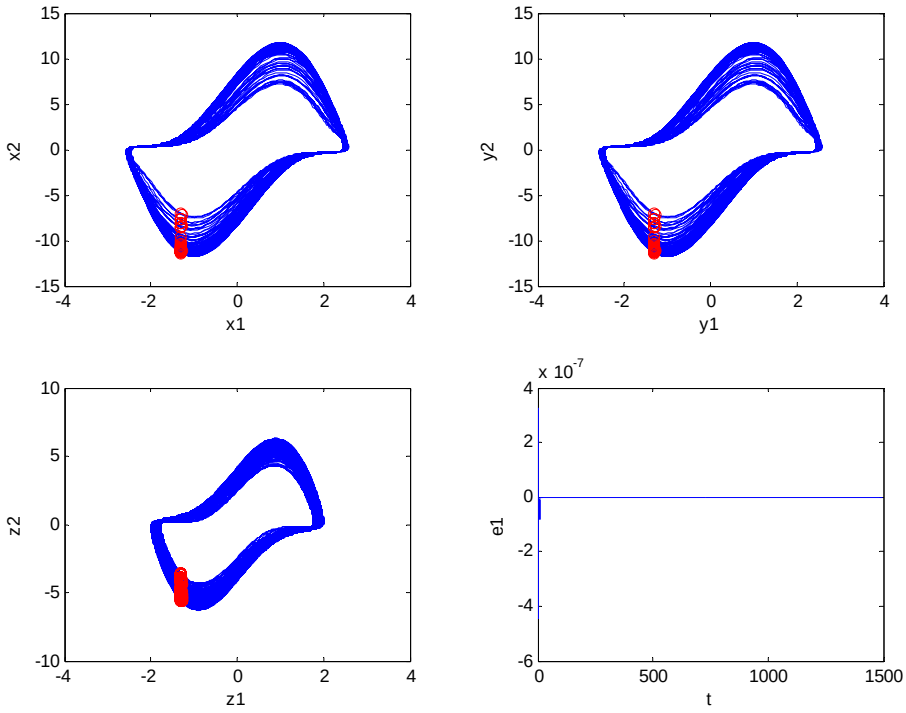

Fig. 3.30 Phase portraits and Poincaré maps of the synchronized fractional order systems and time history of states error for $Z = bgz_2$ with order $\alpha = \beta = 0.9$, $\gamma = 1.1$, ω=0.62, g=3 .

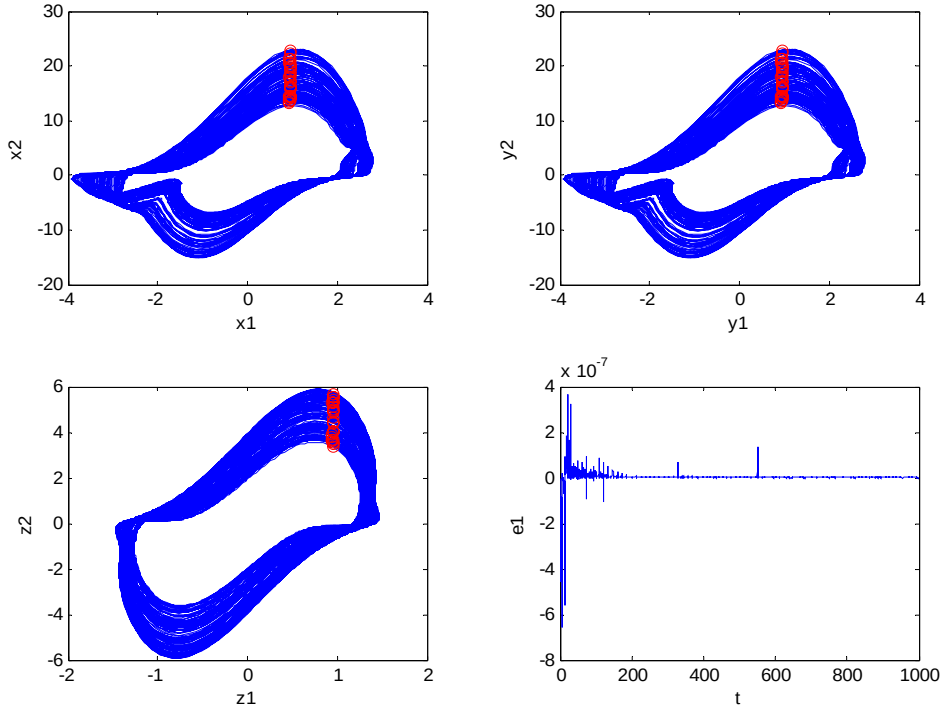

Fig. 3.31 Phase portraits and Poincaré maps of the synchronized fractional order systems and time history of states error for $Z = bgz_2$ with order $\alpha = \beta = 0.8,\ \gamma = 1.1,\ \omega$ =0.2807, g=13.5 .

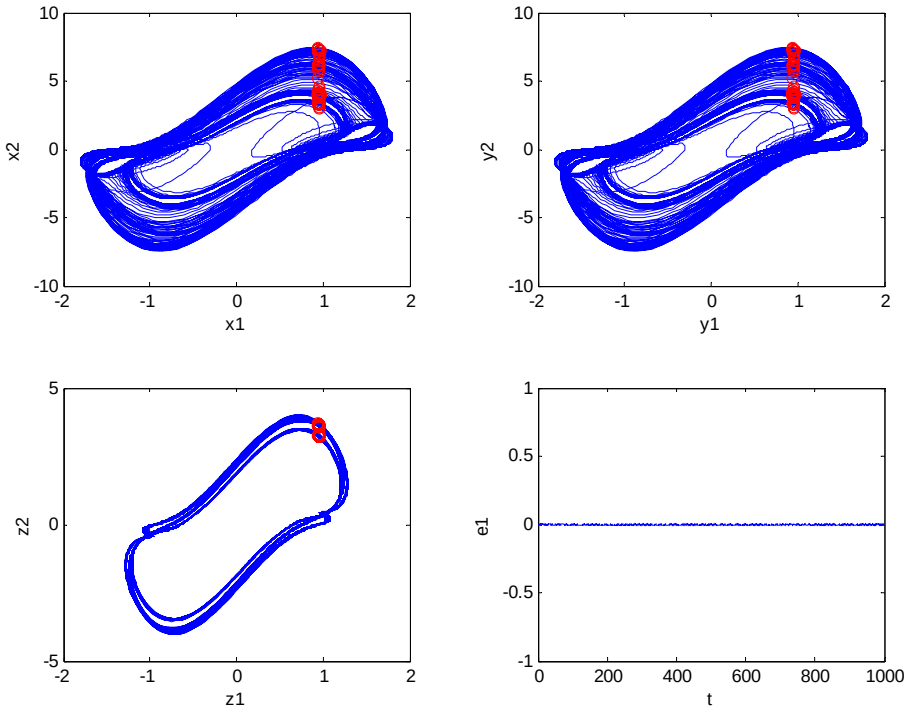

Fig. 3.32 Phase portraits and Poincaré maps of the synchronized fractional order systems and time history of states error for $Z = bgz_2$ with order $\alpha = \beta = 0.7,\ \gamma = 1.1,\ \omega$ =0.144, g=3 .

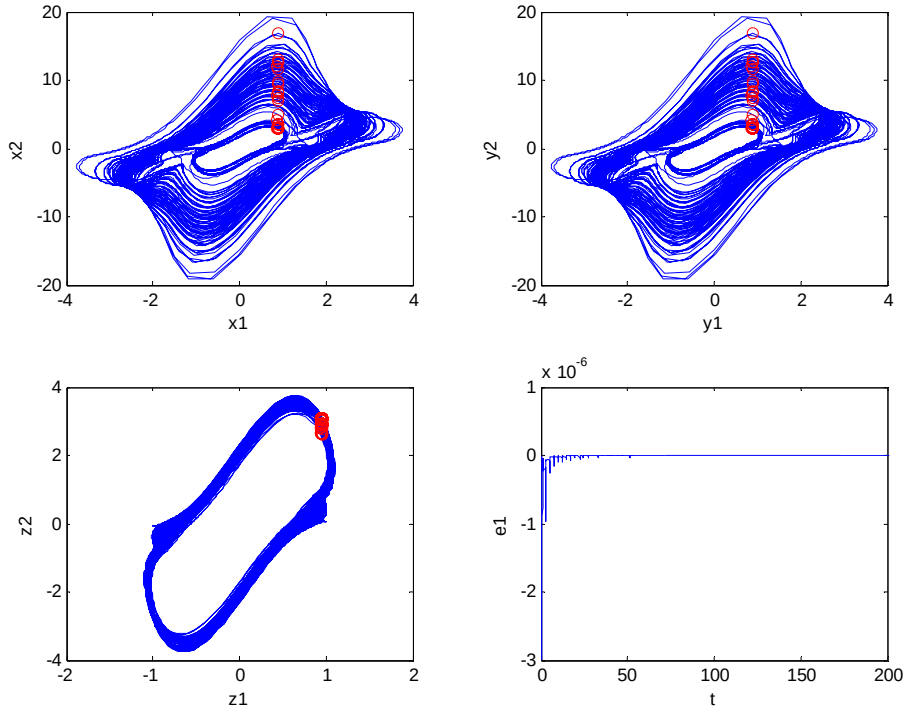

Fig. 3.33 Phase portraits and Poincaré maps of the synchronized fractional order systems and time history of states error for $Z = bgz_2$ with order $\alpha = \beta = 0.6,\ \gamma = 1.1,\ \omega$ =0.0107, g=21.3 .

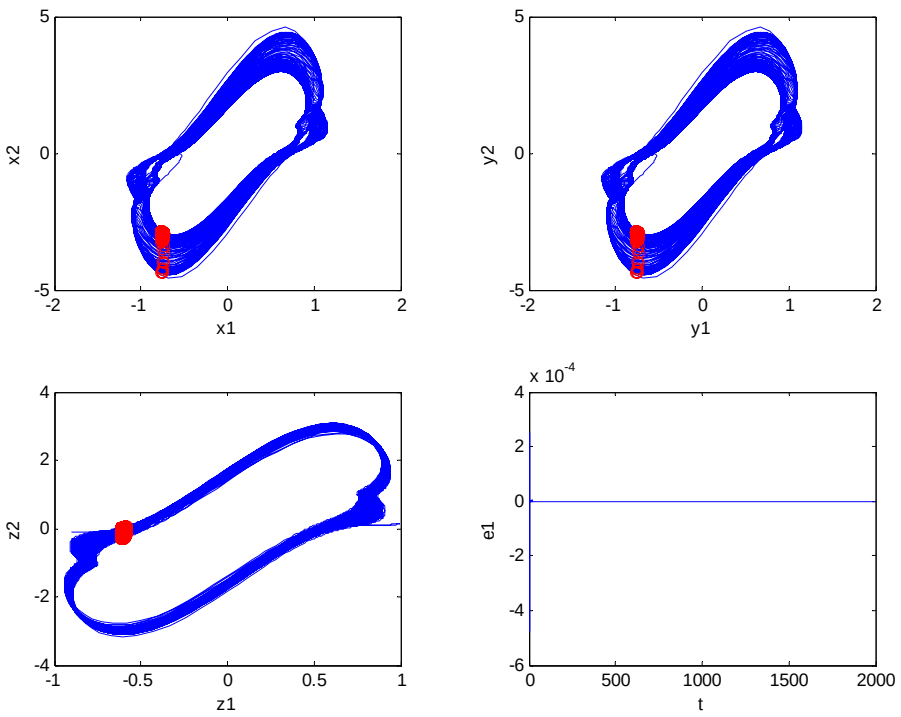

Fig. 3.34 Phase portraits and Poincaré maps of the synchronized fractional order systems and time history of states error for $Z = bgz_2$ with order $\alpha = \beta = 0.5,\ \gamma = 1.1,\ \omega$ =0.001, g=1 .

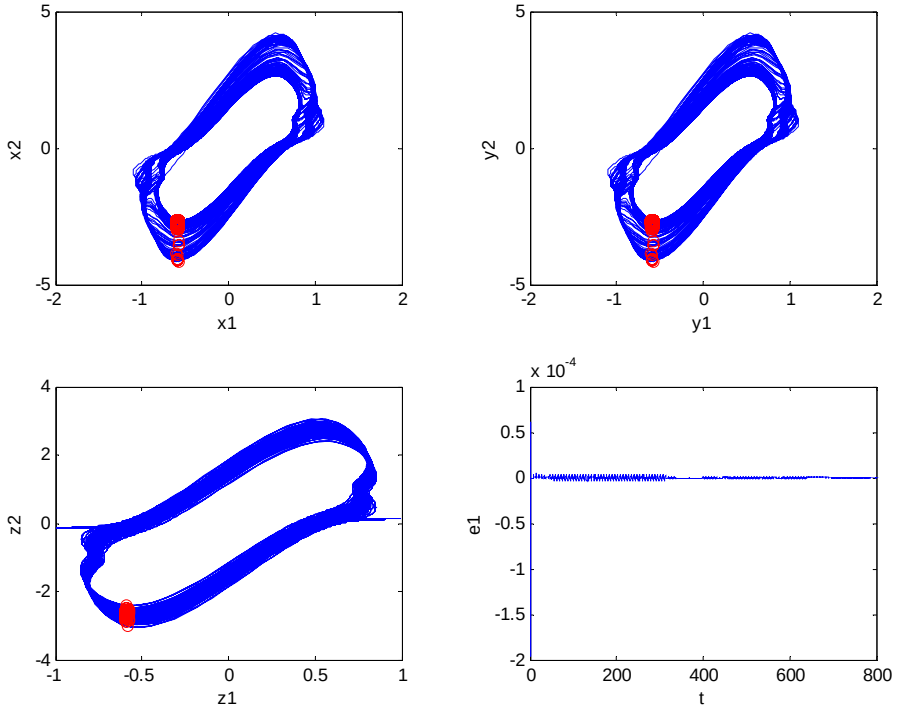

Fig. 3.35 Phase portraits and Poincaré maps of the synchronized fractional order systems and time history of states error for $Z = bgz_2$ with order $\alpha = \beta = 0.4,\ \gamma = 1.1,\ \omega$ =0.005, g=1 .

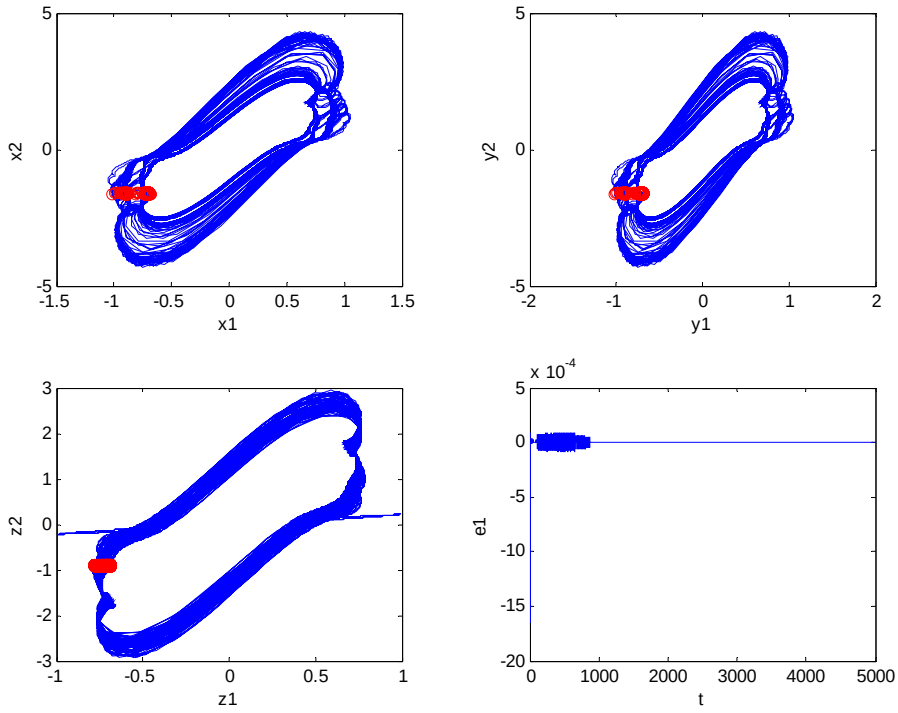

Fig. 3.36 Phase portraits and Poincaré maps of the synchronized fractional order systems and time history of states error for $Z = bgz_2$ with order $\alpha = \beta = 0.3,\ \gamma = 1.1,\ \omega$ =0.0017, g=1 .

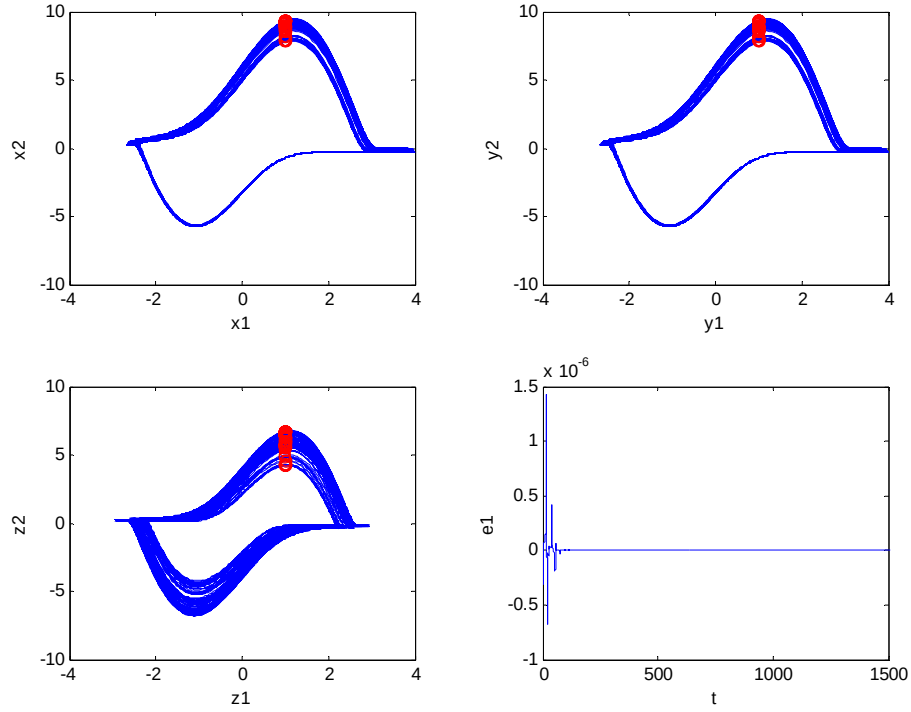

Fig. 3.37 Phase portraits and Poincaré maps of the synchronized fractional order systems and time history of error for $Z = bge^{z_1}$ with order $\alpha = \beta = \gamma = 1.1$, ω=0.34, g=0.29 .

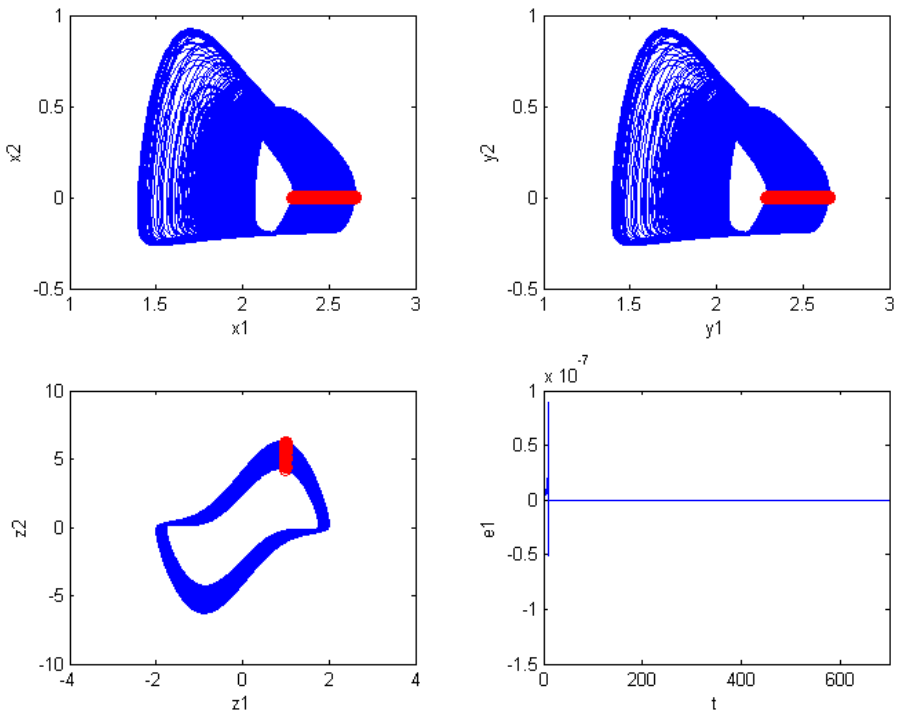

Fig. 3.38 Phase portraits and Poincaré maps of the synchronized fractional order systems and time history of states error for $Z = bge^{z_1}$ with order $\alpha = \beta = 0.9$, $\gamma = 1.1$, ω=0.555, g=1 .

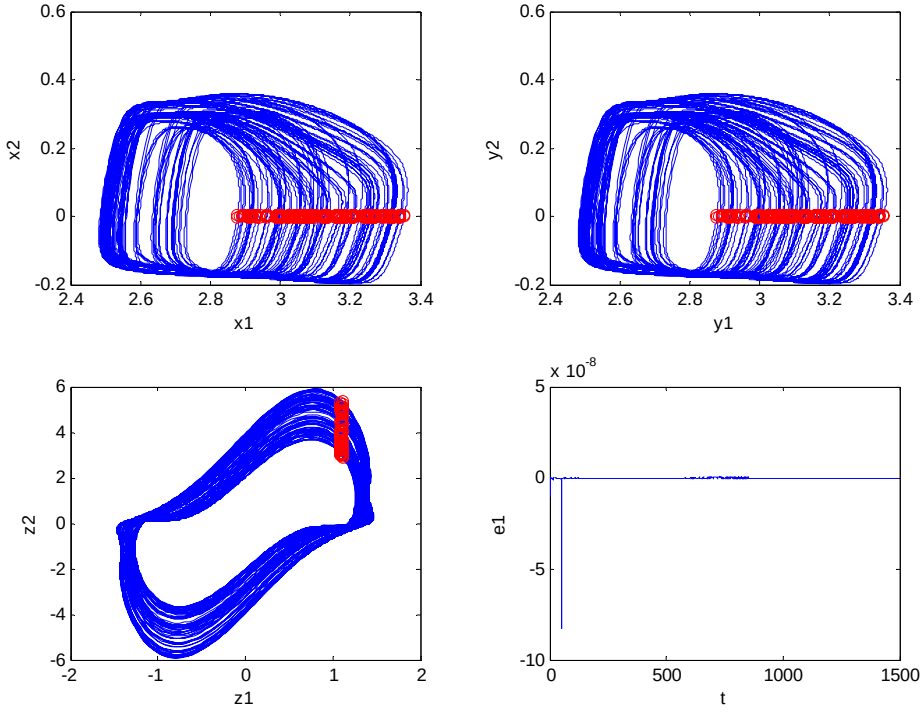

Fig. 3.39 Phase portraits and Poincaré maps of the synchronized fractional order systems and time history of states error for $Z = bge^{z_1}$ with order $\alpha = \beta = 0.8,\ \gamma = 1.1, \omega$ =0.2807, g=1.8 .

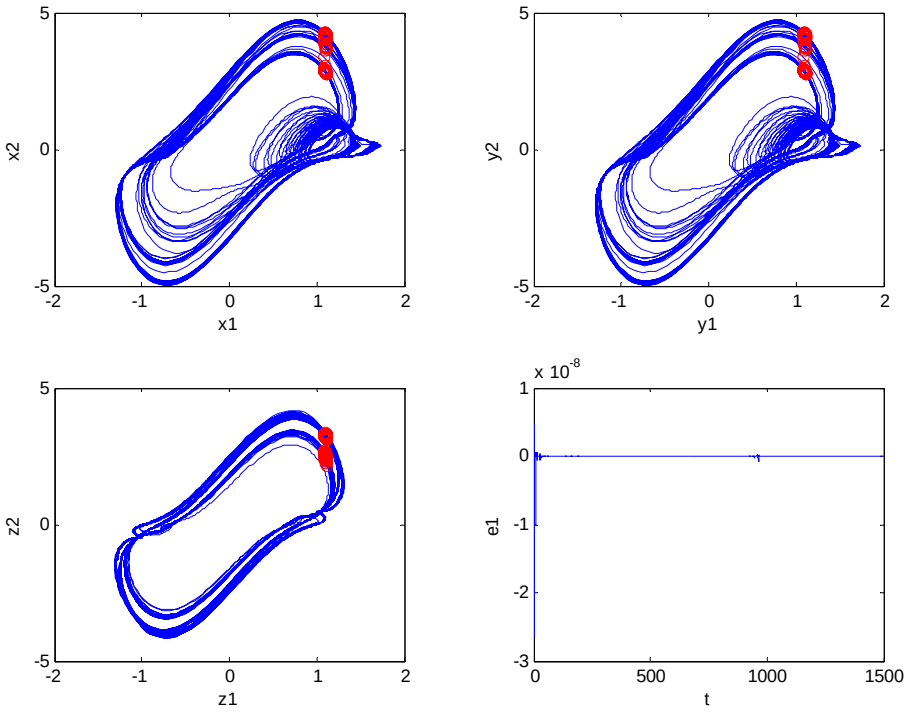

Fig. 3.40 Phase portraits and Poincaré maps of the synchronized fractional order systems and time history of states error for $Z = bge^{z_1}$ with order $\alpha = \beta = 0.7,\ \gamma = 1.1,\ \omega$ =0.144, g=1 .

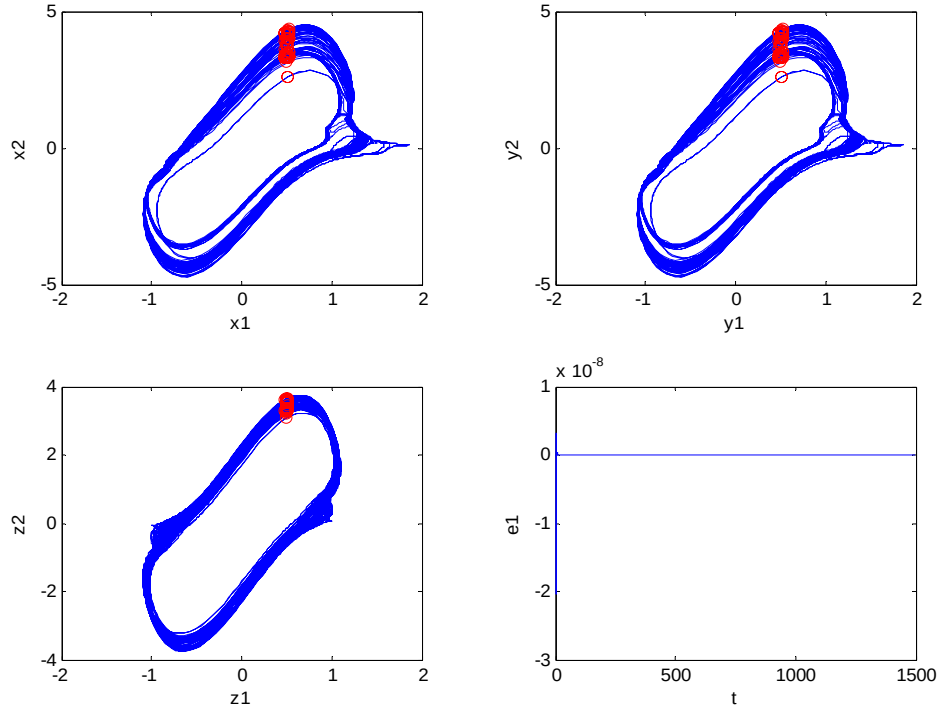

Fig. 3.41 Phase portraits and Poincaré maps of the synchronized fractional order systems and time history of states error for $Z = bge^{z_1}$ with order $\alpha = \beta = 0.6,\ \gamma = 1.1,\ \omega$ =0.0107, g=1 .

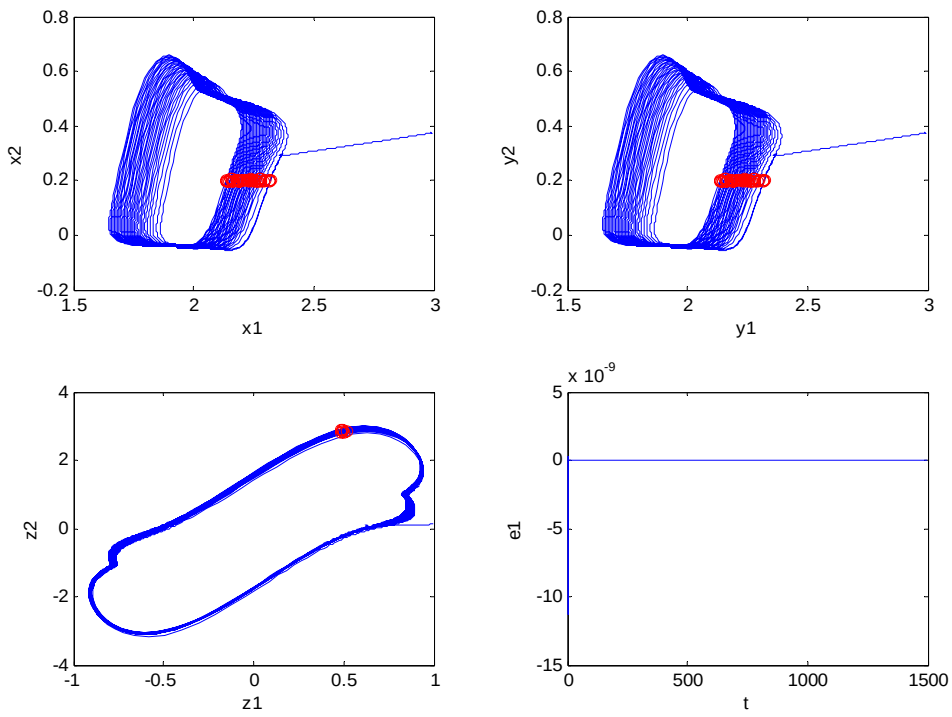

Fig. 3.42 Phase portraits and Poincaré maps of the synchronized fractional order systems and time history of states error for $Z = bge^{z_1}$ with order $\alpha = \beta = 0.5,\ \gamma = 1.1,\ \omega$ =0.001, g=3 .

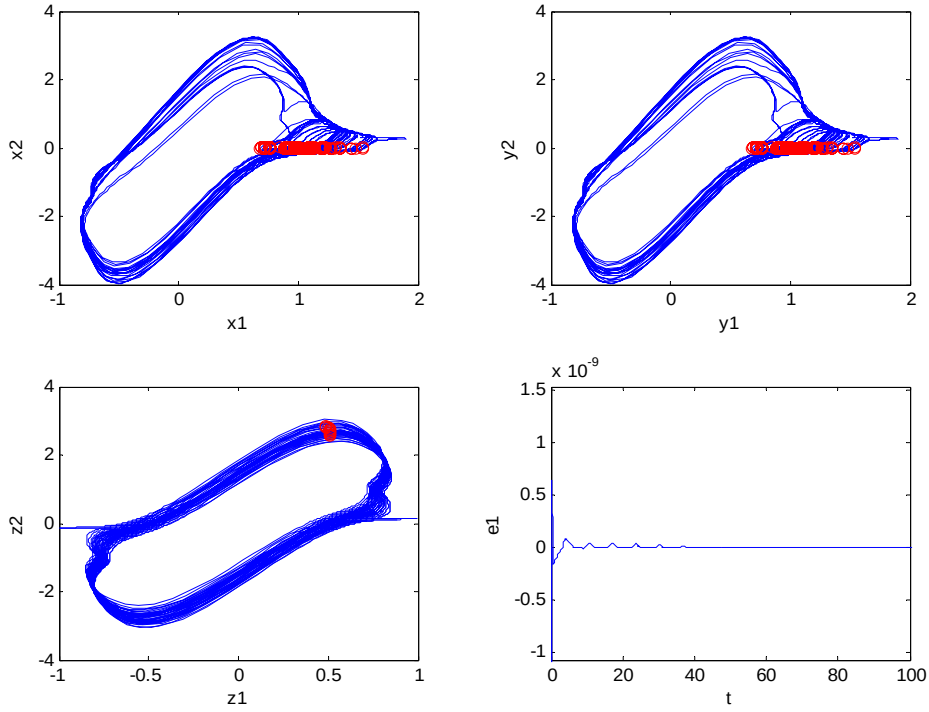

Fig. 3.43 Phase portraits and Poincaré maps of the synchronized fractional order systems and time history of states error for $Z = bge^{z_1}$ with order $\alpha = \beta = 0.4,\ \gamma = 1.1,\ \omega$ =0.005, g=1.5 .

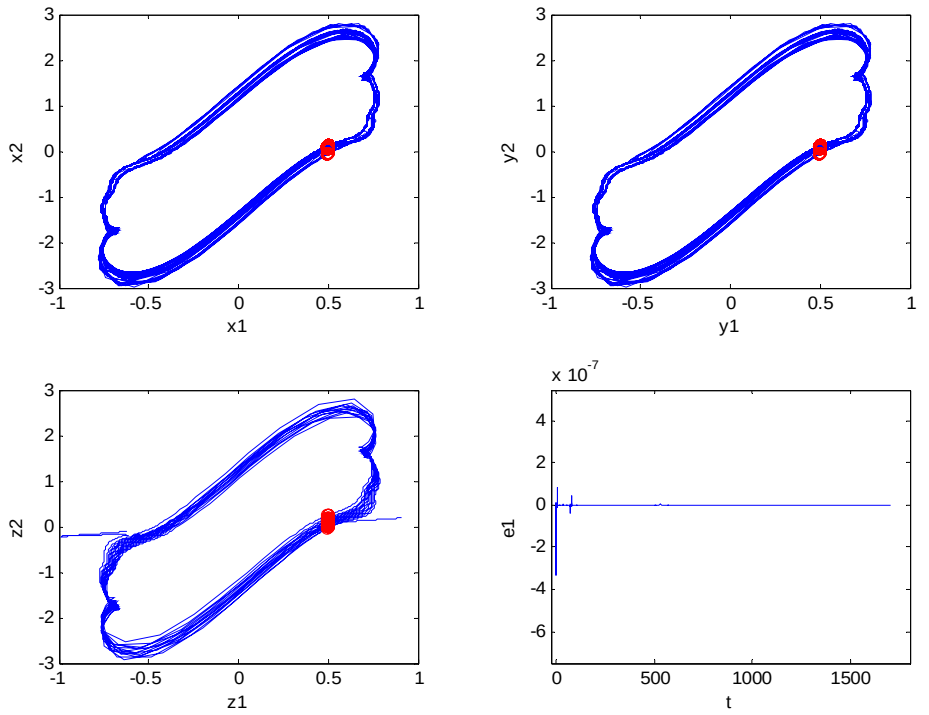

Fig. 3.44 Phase portraits and Poincaré maps of the synchronized fractional order systems and time history of states error for $Z = bge^{z_1}$ with order $\alpha = \beta = 0.3,\ \gamma = 1.1, \omega$ =0.0017, g=0.1 .

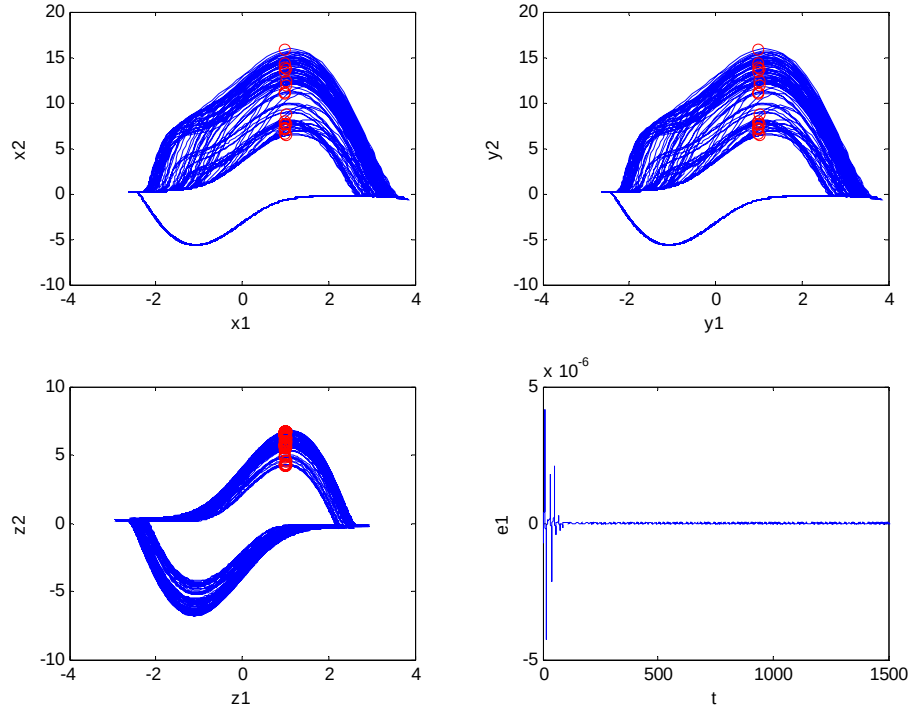

Fig. 3.45 Phase portraits and Poincaré maps of the synchronized fractional order systems and time history of states error for $Z = bge^{z_2}$ with order $\alpha = \beta = \gamma = 1.1$, ω=0.34, g=0.2 .

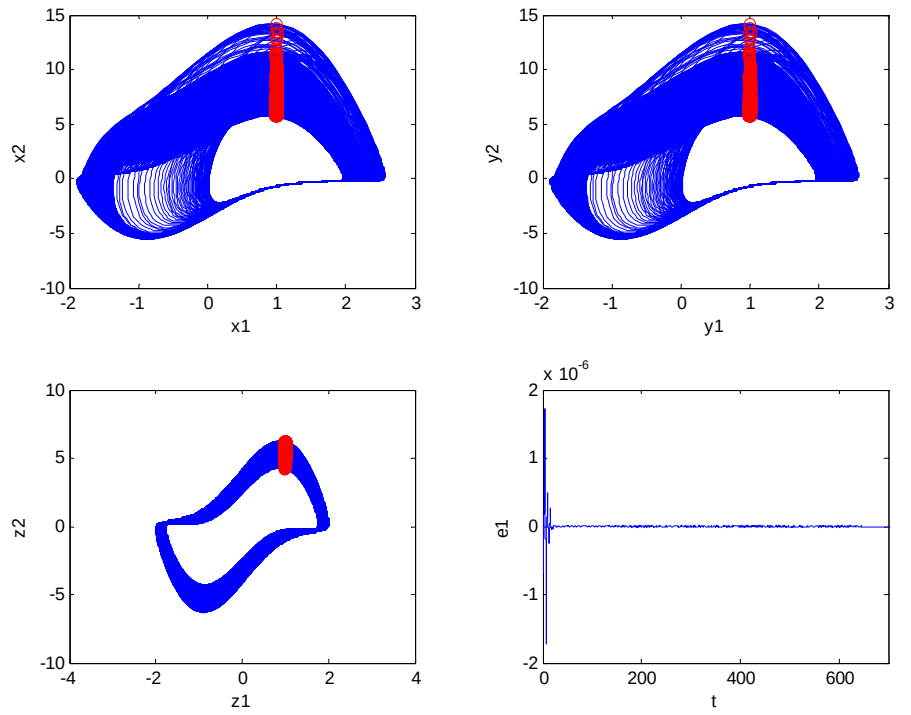

Fig. 3.46 Phase portraits and Poincaré maps of the synchronized fractional order systems and time history of states error for $Z = bge^{z_2}$ with order $\alpha = \beta = 0.9$, $\gamma = 1.1$, ω=0.555, g=0.1 .

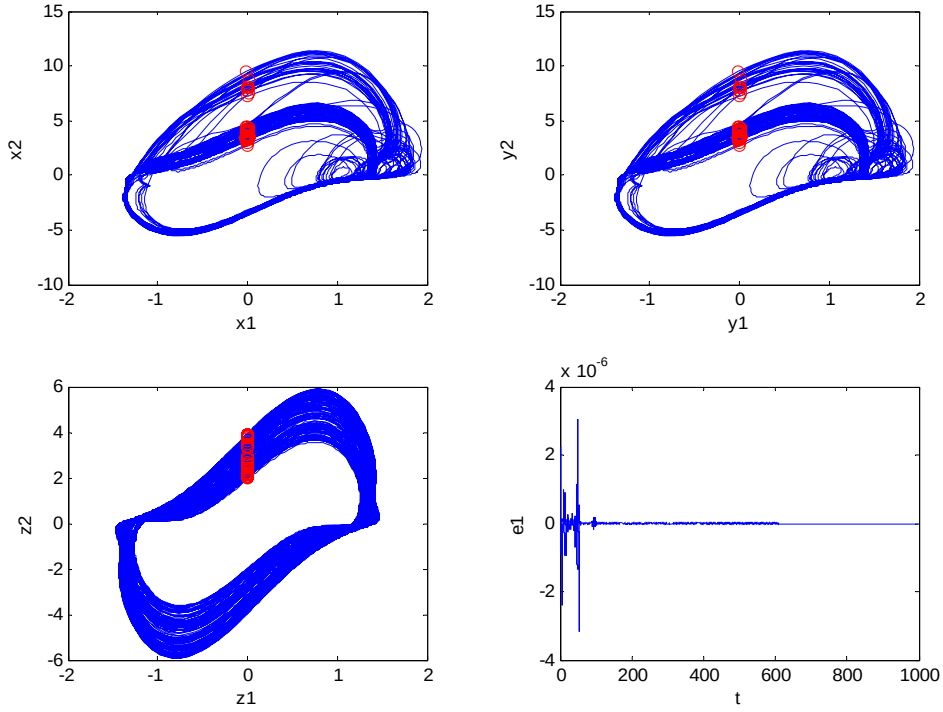

Fig. 3.47 Phase portraits and Poincaré maps of the synchronized fractional order systems and time history of states error for $Z = bge^{z_2}$ with order $\alpha = \beta = 0.8,\ \gamma = 1.1,\ \omega$=02807, g=0.1 .

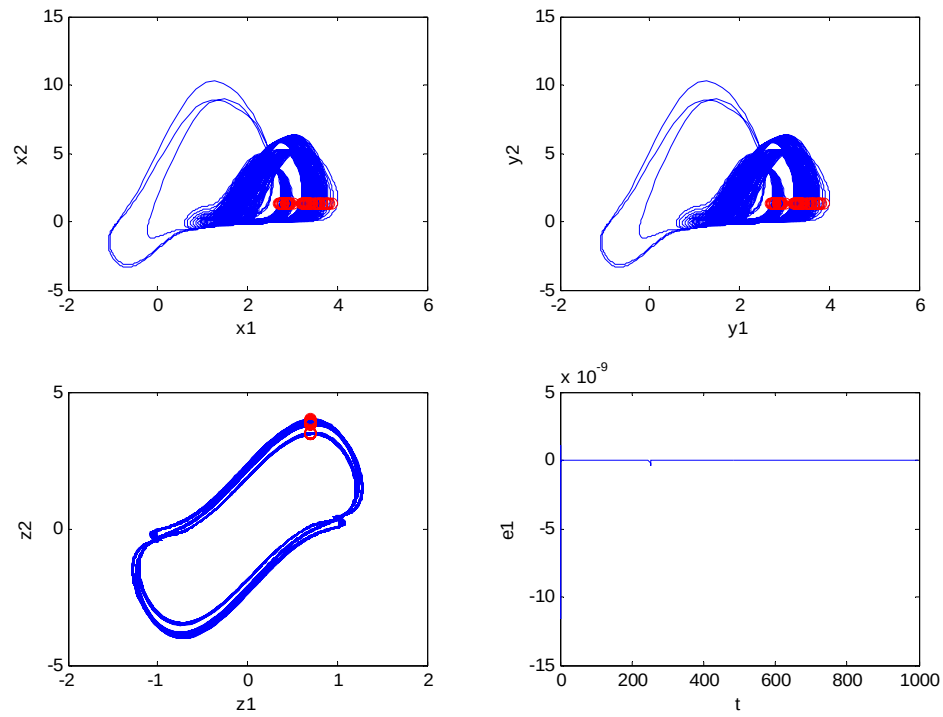

Fig. 3.48 Phase portraits and Poincaré maps of the synchronized fractional order systems and time history of states error for $Z = bge^{z_2}$ with order $\alpha = \beta = 0.7,\ \gamma = 1.1,\ \omega$=0.144, g=1.9 .

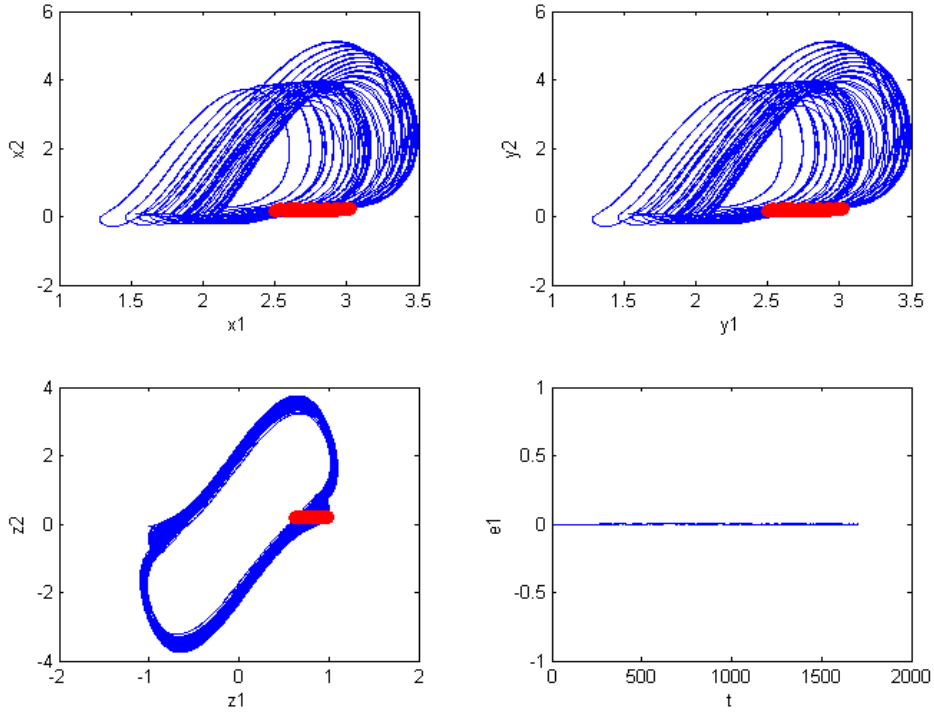

Fig. 3.49 Phase portraits and Poincaré maps of the synchronized fractional order systems and time history of states error for $Z = bge^{z_2}$ with order $\alpha = \beta = 0.6,\ \gamma = 1.1,\ \omega$ =0.0107, g=2 .

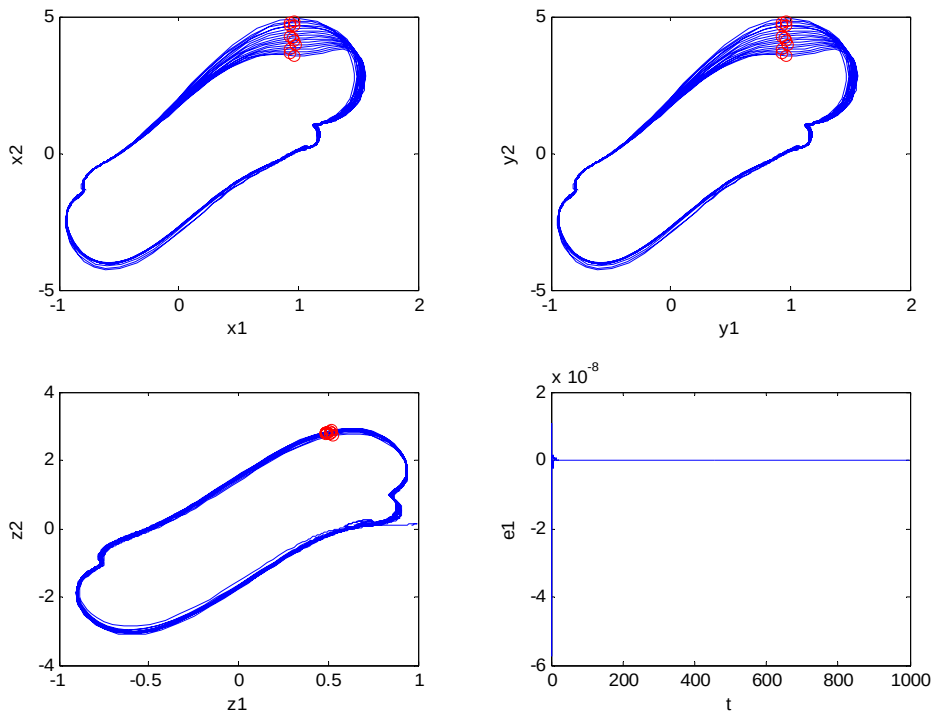

Fig. 3.50 Phase portraits and Poincaré maps of the synchronized fractional order systems and time history of states error for $Z = bge^{z_2}$ with order $\alpha = \beta = 0.5,\ \gamma = 1.1,\ \omega$ =0.001, g=1 .

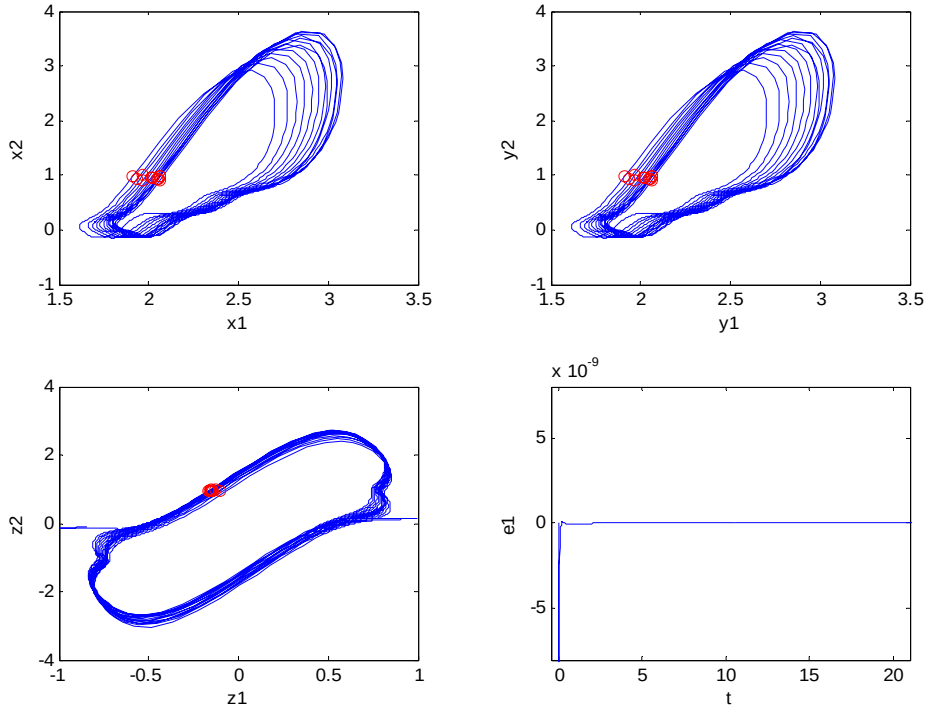

Fig. 3.51 Phase portraits and Poincaré maps of the synchronized fractional order systems and time history of states error for $Z = bge^{z_2}$ with order $\alpha = \beta = 0.4,\ \gamma = 1.1,\ \omega$ =0.005, g=4 .

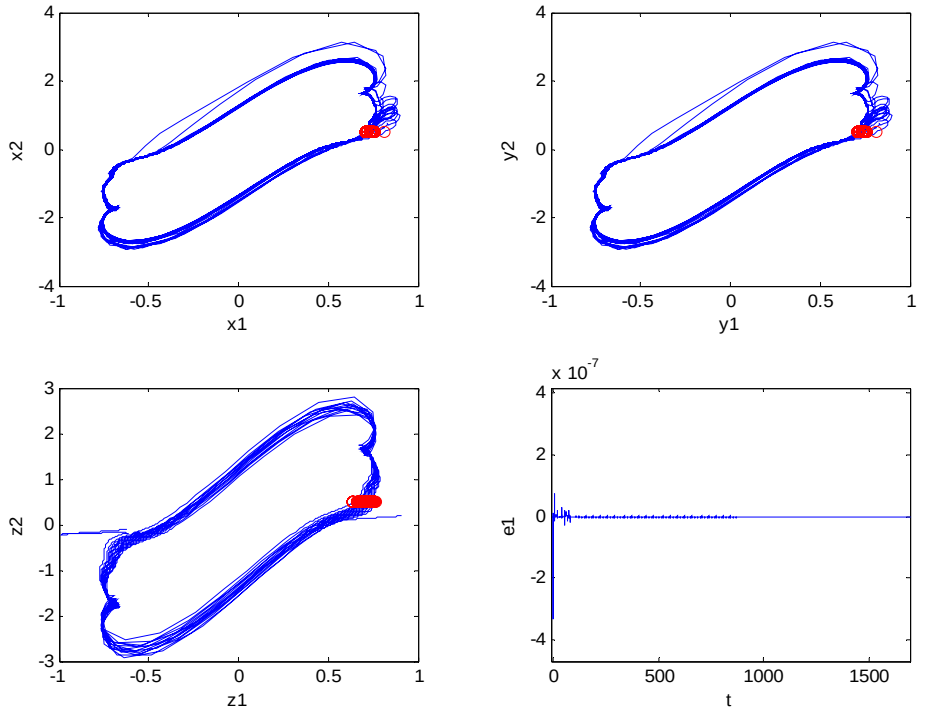

Fig. 3.52 Phase portraits and Poincaré maps of the synchronized fractional order systems and time history of states error for $Z = bge^{z_2}$ with order $\alpha = \beta = 0.3,\ \gamma = 1.1,\ \omega$ =0.0017,g=0.1 .

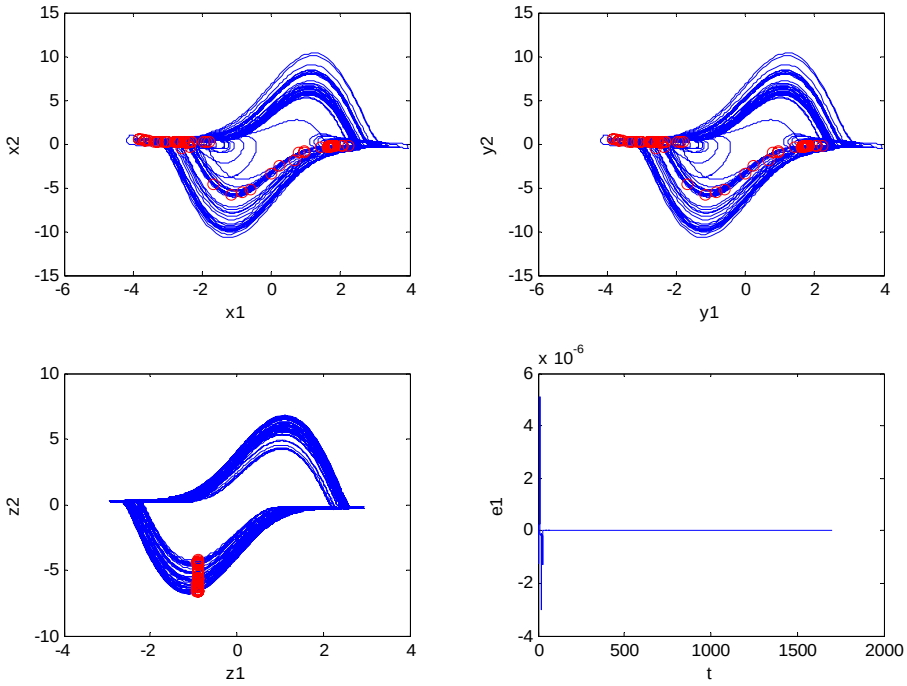

Fig. 3.53 Phase portraits and Poincaré maps of the synchronized fractional order systems and time history of states error for $Z = ge^{z_1}\sin(\omega t)$ with order $\alpha = \beta = \gamma = 1.1$, ω =0.445, ω_z =0.34,g=0.43 .

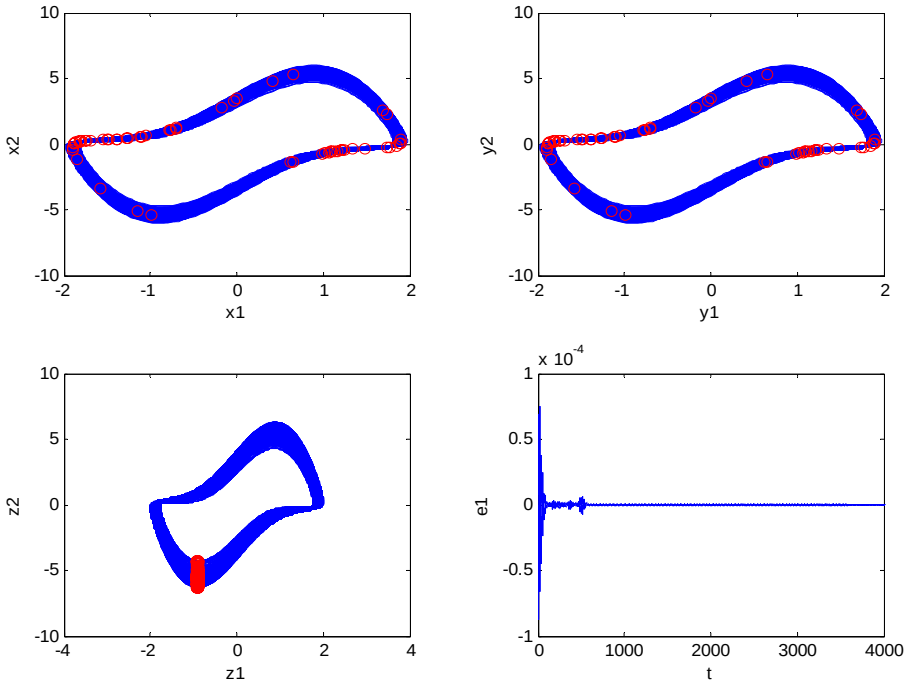

Fig. 3.54 Phase portraits and Poincaré maps of the synchronized fractional order systems and time history of states error for $Z = ge^{z_1}\sin(\omega t)$ with order $\alpha = \beta = 0.9$, $\gamma = 1.1$, ω =0.1275, ω_z =0.555,g=0.1 .

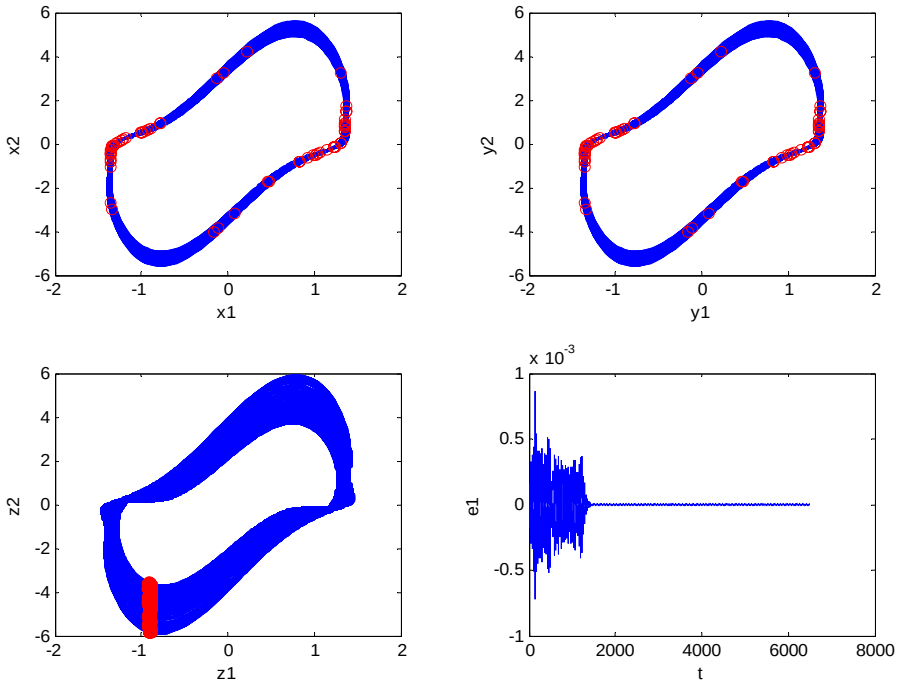

Fig. 3.55 Phase portraits and Poincaré maps of the synchronized fractional order systems and time history of states error for $Z = ge^{z_1}\sin(\omega t)$ with order $\alpha = \beta = 0.8,\ \gamma = 1.1, \omega$ =0.1315, ω_z =0.2807,g=0.1 .

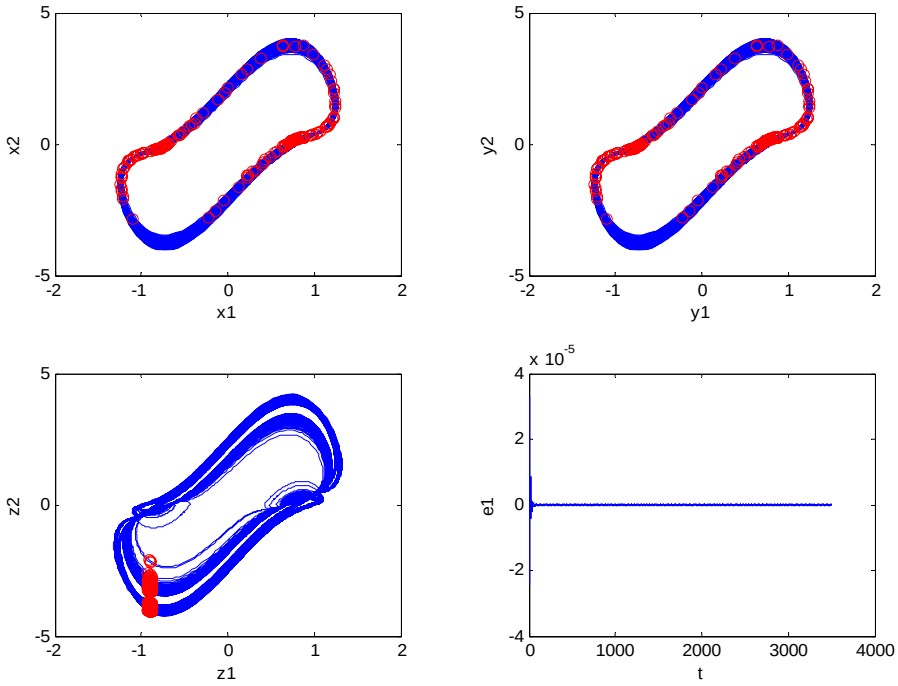

Fig. 3.56 Phase portraits and Poincaré maps of the synchronized fractional order systems and time history of states error for $Z = ge^{z_1}\sin(\omega t)$ with order $\alpha = \beta = 0.7,\ \gamma = 1.1, \omega$ =0.31812, ω_z =0.144,g=0.1 .

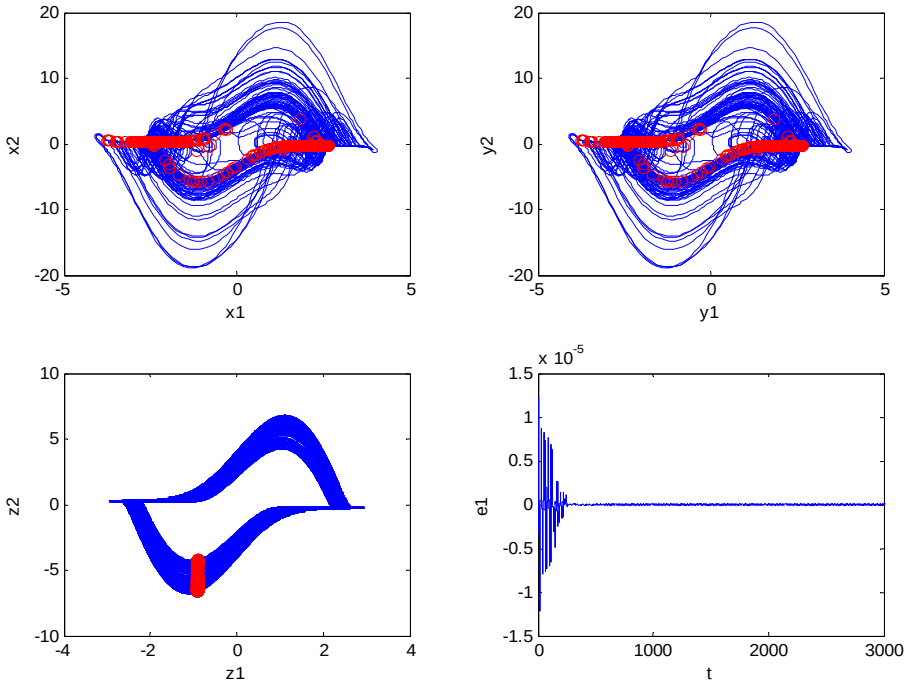

Fig. 3.57 Phase portraits and Poincaré maps of the synchronized fractional order systems and time history of states error for $Z = ge^{z_2}\sin(\omega t)$ with order $\alpha = \beta = \gamma = 1.1$, ω =0.445, ω_z =0.34,g=0.1 .

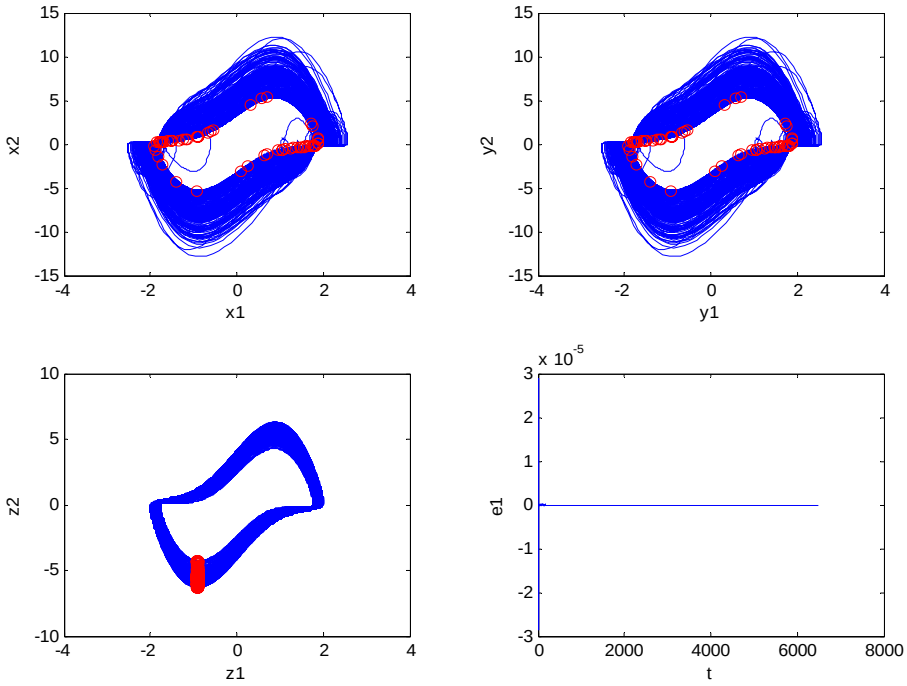

Fig. 3.58 Phase portraits and Poincaré maps of the synchronized fractional order systems and time history of states error for $Z = ge^{z_2}\sin(\omega t)$ with order $\alpha = \beta = 0.9$, $\gamma = 1.1$, ω =0.1275, ω_z =0.555,g=0.1 .

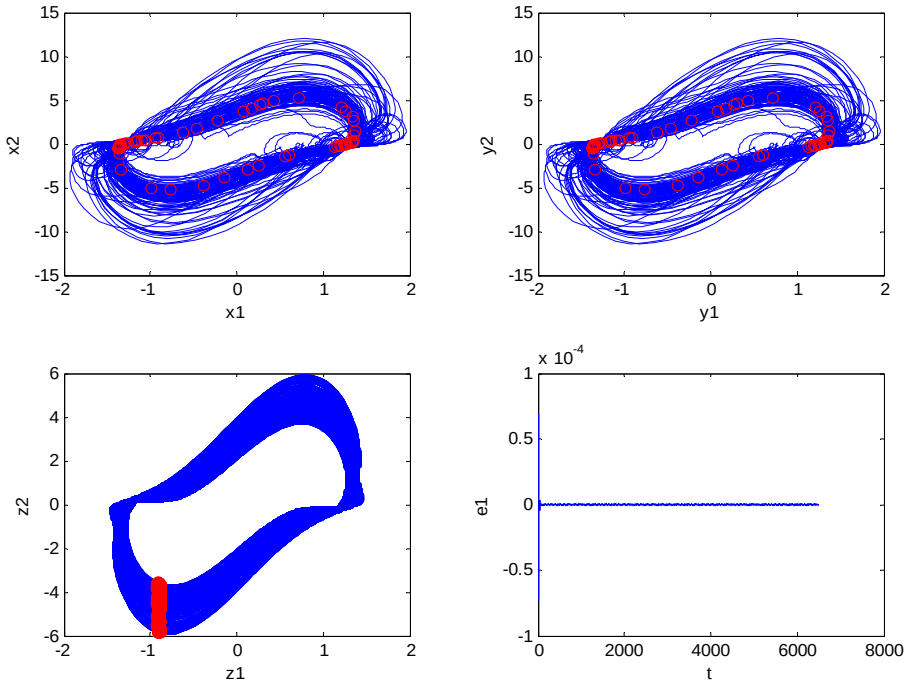

Fig. 3.59 Phase portraits and Poincaré maps of the synchronized fractional order systems and time history of states error for $Z = ge^{z_2}\sin(\omega t)$ with order $\alpha = \beta = 0.8,\ \gamma = 1.1, \omega$ =0.1315, ω_z =0.2807,g=0.1 .

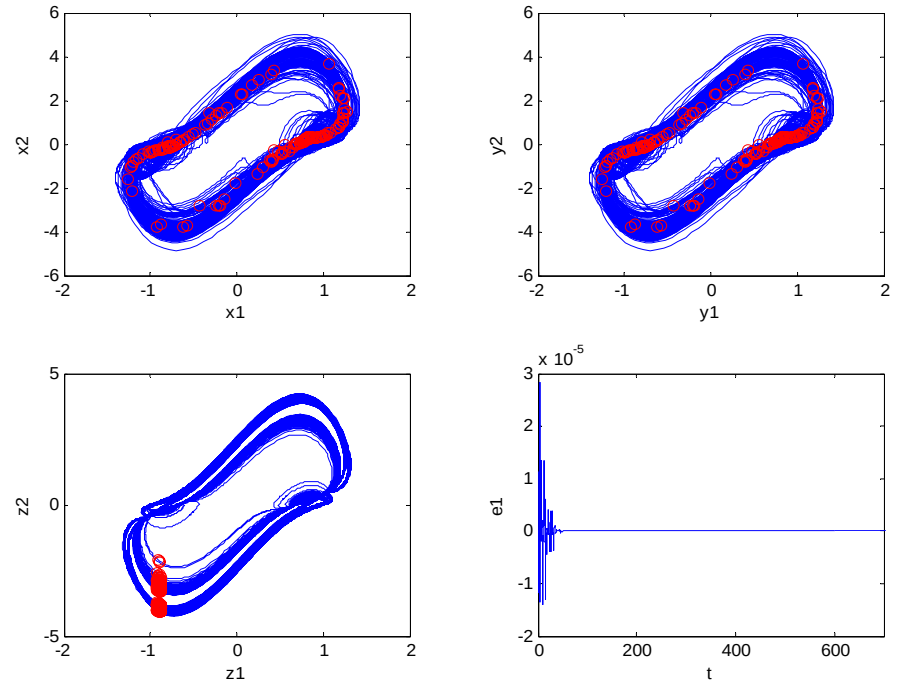

Fig. 3.60 Phase portraits and Poincaré maps of the synchronized fractional order systems and time history of states error for $Z = ge^{z_2}\sin(\omega t)$ with order $\alpha = \beta = 0.7,\ \gamma = 1.1, \omega$ =0.31812, ω_z =0.144,g=0.1 .

Chapter 4

Anticontrol of Chaos for Integral and Fractional Order Generalized Nonautonomous Heartbeat Systems

4.1. Preliminaries

In this chapter, anticontrol of chaos for integral and fractional order generalized nonautonomous van der Pol system is obtained effectively by adding a constant term to the system. By numerical analyses, such as phase portraits, Poincaré maps and bifurcation diagrams, periodic and chaotic motions are observed.

4.2. The Integral and Fractional Order Generalized Nonautonomous Heartbeat Systems and Its Anticontrol Forms

The van der Pol system was first given to study the oscillations in vacuum tube circuits [1-10]. The state equations are in the form of an autonomous system:

$$\begin{aligned} \frac{dx_1}{dt} &= x_2 \\ \frac{dx_2}{dt} &= -x_1 - \varepsilon(x_1^{\,2} - 1)x_2 \end{aligned} \tag{4.1}$$

where ε is a parameter. The generalized van der Pol system has the form of a nonautonomous system which is written as:

$$\begin{aligned} \frac{dx_1}{dt} &= x_2 \\ \frac{dx_2}{dt} &= -x_1 - \varepsilon(1 - x_1^{\,2})(c - ax_1^{\,2})x_2 + b\sin\omega t \end{aligned} \tag{4.2}$$

where ε, a, b, c are parameters, and ω is the circular frequency of the external excitation $b\sin\omega t$. The corresponding nonautonomous fractional order system is

$$\begin{aligned} \frac{d^{\alpha}x_1}{dt^{\alpha}} &= x_2 \\ \frac{d^{\beta}x_2}{dt^{\beta}} &= -x_1 - \varepsilon(1 - x_1^{\,2})(c - ax_1^{\,2})x_2 + b\sin\omega t \end{aligned} \tag{4.3}$$

where α, β are fractional numbers.

In this thesis, the method of the anticontrol chaos by adding constant term is used. The method to control system dynamics from periodic motion to chaotic motion is adding constant terms. Eq.(4.3) can be rewritten as

$$\begin{aligned} \frac{d^{\alpha} x_1}{dt^{\alpha}} &= x_2 + k_1 \\ \frac{d^{\beta} x_2}{dt^{\beta}} &= -x_1 - \varepsilon(1 - x_1^{\,2})(c - a x_1^{\,2}) x_2 + b \sin \omega t + k_2 \end{aligned} \tag{4.4}$$

where k_1, k_2 are constants.

4.3. Numerical Simulations for Anticontrol of Chaos

The systems to be anticontrol are Eq.(4.4) in following three cases. The parameters a=0.07, b=1.0091, c=1.2, ε=3 and $\omega = 0.1309$ of system Eq.(4.4) are fixed. The anticontrol chaos schemes consists of three cases:

Case 1: Add a constant term, k_1 is an ajustable constant and $k_2 = 0$. Fig. 4.1 shows the bifurcation diagram for the nonautonomous integral order generalized van der Pol system (4.4) with k_1 as abscissa, and Fig. 4.2 shows the corresponding phase portrait and Poincaré maps. The chaotic phase portraits and Poincaré maps for the fractional order systems (4.4) where α, β take the same fractional numbers and vary from 1.3 to 0.2 in steps of 0.1, can be successfully obtained. When α, β take the fractional number less than 0.2, no chaotic motion is found. In order to save space, only six cases, fractional numbers 1.3, 1.1, 0.8, 0.5, 0.3, 0.2, are shown in Fig. 4.3~ Fig. 4.8.

Case 2: Add a constant term, k_2 is an ajustable constant and $k_1 = 0$. Fig. 4.9 shows the bifurcation diagram for the nonautonomous integral order generalized van der Pol system (4.4) with k_2 as abscissa, and Fig. 4.10 shows the corresponding phase portrait and Poincaré maps. The chaotic phase portraits and Poincaré maps for the fractional order systems (4.4) where α, β take the same fractional numbers and vary from 1.3 to 0.7 in steps of 0.1, can be successfully obtained. When α, β take the fractional number

less than 0.7, no chaotic motion is found. In order to save space, only five cases, fractional numbers 1.3, 1.1, 0.9, 0.8, 0.7, are shown in Fig. 4.11~ Fig. 4.15.

Case 3: Add two constant terms, k_1 and k_2 are ajustable constants. We take $k_1 = k_2$. Fig. 4.16 shows the bifurcation diagram for the nonautonomous integral order generalized van der Pol system (4.4) with $k_1 = k_2$ as abscissa, and Fig. 4.17 shows the corresponding phase portrait and Poincaré maps. The chaotic phase portraits and Poincaré maps for the fractional order systems (4.4) where α, β take the same fractional numbers and vary from 1.3 to 1.1 in steps of 0.1, can be successfully obtained. When α, β take the fractional number less than 0.7, no chaotic motion is found. In order to save space, only three cases, fractional numbers 1.3, 1.2, 1.1, are shown in Fig. 4.18~ Fig. 4.20.

By the results of simulation, it is found that anticontrols of chaos for integral and fractional order generalized nonautonomous van der Pol systems by adding one constant term are effective.

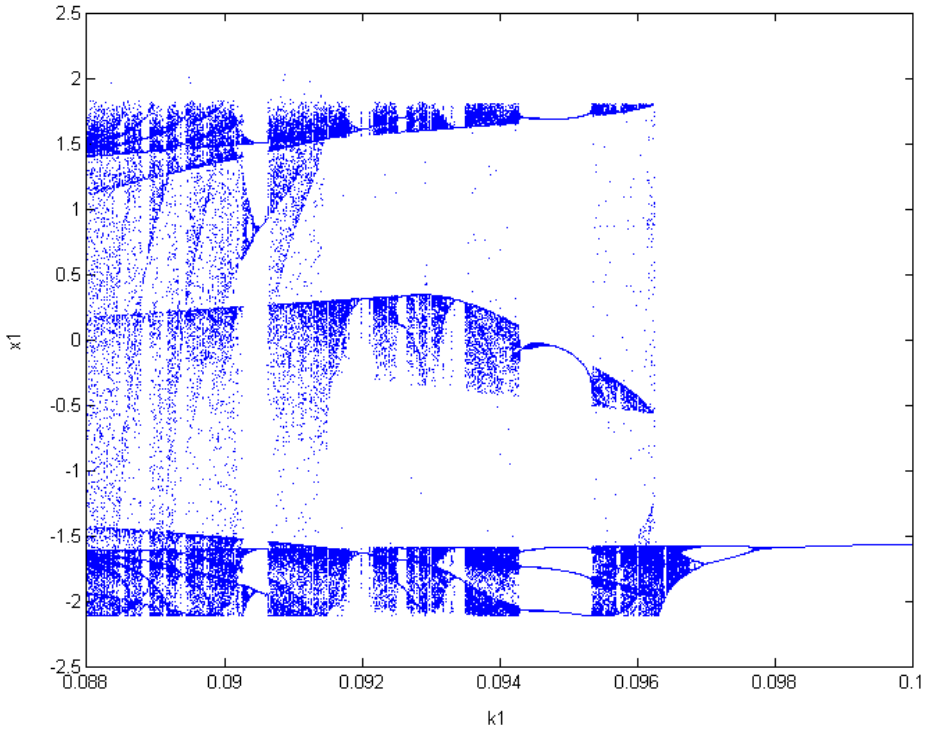

Fig. 4.1 Bifurcation diagram of the integral order system with k_1 as abscissa.

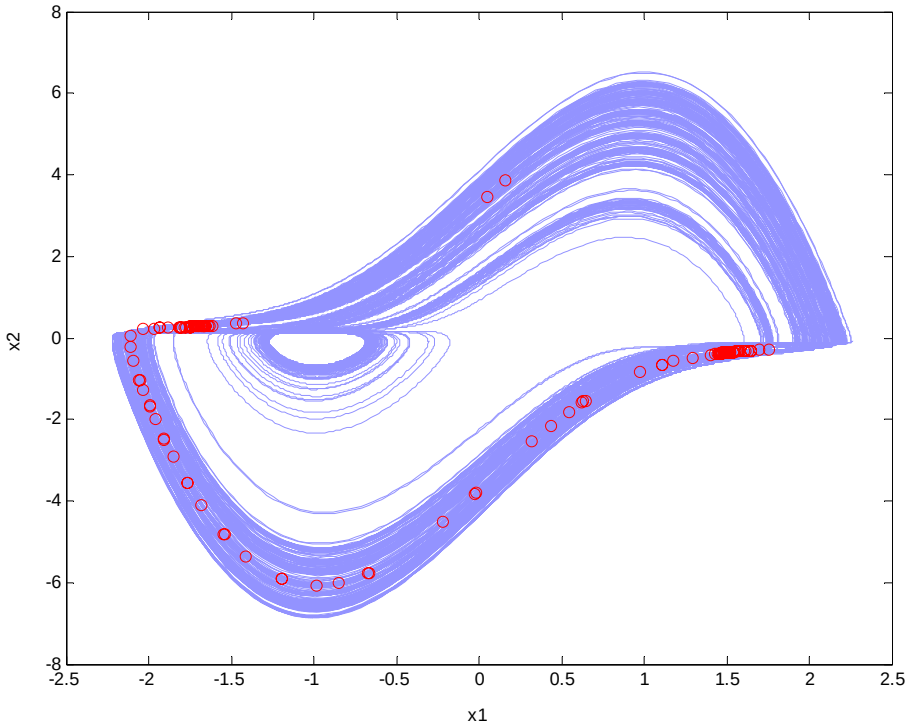

Fig. 4.2 Phase portrait and Poincaré maps of the integral order system for $k_1 = 0.088$, $k_2 = 0$.

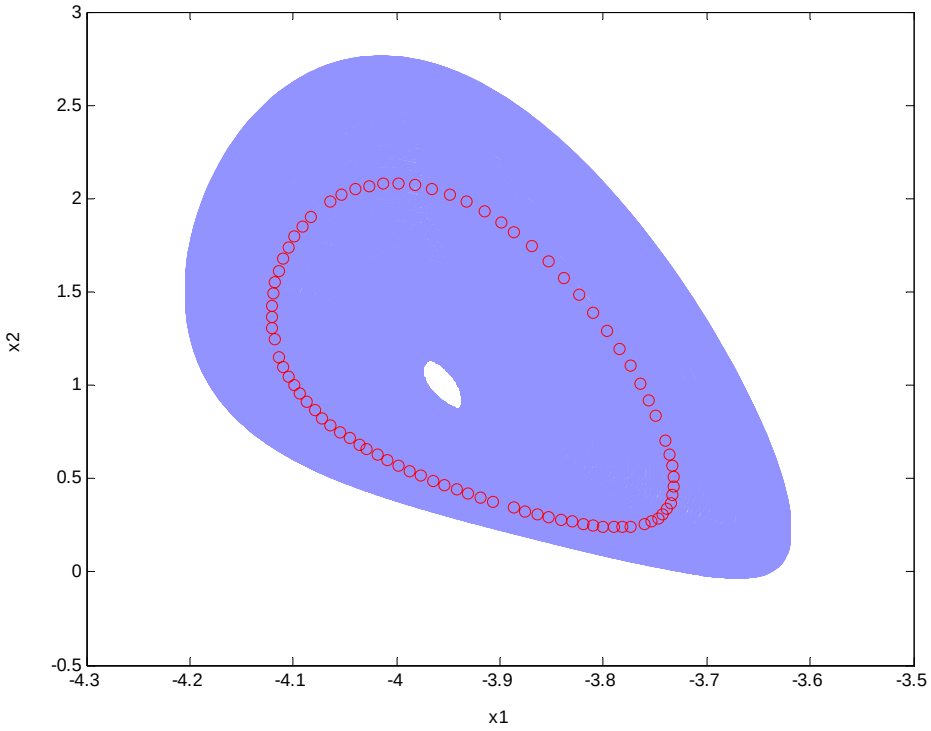

Fig. 4.3 Phase portrait and Poincaré maps of the fractional order system for $\alpha = \beta = 1.3$, $k_1 = -1$, $k_2 = 0$.

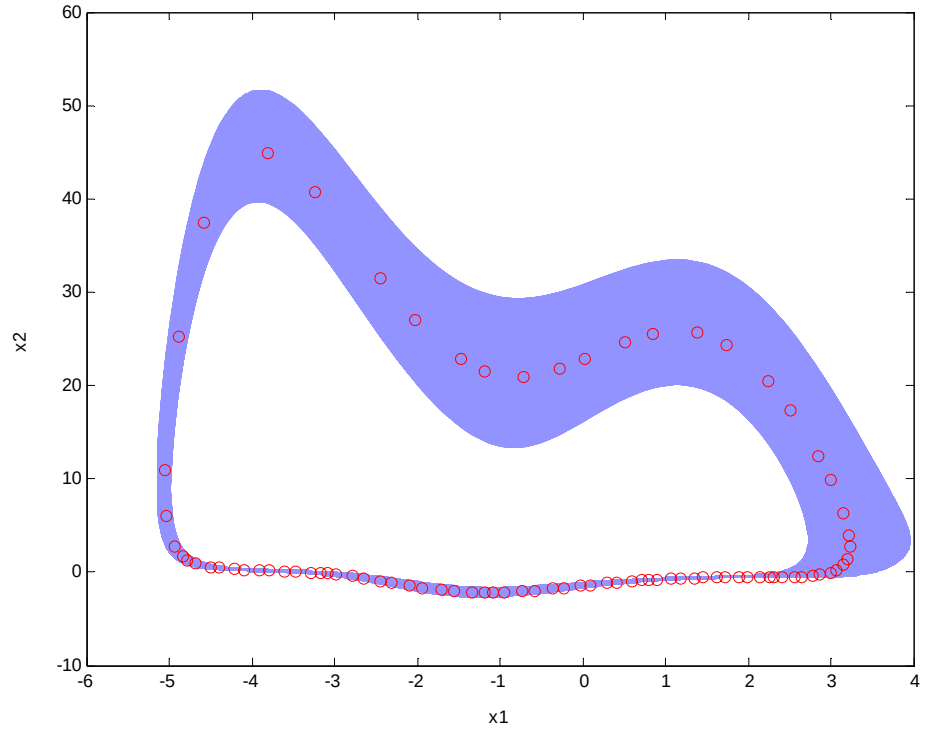

Fig. 4.4 Phase portrait and Poincaré maps of the fractional order system for $\alpha = \beta = 1.1$, $k_1 = -6$, $k_2 = 0$.

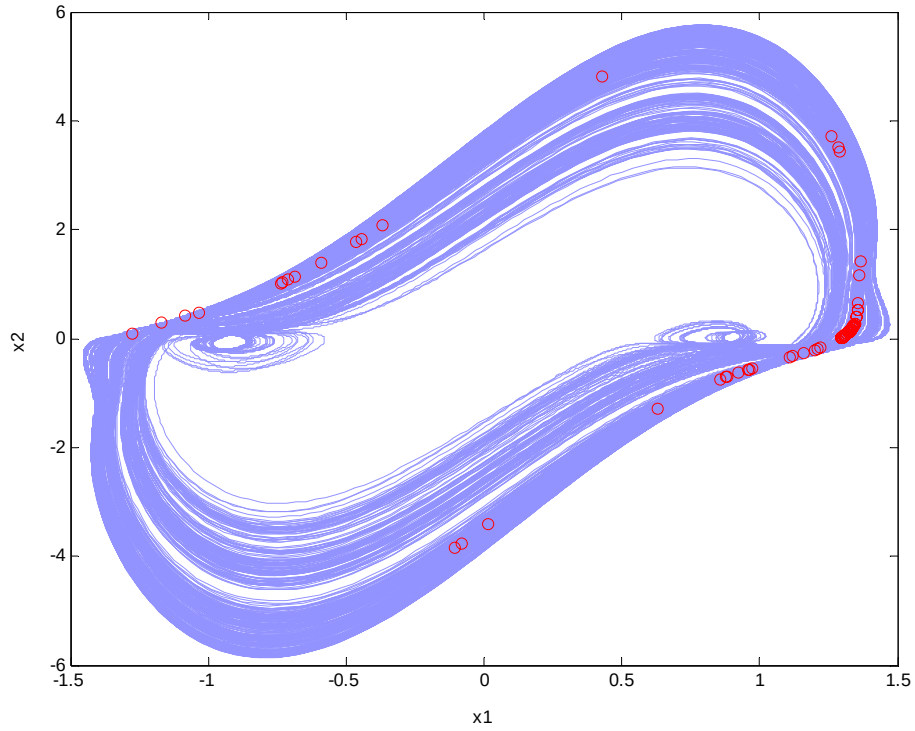

Fig. 4.5 Phase portrait and Poincaré maps of the fractional order system for $\alpha = \beta = 0.8$, $k_1 = 0.02$, $k_2 = 0$.

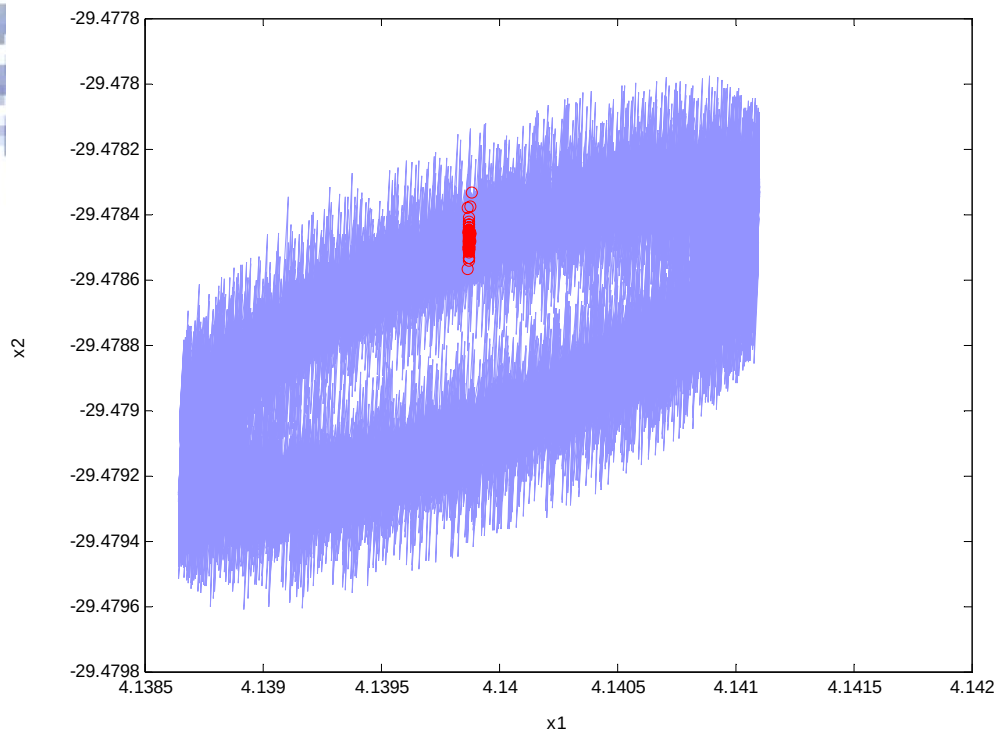

Fig. 4.6 Phase portrait and Poincaré maps of the fractional order system for $\alpha = \beta = 0.5$, $k_1 = 30$, $k_2 = 0$.

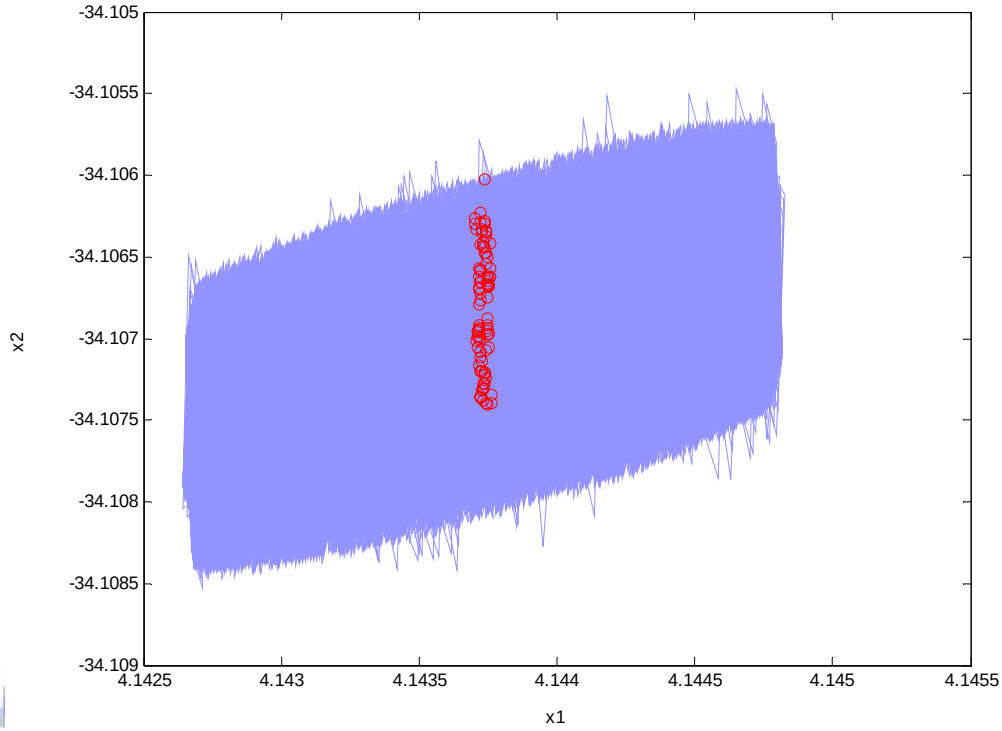

Fig. 4.7 Phase portrait and Poincaré maps of the fractional order system for $\alpha = \beta = 0.3$, $k_1 = 35$, $k_2 = 0$.

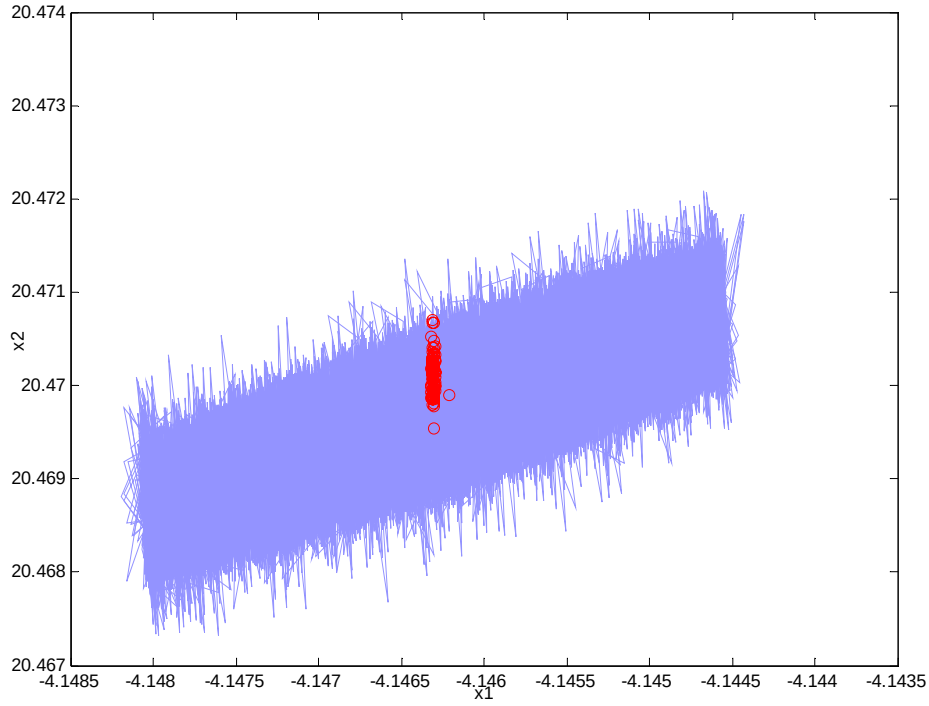

Fig. 4.8 Phase portrait and Poincaré maps of the fractional order system for $\alpha = \beta = 0.2$, $k_1 = -22$, $k_2 = 0$.

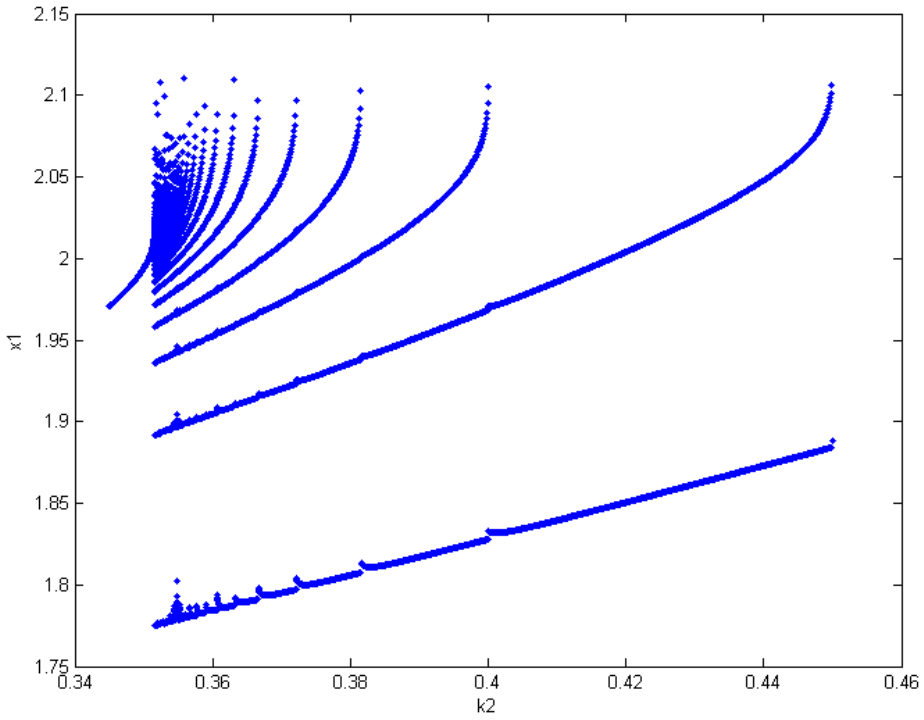

Fig. 4.9 Bifurcation diagram of the integral order system with k_2 as abscissa.

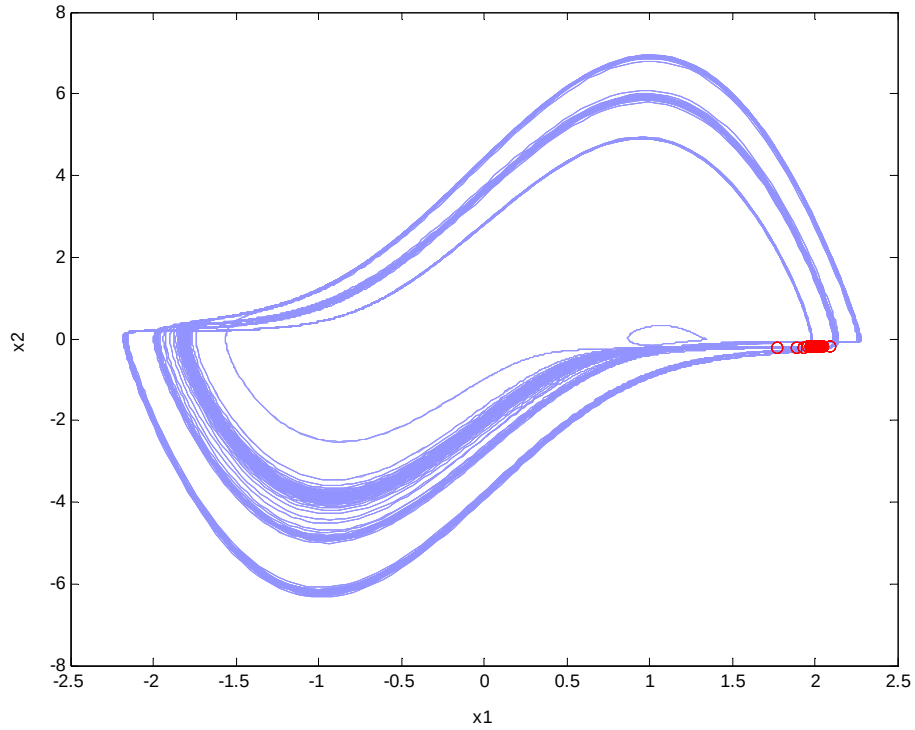

Fig. 4.10 Phase portrait and Poincaré maps of the integral order system for $k_1 = 0$, $k_2 = 0.3518$.

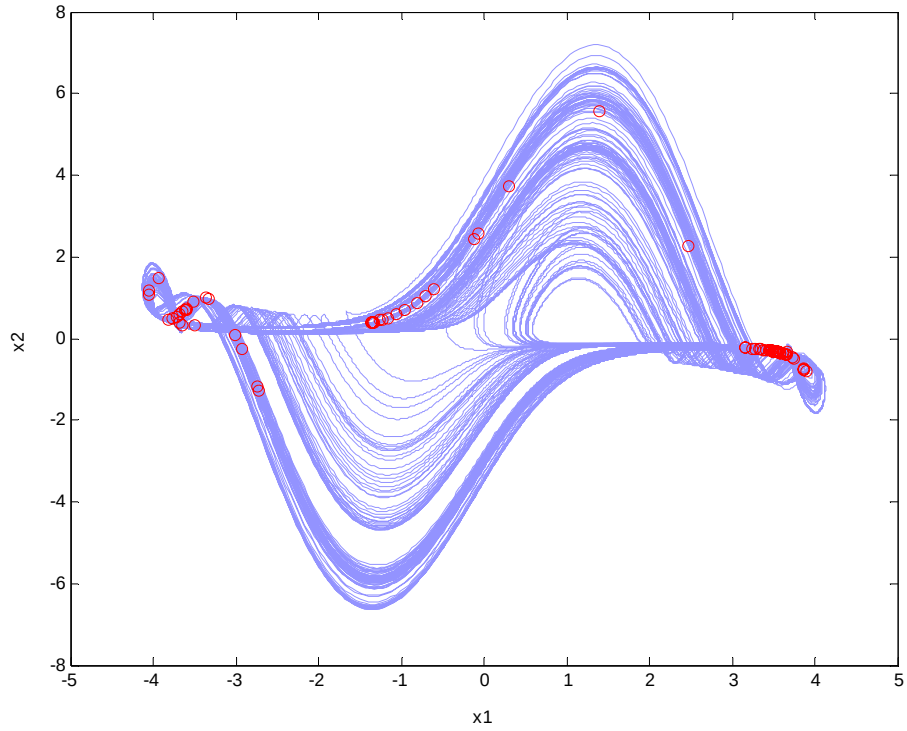

Fig. 4.11 Phase portrait and Poincaré maps of the fractional order system for $\alpha = \beta = 1.3$, $k_1 = 0$, $k_2 = 0.005$.

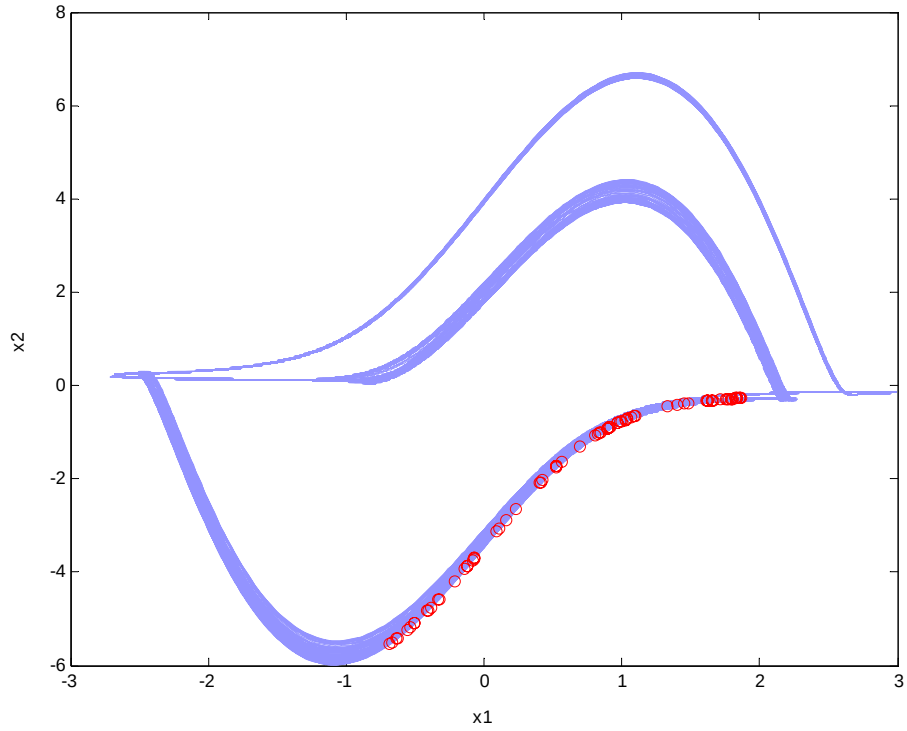

Fig. 4.12 Phase portrait and Poincaré maps of the fractional order system for $\alpha = \beta = 1.1$, $k_1 = 0$, $k_2 = -0.052$.

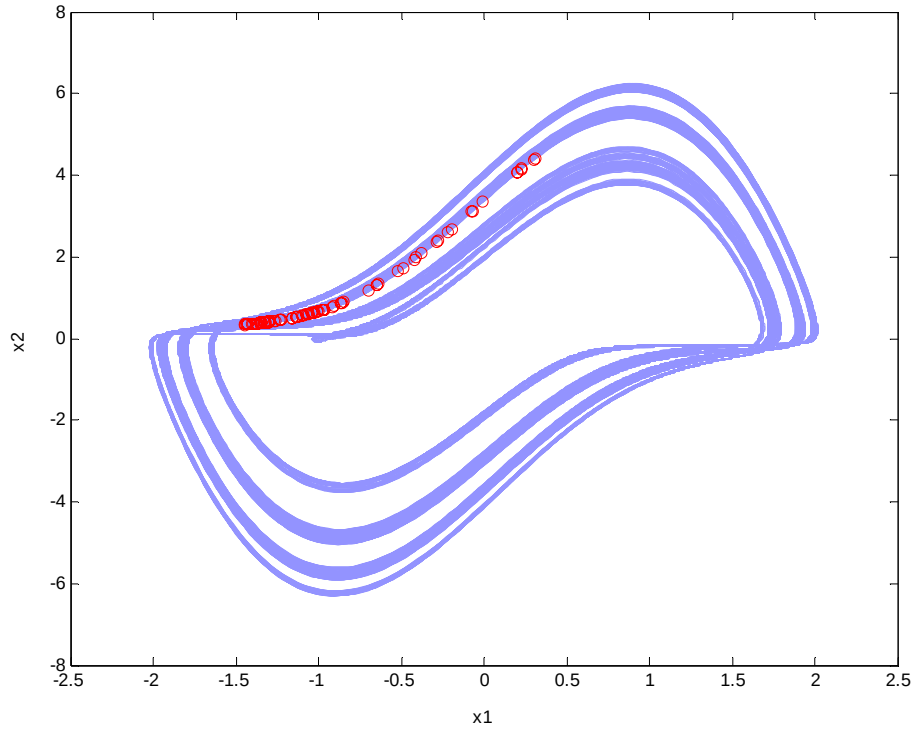

Fig. 4.13 Phase portrait and Poincaré maps of the fractional order system for $\alpha = \beta = 0.9$, $k_1 = 0$, $k_2 = -0.05$.

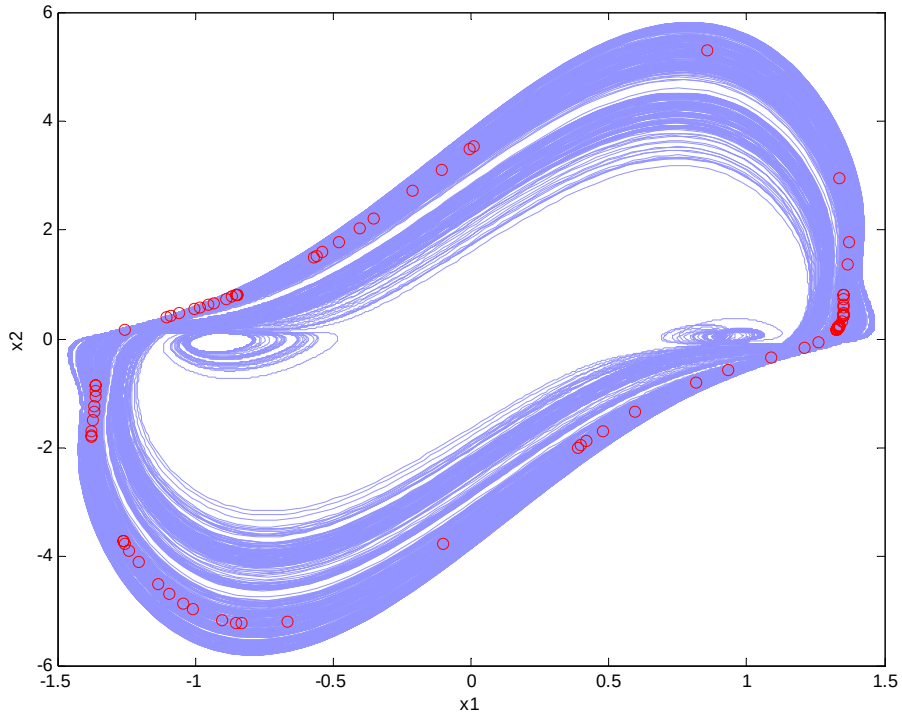

Fig. 4.14 Phase portrait and Poincaré maps of the fractional order system for $\alpha = \beta = 0.8$, $k_1 = 0$, $k_2 = 0.02$.

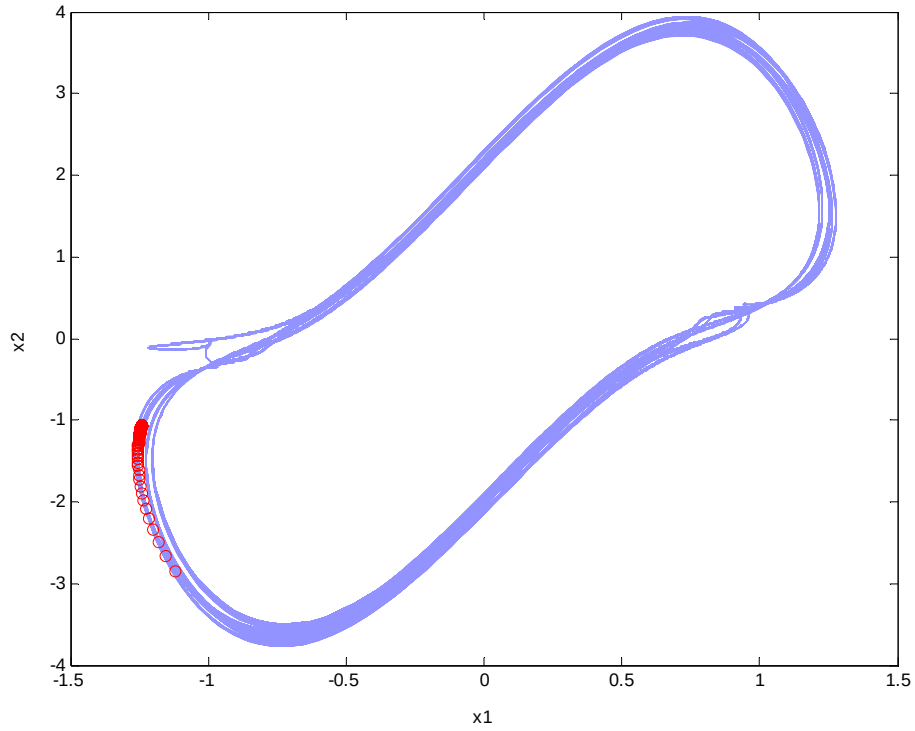

Fig. 4.15 Phase portrait and Poincaré maps of the fractional order system for $\alpha = \beta = 0.7$, $k_1 = 0$, $k_2 = -0.4$.

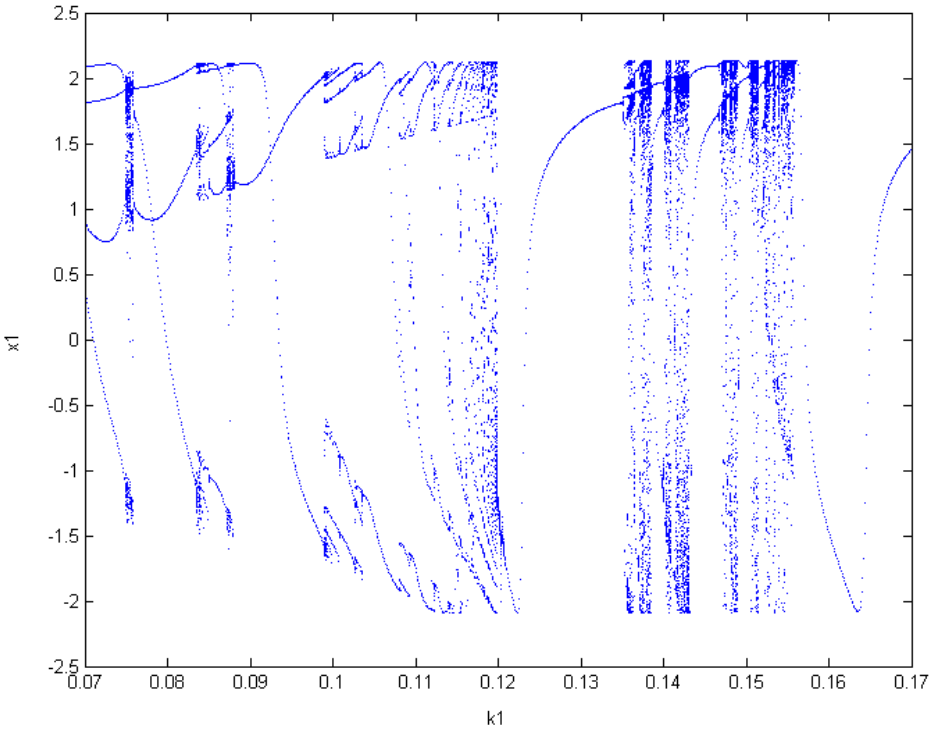

Fig. 4.16 Bifurcation diagram of the integral order system with $k_1 = k_2$ as abscissa.

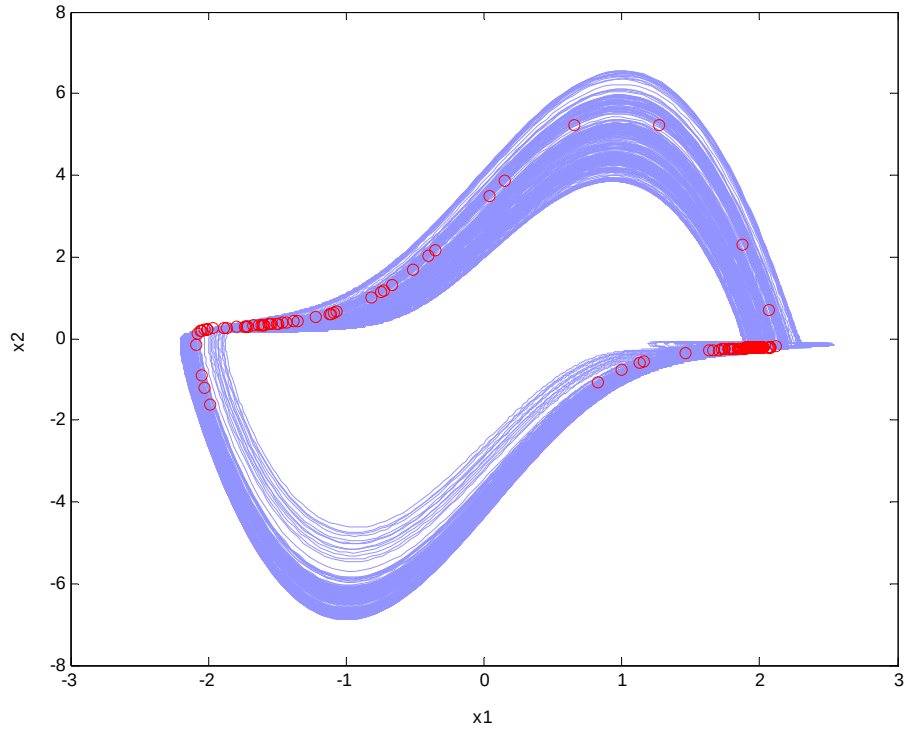

Fig. 4.17 Phase portrait and Poincaré maps of the integral order system for $k_1 = k_2$ =0.1422.

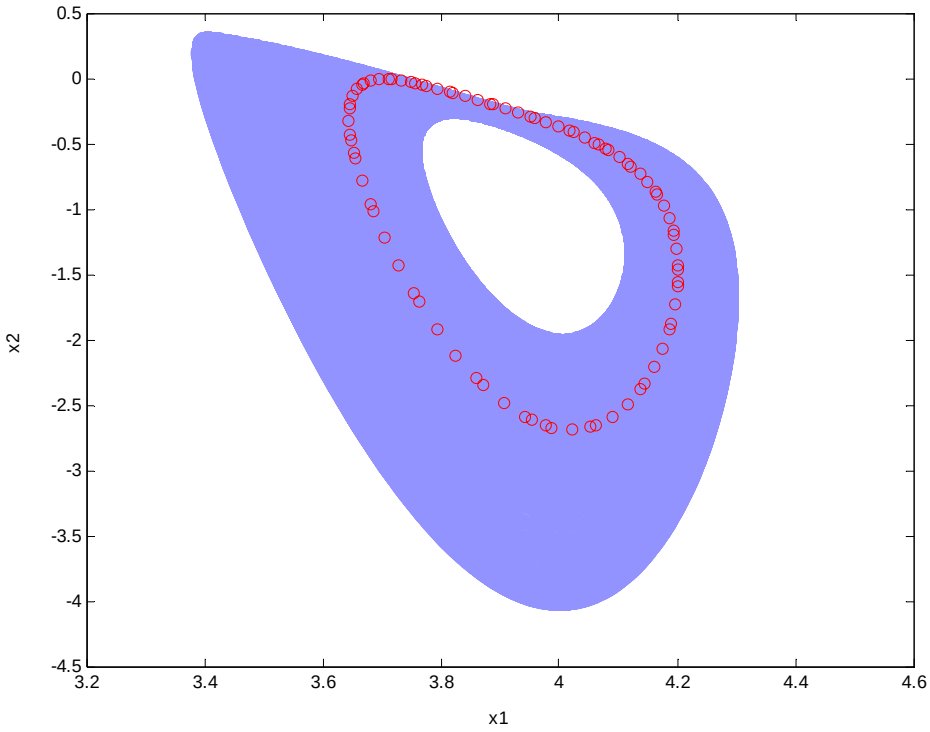

Fig. 4.18 Phase portrait and Poincaré maps of the fractional order system for $\alpha = \beta = 1.3$, $k_1 = k_2 = 1$.

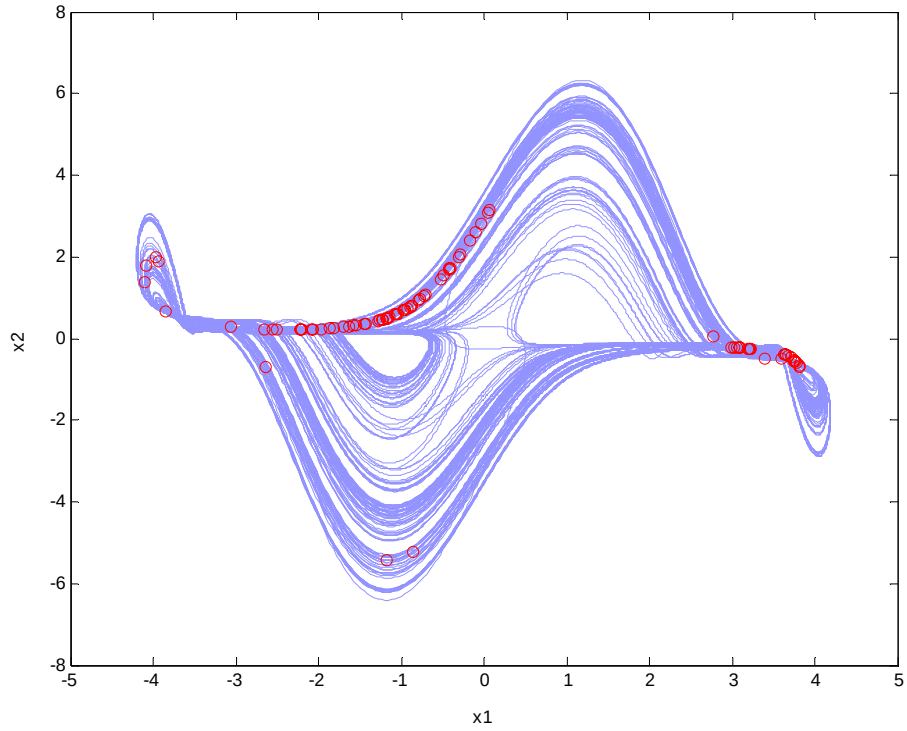

Fig. 4.19 Phase portrait and Poincaré maps of the fractional order system for $\alpha = \beta = 1.2$, $k_1 = k_2 = -0.01$.

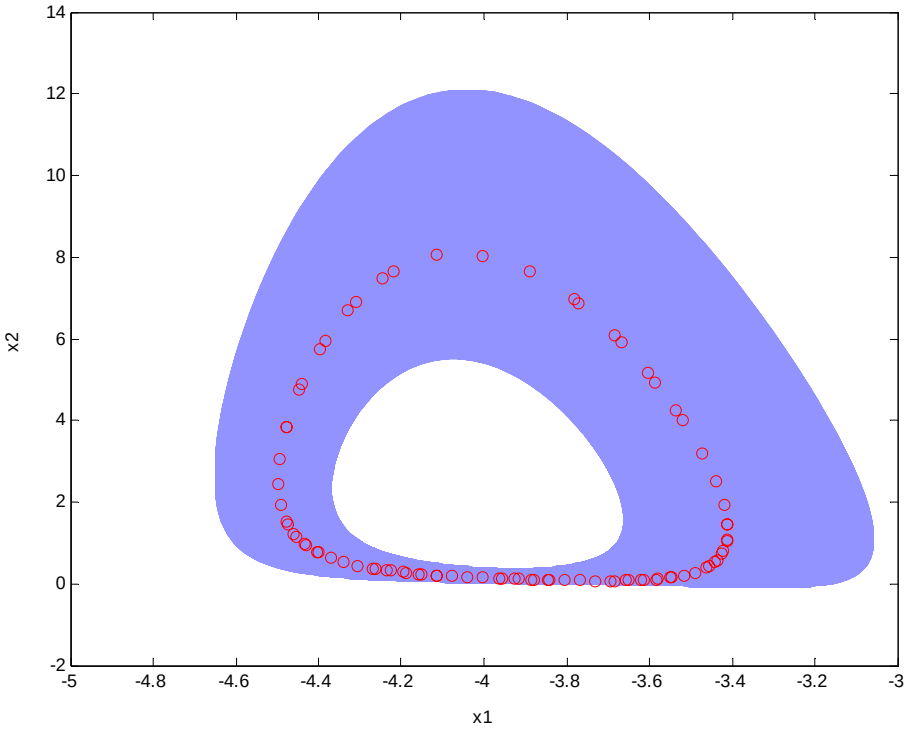

Fig. 4.20 Phase portrait and Poincaré maps of the fractional order system for $\alpha = \beta = 1.1$, $k_1 = k_2 = -2$.

Chapter 5
Conclusions

In this thesis, chaos of a generalized heartbeat system, i.e. a generalized van der Pol system, both with integral order and with fractional orders is studied. Both autonomous and nonautonomous systems are studied in detail. It is found that chaotic motions exist in the nonautonomous generalized van der Pol system excited by a sinusoidal time function. For fractional order systems, when $\gamma = 1$, α, β vary from 1.1 to 0.7 in the steps of 0.1, chaos exists. Next, chaotic motions exist when the fraction orders $\alpha = \beta = \gamma = 1.1$. When $\gamma = 1.1$ with $\alpha = \beta$ varying from 1.1 to 0.3, chaotic motions also exist.

Chaos excited chaos synchronization of a generalized van der Pol system with integral and fractional order is studied. Synchronizations of two identical generalized van der Pol chaotic systems are obtained by replacing the amplitude or the sine time function of their corresponding exciting terms by the same function of chaotic states of a third nonautonomous or autonomous, respectively. Numerical simulations, such as phase portraits, Poincaré maps and state error plots are given. It is found that chaos excited chaos synchronizations exist for the fractional order systems with the total fractional order both less than and more than the number of the states of the integer order generalized van der Pol system. Synchronizations are obtained for lowest total fractional order $0.7 \times 2 = 1.4$ where the third system is an autonomous system with three states. Synchronizations also can be achieved for lowest total fractional order $0.3 \times 2 = 0.6$ where the third system is a nonautonomous system with two states.

Anticontrol of chaos for integral and fractional order generalized nonautonomous van der Pol system is obtained effectively by adding a constant term. By numerical analyses, such as phase portraits, Poincaré maps and bifurcation diagrams, it is found that the periodic motions of the system are transformed to chaotic ones effectively by the proposed anticontrol scheme of adding a constant term. Adding two constant terms is not effective for systems with fractional order less than one, but is effective for systems with fractional order more than one.

References

[1]. L. Glass, *Theory of Heart*, Springer, New York-Heidelberg-Berlin, 1990.

[2]. B.Van der Pol, “Forced Oscillations in a Circuit with Nonlinear Resistance (Receptance with Reactive Triode)”, London, Edinburgh, and Dublin Philosphical Magazine 3, pp.65-80, 1927.

[3]. Qinsheng Bi, “Dynamical Analysis of Two Coupled Parametrically Excited Van der Pol Oscillators”, International Journal of Nonlinear Mechanics, Vol.39, pp.33-54, 2004.

[4]. Hsien-Keng Chen, Zheng-Ming Ge, “Bifurcation and Chaos of a Two-Degree-of Freedom Dissipative Gyroscope”, Chaos, Solitons and Fractals, Vol.24, pp.125-136, 2005.

[5]. R.E. Mickens, “Analysis of Nonlinear Oscillators Having Non-polynomial Elastic Terms”, Journal of Sound and Vibration, Vol.255, pp.789–792, 2002.

[6]. A. M. dos Santos, S. R. Lopes, and R. L. Viana, “Rhythm Synchronization and Chaotic Modulation of Coupled Van der Pol Oscillators in a Model for the Heartbeat”, Physica A, Vol.338, pp.335-355, 2004.

[7]. W. Addo-Asah, H. C. Akpati, R. E. Mickens, “Investigation of a Generalized Van der Pol Oscillator Differential Equation”, Journal of Sound and Vibration, Vol.179, pp. 733-735, 1995.

[8]. Gamal M. Mahmoud, Ahmed A. M. Farghaly, “Chaos Control of Chaotic Limit Cycles of Real and Complex Van der Pol Oscillators”, Chaos, Solitons and Fractals, Vol. 21, pp. 915-924,2004.

[9]. S.B. Waluya, W.T. van Horssen, “On the Periodic Solutions of a Generalized Nonlinear Van der Pol Oscillator”, Journal of Sound and Vibration, Vol.268, pp.209-215, 2003.

[10]. Qinsheng Bi, “Dynamical Analysis of Two Coupled Parametrically Excited Van der Pol Oscillators”, International Journal of Nonlinear Mechanics, Vol.39, pp.33-54, 2004.

[11]. R.L. Bagley and R.A. Calico, “Fractional Order State Equations for the Control of Viscoelastically Damped Structures”, J. Guid. Contr. Dyn., Vol.14, pp.304-311, 1991.

[12]. C. Li and G. Chen, “Chaos in the Fractional Order Chen System and Its Control”, Chaos, Solitons and Fractals, Vol.22, pp.549-554, 2004.

[13]. Wajdi M. Ahmad, Ahmad M. Harb, “On Nonlinear Control Design for Autonomous Chaotic Systems of Integer and Fractional Orders”, Chaos, Solitons and Fractals, Vol.18, pp.693-701, 2003.

[14]. Wajdi M. Ahmad, Reyad El-Khazali, Yousef Al-Assaf, “Stabilization of Generalized Fractional Order Chaotic Systems Using State Feedback Control”, Chaos, Solitons and Fractals, Vol.22, pp.141-150, 2004.

[15]. W.M. Ahmad, “Hyperchaos in Fractional Order Nonlinear Systems”, Chaos, Solitons and Fractals, Vol.26, pp.1459-1465, 2005.

[16]. S. Nimmo and A. K. Evans, “The Effects of Continuously Varying the Fractional Differential Order of Chaotic Nonlinear Systems”, Chaos, Solitons and Fractals, Vol.10, pp.1111–1118, 1999.

[17]. Z.M. Ge, P.C. Tzen, S.C. Lee, “Parametric Analysis and Fractal-Like Basins of Attraction by Modified Interpolates Cell Mapping”, Journal of Sound and Vibration Vol. 253; No. 3, 2002.

[18]. Wajdi M. Ahmad, and J. C. Sprott, “Chaos in a Fractional-Order Autonomous Nonlinear Systems”, Chaos, Solitons and Fractals, Vol.16, pp.339-351, 2003.

[19]. Ramiro S. Barbosa, J.A. Tenreiro Machado, Isabel M. Ferreira, József. K. Tar, “Dynamics of the Fractional-Order Van der Pol Oscillator”, Proc. of the 2nd 2nd IEEE International Conference on Computational Cybernetics (ICCC'04), pp. 373-378, ISBN 3-902463-01-5, 2004.

[20]. Changpin Li, Guojun Peng, “Chaos in Chen’s System with a Fractional Order”, Chaos, Solitons and Fractals, Vol. 22, pp.443–450, 2004.

[21]. A. Charef, H.H. Sun, Y.Y. Tsao, and B. Onaral, “Fractal System as Represented by Singularity Function”, IEEE Trans. Automat. Contr., Vol.37, pp.1465-1470, 1992.

[22]. T.T. Hartley, C.F. Lorenzo, and H.K. Qammer, “Chaos in a Fractional Order Chua’s System”, IEEE Trans CAS-I, Vol.42, pp.485-490, 1995.

[23]. Z.M. Ge, Shiue, “Non-Linear Dynamics and Control of Chaos for Tachometer”, Journal of Sound and Vibration Vol. 253; No4, 2002.

[24]. Z.M. Ge, C.I. Lee, “Non-Linear Dynamics and Control of Chaos for a Rotational Machine with a Hexagonal Centrifugal Governor with a Spring”, Journal of Sound and Vibration Vol. 262, pp.845-64, 2003.

[25]. Z.M. Ge, C.M. Hsiao, Y.S. Chen, “Non-Linear Dynamics and Chaos Control for a Time Delay Duffing System”, Int. J. of Nonlinear Sciences and Numerical Vol. 6; No. 2, pp.187-199, 2005.

[26]. Z.M. Ge, S.C. Lee, “Parameter Used and Accuracies Obtain in MICM Global Analyses”, Journal of Sound and Vibration Vol. 272, pp.1079-85, 2004.

[27]. Zheng-Ming Ge and Wei-Ying Leu, “Anti-Control of Chaos of Two-degrees-of-Freedom Louderspeaker System and Chaos Synchronization of Different Order Systems”, Chaos, Solitons and Fractals, Vol.20, pp.503-521, 2004.

[28]. Zheng-Ming Ge, Jui-Wen Cheng, Yen-Sheng Chen, “Chaos Anticontrol and Synchronization of Three Time Scales Brushless DC Motor System”, Chaos, Solitons and Fractals, Vol.22, pp.1165-1182, 2004.

[29]. Zheng-Ming Ge, Ching-I Lee, “Control, Anticontrol and Synchronization of Chaos for an Autonomous Rotational Machine System with Time-Delay”, Chaos, Solitons and Fractals, Vol.23, pp.1855-1864, 2005.

[30]. Z.-M. Ge, C.-M. Chang, Y.-S. Chen, “Anti-Control of Chaos of Single Time Scale Brushless DC Motor and Chaos Synchronization of Different Order Systems”, accepted by Chaos, Solitons and Fractals, 2005.

[31]. C.M. Kim, S. Rim, W.H. Kye, J.W. Ryu, Y.J. Park, “Anti-Synchronization of Chaotic Oscillators”, Phys. Lett. A, Vol.320, pp.39–46, 2003.

[32]. H.K. Chen, C.I. Lee, “Anti-Control of Chaos in Rigid Body Motion”, Chaos, Solitons and Fractals Vol. 21, pp.957-965, 2004.

[33]. Z.M. Ge, H.W. Wu, “Chaos Synchronization and Chaos Anticontrol of a Suspended Track with Moving Loads”, Journal of Sound and Vibration Vol. 270, pp.685-712, 2004.

[34]. Z.M. Ge, C.Y. Yu, Y.S. Chen, “Chaos Synchronization and Chaos Anticontrol of a

Rotational Supported Simple Pendulum", JSME International Journal, Series C,Vol. 47; No. 1, pp.233-41, 2004.

[35]. Z.M. Ge, C.I. Lee, "Anticontrol and Synchronization of Chaos for an Autonomous Rotational Machine System with a Hexagonal Centrifugal Governor", Chaos, Solitons and Fractals Vol. 282; 635-48, 2005.

[36]. Ruoting Yang, Yiguang Hong, Huashu Qin, Guanrong Chen, "Anticontrol of Chaos for Dynamic Systems in ρ–normal Form: A Homogeneity-based Approach", Chaos, Solitons and Fractals Vol. 25; 687-697, 2005.

[37]. Cristina Morel, Marc Bourcerie, Francois Chapeau-Blondeau, "Generating Independent Chaotic by Chaos Anticontrol in Nonlinear Circuits", Chaos, Solitons and Fractals Vol. 26; 541-549, 2005.

[38]. Xiao Fan Wang, Guanrong Chen, Xinghuo Yu, "Anticontrol of chaos in continuous-time systems via time-delay feedback", CHAOS Vol. 10; 771-779, 2000.

[39]. Hongtao Lu, Xinzhen Yu, "Local bifurcations in delayed chaos anticontrol systems", Journal of Computational and Applied Mathematics Vol. 181; 188-199, 2005.

[40]. Zheng-Ming Ge and Yen-Sheng Chen, "Synchronization of Unidirectional Coupled Chaotic Systems via Partial Stability", Chaos, Solitons and Fractals, Vol.21, pp.101-111, 2004.

[41]. Zheng-Ming Ge and Wei-Ying Leu, "Chaos Synchronization and Parameter Identification for Louderspeaker System", Chaos, Solitons and Fractals, Vol.21, pp.1231-1247, 2004.

[42]. Zheng-Ming Ge and Chien-Cheng Chen, "Phase Synchronization of Coupled Chaotic Multiple Time Scale Systems", Chaos, Solitons and Fractals, Vol.20, pp.639-647, 2004.

[43]. Z.-M. Ge and C.-M. Chang, "Chaos Synchronization and Parameter Identification of Single Time Scale Brushless DC Motors", Chaos, Solitons and Fractals, Vol.20, pp.883-903, 2004.

[44]. Z.-M. Ge, J.-W. Cheng, "Chaos Synchronization and Parameter Identification of Three

Time Scales Brushless DC Motor System", Chaos, Solitons and Fractals, Vol.24, pp.597-616, 2005.

[45]. Zheng-Ming Ge, Yen-Sheng Chen, "Adaptive Synchronization of Unidirectional and Mutual Coupled Chaotic Systems", Chaos, Solitons and Fractals, Vol.26, pp.881-888, 2005.

[46]. G. Jiang, W. Zheng , G. Chen, "Global Chaos Synchronization with Channel Time-Delay", Chaos, Solitons and Fractals, Vol.20, pp.267–75,2004.

[47]. G. Chen , S. Liu, "On Generalized Synchronization of Spatial Chaos", Chaos, Solitons and Fractals, Vol.15, pp.311–318, 2003.

[48]. Z. Li, D. Xu, "A Secure Communication Scheme Using Projective Chaos Synchronization", Chaos, Solitons and Fractals, Vol.22, pp.477–481, 2004.

[49]. Guo-Ping Jiang, Wallace Kit-Sang Tang, Guanrong Chen, "A Simple Global Synchronization Criterion for Coupled Chaotic Systems", Chaos, Solitons and Fractals, Vol.15, pp.925-935, 2003.

[50]. Zheng-Ming Ge, Cheng-Hsiung Yang, "Generalized Synchronization of Quantum-CNN Chaotic Oscillator with Different Order Systems", accepted by Chaos, Solitons and Fractals, 2005.

[51]. L.M. Pecora, T.L. Carroll, "Synchronization in Chaotic Systems",Phys. Rev. Lett. Vol.64, pp.821–4, 1990.

[52]. T.L. Carroll, J.F. Heagy, L.M. Pecora, "Transforming Signals with Chaotic Synchronization", Phys. Rev. E, Vol.54, pp.4676–80, 1996.

[53]. L. Kocarev, U. Parlitz, "Generalized Synchronization, Predictability, and Equivalence of Unidirectionally Coupled Dynamical Systems", Phys. Rev. Lett., Vol.76, pp.1816–9, 1996.

[54]. M.G. Rosenblum, A.S. Pikovsky, J. Kurths, "Phase Synchronization of Chaotic Oscillators", Phys. Rev. Lett. , Vol.76, pp.1804–7, 1996.

[55]. S.S. Yang, C.K. Duan, "Generalized Synchronization in Chaotic Systems", Chaos, Solitons

and Fractals, Vol.9, pp.1703–7, 1998.

[56]. G. Chen, S.T. Liu, “On Generalized Synchronization of Spatial Chaos”, Chaos, Solitons and Fractals, Vol.15, pp.311–8, 2003.

[57]. S.P. Yang, H.Y. Niu, G. Tian, et al., “Synchronizing Chaos by Driving Parameter”, Acta Phys. Sin., Vol.50, pp.619–23, 2001.

[58]. D. Dai, X. K. Ma, “Chaos Synchronization by using Intermittent Parametric Adaptive Control Method”, Phys. Lett. A, Vol.288, pp.23–8, 2001.

[59]. H.K. Chen, “Synchronization of Two Different Chaotic Systems: A New System and each of the Dynamical Systems Lorenz, Chen and Lü ”, Chaos, Solitons and Fractals Vol. 25, pp.1049-56, 2005.

[60]. H.K. Chen, T.N. Lin, “Synchronization of Chaotic Symmetric Gyros by One-Way Coupling Conditions”, ImechE Part C: Journal of Mechanical Engineering Science Vol. 217, pp.331-40, 2003.

[61]. H.K. Chen, “Chaos and Chaos Synchronization of a Symmetric Gyro with Linear-Plus-Cubic Damping”, Journal of Sound & Vibration, Vol. 255, pp.719-40, 2002.

[62]. Z.M. Ge, T.C. Yu, Y.S. Chen, “Chaos Synchronization of a Horizontal Platform System”, Journal of Sound and Vibration, pp.731-49, 2003.

[63]. Z.M. Ge, T.N. Lin, “Chaos, Chaos Control and Synchronization of Electro-Mechanical Gyrostat System”, Journal of Sound and Vibration Vol. 259; No.3, 2003.

[64]. Z.M. Ge, C.C. Lin, Y.S. Chen, “Chaos, Chaos Control and Synchronization of Vibromrter System”, Journal of Mechanical Engineering Science Vol. 218, pp.1001-20, 2004.

[65]. H.K. Chen, T.N. Lin, J.H. Chen, “The Stability of Chaos Synchronization of the Japanese Attractors and its Application”, Japanese Journal of Applied Physics Vol. 42; No. 12, pp.7603-10, 2003.

[66]. Z.M. Ge, J.K. Lee, “Chaos Synchronization and Parameter Identification for Gyroscope System”, Applied Mathematics and Computation, Vol. 63, pp.667-82, 2004.

[67]. H.K. Chen, “Global Chaos Synchronization of New Chaotic Systems via Nonlinear Control”, Chaos, Solitons & Fractals, Vol.4, pp.1245-51, 2005.

APPENDIX

FRACTIONAL OPERATORS WITH APPROXIMATELY
2 db ERROR FROM ω = 10^{-2} TO 10^{2} rad/sec

$\frac{1}{s^{0.1}} \approx \frac{220.4s^4 + 5004s^3 + 503s^2 + 234.5s + 0.484}{s^5 + 359.8s^4 + 5742s^3 + 4247s^2 + 147.7s + 0.2099}$
$\frac{1}{s^{0.2}} \approx \frac{60.95s^4 + 816.9s^3 + 582.8s^2 + 23.24s + 0.04934}{s^5 + 134s^4 + 956.5s^3 + 383.5s^2 + 8.953s + 0.01821}$
$\frac{1}{s^{0.3}} \approx \frac{23.76s^4 + 224.9s^3 + 129.1s^2 + 4.733s + 0.01052}{s^5 + 64.51s^4 + 252.2s^3 + 63.61s^2 + 1.104s + 0.002267}$
$\frac{1}{s^{0.4}} \approx \frac{25s^4 + 558.5s^3 + 664.2s^2 + 44.15s + 0.1562}{s^5 + 125.6s^4 + 840.6s^3 + 317.2s^2 + 7.428s + 0.02343}$
$\frac{1}{s^{0.5}} \approx \frac{15.97s^4 + 593.2s^3 + 1080s^2 + 135.4s + 1}{s^5 + 134.3s^4 + 1072s^3 + 543.4s^2 + 20.1s + 0.1259}$
$\frac{1}{s^{0.6}} \approx \frac{8.579s^4 + 255.6s^3 + 405.3s^2 + 35.93s + 0.1696}{s^5 + 94.22s^4 + 472.9s^3 + 134.8s^2 + 2.639s + 0.009882}$
$\frac{1}{s^{0.7}} \approx \frac{4.406s^4 + 177.6s^3 + 209.6s^2 + 9.179s + 0.0145}{s^5 + 88.12s^4 + 279.2s^3 + 33.3s^2 + 1.927s + 0.0002276}$
$\frac{1}{s^{0.8}} \approx \frac{5.235s^3 + 1453s^2 + 5306s + 254.9}{s^4 + 658.1s^3 + 5700s^2 + 658.2s + 1}$
$\frac{1}{s^{0.9}} \approx \frac{1.766s^2 + 38.27s + 4.914}{s^3 + 36.15s^2 + 7.789s + 0.01}$

Paper List

[1]. Zheng-Ming Ge and Mao-Yuan Hsu, “Chaos in a Generalized Van der Pol System and in Its Fractional Order System”, Chaos, Solitons and Fractals, Dec. 2005. accepted and proofed. (SCI, Impact Factor:1.938)

[2]. Zheng-Ming Ge and Mao-Yuan Hsu, “Chaos Excited Chaos Synchronizations of Integral and Fractional Order Generalized Van der Pol Systems”, submitted to Chaos, Solitons and Fractals, 2006.

[3]. Zheng-Ming Ge and Mao-Yuan Hsu, “Anticontrol of Chaos for Integral and Fractional Order Generalized Nonautonomous Van der Pol Systems”, submitted to Chaos, Solitons and Fractals, 2006.